

LABORATORY FOR ENGINEERING MAN/MACHINE SYSTEMS  
LEMS

**System Identification, Model Reduction and  
Deconvolution Filtering Using Fourier Based  
Modulating Signals and High Order Statistics**

*JianQiang Pan\**

Technical Report LEMS-103  
Division of Engineering, Brown University  
March, 1992

---

\*This work partially funded by NSF Grant #ECS-8713771 and NASA Grant #NAG-1-1065



Abstract of " System Identification, Model Reduction and Deconvolution Filtering Using Fourier Based Modulating Signals and High Order Statistics " by JianQiang Pan, Ph.D., Brown University, May 1992.

This research investigates several important problems in the fields of signal processing and model identification, such as system structure identification, frequency response determination, high order model reduction, high resolution frequency analysis, deconvolution filtering, and etc. Each of these topics involves a wide range of applications and has received considerable attention.

Using the Fourier based sinusoidal modulating signals, it is demonstrated that a discrete autoregressive model can be constructed for the least squares identification of continuous systems. Some identification algorithms are presented for both SISO and MIMO systems frequency response determination utilizing only transient data. Also, several new schemes for model reduction have been developed.

Based upon the complex sinusoidal modulating signals, a parametric least squares algorithm for high resolution frequency estimation is proposed. Numerical examples demonstrate that the proposed algorithm shows better performance than the well-known High-Order Yule-Walker Estimation. Also, we have studied the problem of deconvolution and parameter identification of a general noncausal nonminimum phase ARMA system driven by non-Gaussian stationary random processes. Inverse cumulant and inverse polyspectra are introduced as generalizations of the inverse autocorrelation and inverse power spectrum. Algorithms are presented for estimating the inverse cumulants, both in the frequency domain via the FFT algorithms and in the time domain via the least squares algorithm. Simulation results are provided to demonstrate the performance of the method.

# Table of Contents

Chapter 1: Introduction .....	1
Chapter 2: Input Persistent Excitation and Model Structure Estimation .....	5
Section 2.1: Linear Systems and Moment Functionals .....	5
Section 2.2: System Persistent Excitation .....	10
Section 2.3: A Least Squares Algorithm for System Structure Estimation .....	15
Section 2.4: Computer Simulation Results .....	20
Subsection 2.4.1: Some Computational Considerations .....	20
Subsection 2.4.2 Some Numerical Examples .....	22
Chapter 3: Frequency Analysis Using Short Time Transient Data .....	29
Section 3.1: Introduction .....	29
Section 3.2: Complex Modulating Signal Construction and the Modulating Property .....	32
Section 3.3: Least Squares Estimation (The First Formulation) .....	35
Section 3.4: Least Squares Estimation (The Second Formulation) .....	42
Section 3.5: Least Squares Estimation (The Third Formulation) .....	46
Section 3.6: Computer Simulation Results .....	47
Section 3.7: Frequency Analysis for MIMO Systems .....	46
Section 3.8: Numerical Simulation Results .....	60
Chapter 4: Schemes for Model Reduction and Parameter Identification in the Frequency Domain .....	66
Section 4.1: Scheme 1 .....	69
Section 4.2: Scheme 2 .....	72
Section 4.3: Scheme 3 .....	75

Section 4.4: An Algorithm for Initial Value Estimation .....	80
Section 4.5: Some Numerical Examples .....	83
Chapter 5: High Resolution Frequency Estimation in the Presence of Noise	
Using Complex Sinusoidal Modulating Signals .....	92
Section 5.1: Introduction .....	92
Section 5.2: Overview of the High Order Yule-Walker Estimation .....	94
Section 5.3: The Parametric Least Squares Estimation .....	97
Section 5.4: Performance Analysis for Large SNR Circumstances .....	101
Section 5.5: Some Numerical Examples .....	105
Section 5.6: Concluding Remarks .....	118
Chapter 6: Deconvolution and Parameter Identification for Noncausal	
Nonminimum Phase ARMA Systems Using Inverse Cumulants ...	119
Section 6.1: Introduction .....	119
Section 6.2: Background and Problem Statements .....	122
Section 6.3: The Inverse Cumulants .....	125
Section 6.4: Inverse Cumulants Based Algorithms for System	
Deconvolution and Parameter Identification .....	128
Subsection 6.4.1: Inverse Cumulants Estimation in the	
Frequency Domain .....	132
Subsection 6.4.2: Inverse Cumulants Estimation in the	
Time Domain .....	135
Section 6.5: Numerical Simulation Results .....	138
Section 6.6: Concluding Remarks .....	149
Bibliography .....	151

## List of Figures

Fig.2.1(a): Prediction error modeling .....	19
Fig.2.1(b): Typical function $E_n$ verse n .....	19
Fig.2.2(a): Input signal $u(t)$ collected in 40 sec. ....	23
Fig.2.2(b): Output signal $y(t)$ contaminated by 10% white noise .....	23
Fig.2.3: $D_n$ verses n .....	25
Fig.2.4: Magnitude response of the original and estimated systems .....	25
Fig.2.5(a): Output signal $y(t)$ contaminated by 10% white noise .....	27
Fig.2.5(b): $D_n$ verses n .....	27
Fig.2.5(c): Magnitude response of original and estimated systems .....	28
Fig.3.1(a): A random binary input signal collected in 8 seconds .....	49
Fig.3.1(b): Output signal contaminated by noise with SNR=15(dB) .....	50
Fig.3.2(a): Estimated magnitude response in noise-free case .....	50
Fig.3.2(b): Estimated phase response in noise-free case .....	51
Fig.3.3(a): Estimated magnitude response in SNR=15(dB) case .....	51
Fig.3.3(b): Estimated phase response in SNR=15(dB) case .....	52
Fig.3.4: Output signal contaminated by noise with SNR=20(dB) .....	53
Fig.3.5(a): Estimated magnitude response in noise-free case .....	54
Fig.3.5(b): Estimated phase response in noise-free case .....	54
Fig.3.6(a): Estimated magnitude response in SNR=20(dB) case .....	55
Fig.3.6(b): Estimated phase response in SNR=20(dB) case .....	55
Fig.3.7(a): Estimated mag. response of subsystem one in noise-free case .....	62
Fig.3.7(b): Estimated phase response of subsystem one in noise-free case .....	62
Fig.3.7(c): Estimated mag. response of subsystem two in noise-free case .....	63
Fig.3.7(d): Estimated phase response of subsystem two in noise-free case .....	63

Fig.3.8(a): Estimated magnitude response of subsystem one in noise case	64
Fig.3.8(b): Estimated phase response of subsystem one in noise case	64
Fig.3.8(c): Estimated magnitude response of subsystem two in noise case	65
Fig.3.8(d): Estimated phase response of subsystem two in noise case	65
Fig.4.1(a): Magnitude response vs. frequency. The MFFM uses the low frequency matching	85
Fig.4.1(b): Phase response vs. frequency. The MFFM uses the low frequency matching	85
Fig.4.1(c): Nichols plots. The MFFM uses the low frequency matching	86
Fig.4.2(a): Magnitude response vs. frequency. The MFFM uses the high frequency matching	86
Fig.4.2(b): Phase response vs. frequency. The MFFM uses the high frequency matching	87
Fig.4.2(c): Nichols plots. The MFFM uses the low frequency matching	87
Fig.4.3(a): Magnitude response vs. frequency	90
Fig.4.3(b): Phase response vs. frequency	90
Fig.4.3(c): Nichols plots	91
Fig.5.1(a): The variance of estimation of $\omega_1$ in different SNR cases	109
Fig.5.1(b): The variance of estimation of $\omega_2$ in different SNR cases	109
Fig.5.1(c): The variance of estimation of $\omega_3$ in different SNR cases	109
Fig.5.2(a): The estimation bias(dB) verses different SNR for $\omega_1$	110
Fig.5.2(b): The estimation bias(dB) verses different SNR for $\omega_2$	110
Fig.5.2(c): The estimation bias(dB) verses different SNR for $\omega_3$	110
Fig.5.3: Power spectrum of the estimated filter $1/C(z^{-1})$ using the HOYW equations for SNR=0(dB)	111
Fig.5.4(a): Variance of estimation of $\omega_1$ against resolving frequency $\omega_0$	113
Fig.5.4(b): Variance of estimation of $\omega_2$ against resolving frequency $\omega_0$	114
Fig.5.4(c): Variance of estimation of $\omega_3$ against resolving frequency $\omega_0$	114

Fig.5.5(a): The variance of estimation of $\omega_1$ in different SNR cases .....	116
Fig.5.5(b): The variance of estimation of $\omega_2$ in different SNR cases .....	116
Fig.5.5(c): The variance of estimation of $\omega_3$ in different SNR cases .....	116
Fig.5.5(d): The variance of estimation of $\omega_4$ in different SNR cases .....	117
Fig.5.6: Power spectrum of the estimated filter $1/C(z^{-1})$ using the HOYW equations for SNR=0(dB) .....	117
Fig.6.1(a): The true third order inverse cumulants .....	139
Fig.6.1(b): The estimated third order inverse cumulants $ci_{3,F}(i, j)$ .....	140
Fig.6.1(c): The error for the estimated $ci_{3,F}(i, j)$ .....	140
Fig.6.1(d): The estimated third order inverse cumulants $ci_{3,T}(i, j)$ .....	141
Fig.6.1(e): The error for the estimated $ci_{3,T}(i, j)$ .....	141
Fig.6.2(a): The true AR filter and the estimated parameters via the frequency domain formulations .....	142
Fig.6.2(b): The true AR filter and the estimated parameters via the time domain formulations .....	142
Fig.6.3(a): The true fourth order inverse cumulants $ci_4(i, j, 0)$ .....	144
Fig.6.3(b): The true fourth order inverse cumulants $ci_4(i, j, 1)$ .....	144
Fig.6.4(a): The estimated $ci_{4,F}(i, j, 0)$ via a FFT algorithm .....	145
Fig.6.4(b): The estimated $ci_{4,F}(i, j, 1)$ via a FFT algorithm .....	145
Fig.6.4(c): The error for the estimated $ci_4(i, j, 0)$ via the FFT algorithm ....	145
Fig.6.4(d): The error for the estimated $ci_4(i, j, 1)$ via the FFT algorithm ....	145
Fig.6.5(a): The estimated $ci_{4,F}(i, j, 0)$ via a LS algorithm .....	146
Fig.6.5(b): The estimated $ci_{4,F}(i, j, 1)$ via a LS algorithm .....	146
Fig.6.5(c): The error for the estimated $ci_4(i, j, 0)$ via the LS algorithm .....	146
Fig.6.5(d): The error for the estimated $ci_4(i, j, 1)$ via the LS algorithm .....	146
Fig.6.6(a): The true AR filter and the estimated parameters using the frequency domain formulation .....	147
Fig.6.6(b): The true AR filter and the estimated parameters using the	



time domain formulation .....	147
Fig.6.7: The probability error of reconstruction .....	148

## List of Tables

Table 2.1: Least Squares Estimation of The Chevbyshhev System .....	24
Table 2.2: Least Squares Estimation of the Band Pass System .....	26
Table 5.1: Normalized Variance of $\hat{\omega}_1$ in Decibels .....	107
Table 5.2: Normalized Variance of $\hat{\omega}_3$ in Decibels .....	107

# Chapter 1

## Introduction

This research investigates several important problems in the fields of signal filtering, model identification, such as system and structure identification, frequency response determination, high-order model reduction, high resolution frequency analysis, deconvolution filtering, and etc. All these topics involve a wide range of applications and have received considerable attention.

System modeling and structure identification play a very important role in process control and analysis. Much investigation has been carried out in modeling linear systems, both in a deterministic and stochastic vein. In a deterministic setting, we can use the classical state steady frequency domain approaches , or the time domain approaches, like the Bellman-Kalaba quasilinearization technique [Bell65, Kala82], model adaptive observer , state variable filters , and etc. In a stochastic setting, we could use the well-known Kalman filter technique , instrumental variable method, least squares prediction error approach , and etc.[Astr81, Youn81].

In chapter 2, the modulating function approach is formulated for system identification, including order determination. Using the Fourier based commensurable sinusoids as modulating functions, it is demonstrated that a discrete autoregressive model for the least squares identification of continuous differential systems can be constructed in a way utilizing the computationally efficient FFT technique while avoiding the complicated problem of estimating unknown initial values of the system. We discuss the issue of input persistent excitation based upon the autoregressive model. It is shown how an AR model can be constructed to estimate the system parameters and to determine the order of the system. It is proposed that the choice of sinusoidal modulating functions can be based on the heuristic notion of system bandwidth .

Determination of the frequency response of a stable linear system from input-output data is a classical problem of signal processing and system control, and is very important for system synthesis, controller design and the Nyquist stability analysis. Methods for solving this problem include the DFT technique, the cross correlation, and etc.[Astr75, Ljun87, Unbe87]. Requirements for employing these nonparametric schemes are the statistical stationarity of the input and output data, or the steady state operating condition of the system. In order to satisfy these assumptions, eliminate the initial value effects and achieve good accuracy, a long data record needs to be collected. Good reviews of these approaches, as well as noise and finite data effects, can be found in [Söde89].

A frequent critical situation is that the model is not initially at rest and the available length of input and output signals is limited. Also the signal involves sensor noise. In this case, the DFT and cross correlation algorithms will entail large error. Chapter 3 deals with this more general situation by using the complex sinusoidal modulating signals, see [PearAE, Pear91]. An algorithm for MIMO systems frequency

response determination has been developed. Numerical examples are also presented to show the performance.

Based upon the algorithms developed in chapter 3, chapter 4 proposes an approach for model reduction. The new method combines the model identification and reduction together. There is no necessity of knowing the original system or assuming statistical stationarity of input-output data which is crucial to existing algorithms. Some comparison with the balanced realization method and the P-L method have been made.

Chapter 5 focuses on the problem of high resolution frequency estimation by using short time data and a simple linear least squares algorithm. An autoregressive differential equation model is constructed to fit the received signal. Using the Fourier based complex sinusoidal modulating signals, we can easily convert the differential equation model into linear algebraic equations. Numerical examples demonstrate that the proposed algorithm shows better performance than the well-known High-Order Yule-Walker Estimation.

In chapter 6, we focus on the problem of deconvolution and parameter identification of a general noncausal nonminimum phase ARMA system driven by non-Gaussian stationary random processes. Inverse cumulant and inverse polyspectra are introduced as generalizations of the inverse autocorrelation and inverse power spectrum proposed in [Chat79, Clev72]. The original noncausal ARMA system is approximated by a noncausal AR model; a direct relationship exists between the inverse cumulants and the parameters of the deconvolution AR filter. The inverse system is then constructed directly by utilizing a gradient type nonlinear optimization algorithm for matching the AR coefficients and the estimated inverse cumulants. Algorithms are

presented for estimating the inverse cumulants, both in the frequency domain via the FFT algorithms and in the time domain via the least squares algorithm. In the time domain estimation, we have used the forward regression orthogonal algorithm proposed in [Bill89] because it can be modified to take advantage of the specific problem structure. Simulation results are provided to demonstrate the performance of the method.

## Chapter 2

# Input Persistent Excitation and Model Structure Estimation

### 2.1 Linear Systems and Moment Functionals

In this section, we focus on linear systems and introduce the modulating functionals which can be used for system identification. A general input-output linear differential system can be specified by :

$$\sum_{i=0}^n a_{n-i} p^i y(t) = \sum_{i=0}^{n-1} b_{n-1-i} p^i u(t) \quad (2.1.1)$$

The object is to estimate the structure and parameters of the system given input-output data  $(u(t), y(t))$  on the time interval  $[0, T]$ .

Shinbrot's method of moment functionals is one of the classical techniques for system identification[Shin57]. It is also called the modulating function approach. We use modulating functions to convert a differential equation into algebraic equations which

makes it easier to solve the identification problems. Shinbrot's modulating function technique avoids dealing with the unknown initial conditions over each time sequence interval  $[t_i, t_{i+1}]$ , and avoids differentiating the original data, thereby avoiding the noise sensitivity in estimating time derivatives of data.

Converting the differential equation into an algebraic equation is a big step, the latter is much easier to handle. As introduced by Shinbrot,  $\phi(t)$  is a modulating function of order  $N$  over a fixed time interval  $[0, T]$  if  $\phi(t)$  is sufficiently smooth and satisfies the end point conditions :

$$\phi^{(i)}(0) = \phi^{(i)}(T) = 0, \quad i = 0, 1, \dots, N - 1$$

where,

$$\phi^{(i)}(t) = p^i \phi(t) = \frac{d^i}{dt^i} \phi(t)$$

The significance of using this property for the model identification relates to the following fact. If equ.(2.1.1) is multiplied by  $\phi(t)$  on both sides and integrated by parts  $n$  times over  $[0, T]$ , while using the end point conditions, the result is the following functional equation:

$$\sum_{i=0}^n (-1)^i a_{n-i} \int_0^T \phi^{(i)}(t) y(t) dt = \sum_{i=0}^{n-1} (-1)^i b_{n-i} \int_0^T \phi^{(i)}(t) u(t) dt \quad (2.1.2)$$

Here we assume  $\phi(t)$  is a  $N^{th}$  order modulating function,  $N \geq n$ . Furthermore, if  $\{\phi_i(t)\}$ ,  $i = 1, 2, \dots, 2M + 1$  is a set of linearly independent modulating functions, then a set of algebraic equations result. From these vector algebraic equations we can use standard least squares techniques to estimate the parameters.

Several researchers have already investigated similar topics using a variety of modulating functions such as Hermite polynomials and splines. However, using these



modulating functions has not significantly reduced the computational cost because they lack some kind of fast algorithm. Motivated by this fact we use modulating functions comprised of linear combinations of commensurable sinusoids because the FFT algorithm can be applied to calculate the following integrals efficiently:

$$\int_0^T Z(t)[\sin(m\omega_0 t) \text{ or } \cos(m\omega_0 t)]dt, \quad \omega_0 = \frac{2\pi}{T}$$

especially for large  $M$ . Note that  $\omega_0$  plays the role of a “resolving frequency” in the system identification scheme. The saving in computation time is significant, and the use of the FFT makes the procedure possibly to be an on-line algorithm.

With this advantage of using the FFT fast algorithm, we consider the set of commensurable sinusoids  $\{\cos(m\omega_0 t), \sin(m\omega_0 t)\}$  defined on the time interval  $[0, T]$ ,  $\omega_0 = 2\pi/T$ ,  $m = 0, 1, \dots, M$ . Let  $f(t)$  be the sinusoid vector defined as:

$$f(t) = \text{col}[1, \cos \omega_0 t, \sin \omega_0 t, \dots, \cos M\omega_0 t, \sin M\omega_0 t] \quad (2.1.3)$$

It could be expected that if we form the appropriate linear combinations of these sinusoids subject to the end point conditions then we can get a set of linear independent trigonometric modulating functions.

For constructing the  $N^{\text{th}}$  order modulating functions, using the off-line procedure specified in [LeeF84], we can get  $2M+1-N$  linearly independent modulating functions  $\phi_i(t)$ ,  $i = 1, 2, \dots, 2M+1-N$ , which can be represented as the vector-matrix form:

$$\Phi(t) = C f(t), \quad 0 \leq t \leq T \quad (2.1.4)$$

where  $C$  is a  $(2M+1-N)$  by  $(2M+1)$  matrix constructed to make  $\Phi(t)$  satisfy the end point conditions:

$$\Phi^{(i)}(0) = \Phi^{(i)}(T) = 0, \quad i = 0, 1, \dots, N-1 \quad (2.1.5)$$

The rows of matrix  $C$  are determined by the solution of a Vandermonde type matrix equation. Moreover, the matrix  $C$  has full rank .

Because  $\Phi(t)$  is a vector of the  $N^{th}$  order modulating function, from equations (2.1.3) and (2.1.4), the time derivatives of  $\Phi(t)$  can be easily computed in the form of :

$$\Phi^{(i)}(t) = (-1)^i C D^i f(t), \quad i = 0, 1, 2, \dots \quad (2.1.6)$$

where  $D$  is a matrix defined by the block diagonal structure:

$$D = \omega_0 \begin{pmatrix} 0 & & & & & \\ & 0 & 1 & & & \\ & -1 & 0 & & & \\ & & & \ddots & & \\ & & & & 0 & M \\ & & & & -M & 0 \end{pmatrix} \quad (2.1.7)$$

We assume  $D^0 = I$ , the identity matrix.

For identifying a linear time invariant system (2.1.2), multiplying both sides by  $\Phi(t)$ , and integrating by parts  $n$  times results in the following algebraic vector equation:

$$\sum_{i=0}^n (-1)^i a_{n-i} \int_0^T \Phi^{(i)}(t) y(t) dt = \sum_{i=0}^{n-1} (-1)^i b_{n-1-i} \int_0^T \Phi^{(i)}(t) u(t) dt$$

$$a_0 = 1 \quad (2.1.8)$$

Noting equ.(2.1.6), (2.1.8) can be expressed as :

$$\sum_{i=0}^n a_{n-i} C D^i Y = \sum_{i=0}^{n-1} b_{n-1-i} C D^i U$$

$$a_0 = 1 \quad (2.1.9)$$

$(U, Y)$  are corresponding finite Fourier series coefficient vectors of the input and output signals:

$$\begin{aligned} U &= \int_0^T u(t)f(t)dt \\ Y &= \int_0^T y(t)f(t)dt \end{aligned} \quad (2.1.10)$$

Define a parameter vector  $\theta$  and coefficient matrix  $\Gamma$  as :

$$\begin{aligned} \theta &= \text{col}[-a_1, \dots, -a_n, b_0, \dots, b_{n-1}] \\ \Gamma &= [D^{n-1}Y, \dots, Y, D^{n-1}U, \dots, U] \end{aligned} \quad (2.1.11)$$

Then, equ.(2.1.9) can be written equivalently in a regression form as :

$$C\Gamma\theta = CD^nY \quad (2.1.12)$$

We can use the standard least squares technique to solve equation (2.1.12). The dimension of the parameter vector  $\theta$  for (2.1.12) is  $2n$ . The normal equation is:

$$(C\Gamma)^T(C\Gamma)\theta = -(C\Gamma)^TCD^nY \quad (2.1.13)$$

If we choose  $(M, N)$  such that :

$$2M + 1 - N \geq 2n \quad (2.1.14)$$

then there exists a unique solution for a one-shot least squares estimation if and only if we can find input-output data for which  $C\Gamma$  has full rank. Although the matrix  $C$  has full rank  $2M + 1 - N$ , it does not guarantee that  $C\Gamma$  will have full rank. Thus we have to consider  $C$  and  $\Gamma$  together.

Now there are still some questions which have not been answered. For any general system, can we always find some conditions which involve input signals only and

guarantee that  $C\Gamma$  has full rank? Can we find some good input signal which enable us to use some efficient algorithms to estimate  $\theta$  in a robust way? How can we use equ.(2.1.12) to estimate the order of a system? All these questions are related to the existence and uniqueness of a one-shot estimation. These issues will obviously involve the notions of system identifiability, persistent excitation of the system active modes, appropriate structure of the model, and etc. In the following sections we mainly investigate these related issues.

## 2.2 System Persistent Excitation

If we choose the Fourier based modulating functions (2.1.4), then equ.(2.1.2) becomes (2.1.12) and there exists a unique least squares estimation iff the matrix  $C\Gamma$  has full rank. From a practical point of view, we are interested in some conditions which involve the input  $u(t)$  only.

The idea is quite simple. If  $\Phi(t)$  is an  $N^{th}$  order modulating function, then  $\Phi^{(k)}(t)$  is also an  $(N - k)^{th}$  order modulating function for any  $k$ ,  $N - k \geq n$ . Based on the off-line algorithm[Pear85], for fixed  $(M, N)$ , we form the  $N^{th}$  order modulating functions by computing the  $(2M + 1 - N) \times (2M + 1)$  matrix  $C$  in equ.(2.1.4). For the linear time invariant system(2.1.1), multiplying both sides by  $\Phi^{(k)}(t)$ , and taking intergration-by-parts  $n$  times, the results are the algebraic equations:

$$\sum_{i=0}^n a_{n-i} C D^{i+k} Y = \sum_{i=0}^{n-1} b_{n-1-i} C D^{i+k} U$$

$$a_0 = 1, \quad k = 0, 1, \dots, N - n \quad (2.2.1)$$

where  $D, Y, U$  are defined in the equ.(2.1.7) and (2.1.10).

Define:

$$\begin{aligned} W(m) &= CD^m Y, \\ V(m) &= CD^m U, \end{aligned} \tag{2.2.2}$$

then (2.2.1) can be written as:

$$\begin{aligned} \left( \sum_{i=0}^n a_i q^{-i} \right) W(m) &= \left( \sum_{i=0}^{n-1} b_i q^{-i} \right) V(m-1) \\ m &= n, n+1, \dots, N \end{aligned} \tag{2.2.3}$$

where  $q^{-1}$  is the unit delay operator, i.e.  $q^{-1}W(m) = W(m-1)$ .

In equ.(2.2.3)  $W(m)$  depends on the output signal,  $V(m)$  depends on the input signal. The dimension of both  $W(m)$  and  $V(m)$  is  $2M + 1 - N$ . So instead of using the  $n^{th}$  order modulating functions and getting one set of algebraic equations having high dimension of order  $2M + 1 - n$ , here we use the  $N^{th}$  order modulating functions and obtain a sequence of algebraic equations but having the low dimension of  $2M + 1 - N$ . Furthermore, if we choose  $N = 2M$ , we get a sequence of scalar algebraic equations. The essential information about the system parameters contained in these two algebraic equation sets is the same. The advantage of using (2.2.3) is that it has the sequence structure that makes it easy to get some conditions on good input signals and develop some recursive algorithms for identifying the system parameters and estimating the order of the system in a robust manner.

Realizing that if the data involve some measurement noises, equ.(2.2.3) should be replaced by the linear regression model:

$$W(m) = \psi^T(m)\theta + \epsilon(m) \tag{2.2.4}$$

where:

$$\theta = (a_1, a_2, \dots, a_n, b_0, b_1, \dots, b_{n-1})^T$$

$$\psi(m) = (-W(m-1), -W(m-2), \dots, -W(m-n), V(m-1), \dots, V(m-n))^T \quad (2.2.5)$$

Denote:

$$\begin{aligned} A(q^{-1}) &= \sum_{i=0}^n a_i q^{-i} \\ B(q^{-1}) &= \sum_{i=0}^{n-1} b_i q^{-i} \end{aligned} \quad (2.2.6)$$

Now, the standard model persistent excitation analysis tool can be used for the linear regression model (2.2.4). See [Sode89] for more details regarding the analysis we employ in the following.

The condition that there exists a unique solution to the least squares estimation problem of (2.2.4) will be asymptotically equivalent to the nonsingularity of a covariance matrix:

$$R = E\psi\psi^T > 0 \quad (2.2.7)$$

i.e.,  $R$  must be positive definite. So  $R > 0$  will be relevant to the persistent excitation property of input. Actually,  $R$  can be estimated using the following equation:

$$\hat{R} = \frac{1}{N-n} \sum_{m=n}^N \phi(m)\phi^T(m)$$

Now we consider two different cases,  $\epsilon(m) = 0$ , i.e., the system is free of noise, and  $\epsilon(m) \neq 0$ , i.e., the system is contaminated by a significant measurement noise.

**Case 1.**  $\epsilon(m) = 0$

For  $\epsilon = 0$ , we can make the following analysis similar to [Sode89]. Rewrite:

$$\psi(m) = \begin{pmatrix} -b_1 & \dots & -b_{n-1} & & \\ & \ddots & & \ddots & \\ & & -b_1 & \dots & -b_{n-1} \\ 1 & \dots & a_n & & \\ & \ddots & & \ddots & \\ & & 1 & \dots & a_n \end{pmatrix} \begin{pmatrix} \frac{1}{A(q^{-1})}V(m-1) \\ \vdots \\ \frac{1}{A(q^{-1})}V(m-2n-1) \end{pmatrix}$$

$$\psi(m) = \Xi \tilde{\psi}(m) \tag{2.2.8}$$

where,

$$\tilde{\psi}(m) = \begin{pmatrix} \frac{1}{A(q^{-1})}V(m-1) \\ \vdots \\ \frac{1}{A(q^{-1})}V(m-2n-1) \end{pmatrix} \tag{2.2.9}$$

$\Xi$ , the matrix of system coefficients, is the Sylvester matrix associated with the polynomials  $-B(q^{-1})$  and  $A(q^{-1})$ . So if  $A(q^{-1})$  and  $B(q^{-1})$  are coprime, then  $\Xi$  is nonsingular, and vice versa.

$$R = E\psi(m)\psi^T(m) = \Xi \tilde{R} \Xi^T \tag{2.2.10}$$

and

$$\tilde{R} = E\tilde{\psi}(m)\tilde{\psi}^T(m) \tag{2.2.11}$$

So,  $R$  is positive definite if and only if  $\Xi$  is nonsingular and  $\tilde{R}$  is positive definite.

If the system is unidentifiable, which implies  $A(z)$  and  $B(z)$  are not coprime, then we can not find the input which will guarantee to persistently excite the system. Before going further, we will use the following definition:

Define  $\xi(k) = (V^T(k-1), V^T(k-2), \dots, V^T(k-L))^T$ .  $V(k)$  is said to be persistently exciting(p.e.) of order  $L$  if there exist  $\alpha_1, \alpha_2 > 0$ , such that for all  $l$ , there exist  $m$ , corresponding to which the following equation holds,

$$\alpha_1 I \geq \sum_{k=l}^{l+m} \xi(k)\xi^T(k) \geq \alpha_2 I \quad (2.2.12)$$

It is easy to show that  $\tilde{R} > 0$  if and only if  $V(k)$  is persistently exciting of order  $2n-1$ . Since the  $V(k)$  are composed of frequency coefficients of the input signal  $u(t)$ , it means that input signal should have a wide frequency band.

So for noise free systems,  $R > 0$  if and only if  $A(z)$  and  $B(z)$  are coprime and  $V(k)$  is p.e. of order  $2n-1$ .

**Case 2.**  $\epsilon(m) \neq 0$ :

Assume that the signal and noise are not correlated, i.e.

$$EV(i)\epsilon^T(j) = 0 \quad \forall i, j \quad (2.2.13)$$

Let

$$\begin{aligned} Z(k) &= \frac{B(q^{-1})}{A(q^{-1})}V(k) \\ e(k) &= -\frac{1}{A(q^{-1})}\epsilon(k) \end{aligned} \quad (2.2.14)$$

Then

$$R = E \begin{pmatrix} Z(m-1) \\ \vdots \\ Z(m-n) \\ V(m-1) \\ \vdots \\ V(m-n+1) \end{pmatrix} (Z^T(m-1), \dots, Z^T(m-n), V^T(m-1), \dots, V^T(m-n))$$



$$+E \begin{pmatrix} e(m-1) \\ \vdots \\ e(m-n) \\ 0 \\ \vdots \\ 0 \end{pmatrix} (e^T(m-1), \dots, e^T(m-n), 0, \dots, 0) = \begin{pmatrix} R_Z & R_{ZV} \\ R_{ZV}^T & R_V \end{pmatrix} + \begin{pmatrix} R_e & 0 \\ 0 & 0 \end{pmatrix}$$

It is obvious that the necessary condition for  $R > 0$  is  $R_V > 0$ . If we assume  $R_e > 0$ , using the argument of algebra, it is easy to prove that  $R_V > 0$  is the sufficient condition for  $R > 0$  as well because  $R_Z \geq 0$ .

So assuming  $R_e > 0$ , then  $R > 0$  if and only if  $V(k)$  is persistently exciting of order  $n - 1$ .

The above analysis is very useful for system identification because the condition of persistent excitation of  $V(k)$  only depends on the input signal  $u(k)$ , not involving any output signal  $y(t)$ . For the nonlinear polynomial systems, quite same arguments can be advanced and similar results will be obtained. We omit the analysis here.

## 2.3 A Least Squares Algorithm for System Structure Estimation

In this section, we consider to use the least squares algorithms to identify system parameters and estimate the order of a system. The idea is to minimize the mean square error by adjusting the system parameters and order based on the prediction error modeling as depicted in Fig.2.1(a).

Suppose we choose  $n$  as the order of the system. With reference to equ.(2.2.3), we have:

$$\begin{aligned}
W(m) &= -a_{n1}W(m-1) - a_{n2}W(m-2) - \dots - a_{nn}W(m-n) \\
&\quad + b_{n0}V(m-1) + \dots + b_{n,n-1}V(m-n) + e_n(m) \\
N &\geq m \geq n
\end{aligned} \tag{2.3.1}$$

Define:

$$X(k) = \begin{pmatrix} W(k) \\ V(k) \end{pmatrix} \tag{2.3.2}$$

Then, equ.(2.3.1) becomes:

$$\begin{aligned}
[W(n), \dots, W(N)] &= [\theta_{n,1}, \dots, \theta_{n,n}] \begin{pmatrix} X(n-1) & X(n-2) \dots & X(N-1) \\ X(n-2) & X(n-1) \dots & X(N-2) \\ \vdots & \vdots & \vdots \\ X(0) & X(1) \dots & X(N-n) \end{pmatrix} \\
+ [\epsilon_n(n), \epsilon_n(n+1), \dots, \epsilon_n(N)] &= \theta_n^T \Gamma_n^T + \epsilon_n^T
\end{aligned} \tag{2.3.3}$$

where

$$\begin{aligned}
\theta_{n,j} &= (-a_{n,j}, b_{n,j-1}) \\
\theta_n^T &= [\theta_{n,1}, \theta_{n,n-2}, \dots, \theta_{n,n}] \\
\epsilon_n^T &= [\epsilon_n(n), \epsilon_n(n+1), \dots, \epsilon_n(N)] \\
\Gamma_n^T &= \begin{pmatrix} X(n-1) & \dots & X(N-1) \\ \vdots & \ddots & \vdots \\ X(0) & \dots & X(N-n) \end{pmatrix}
\end{aligned} \tag{2.3.4}$$

The parameter vector  $\theta_n$  is determined by minimizing a weighted least squares criterion:

$$E_n = \sum_{k=n}^N e_n^T(k) e_n(k) \tag{2.3.5}$$

By some algebraic calculation, the LS estimation of  $\theta_n$  can be specified by :

$$\hat{\theta}_n = [\Gamma_n^T \Gamma_n]^{-1} \Gamma_n^T W_n(N) \quad (2.3.6)$$

$$W_n(N) = [W(n), W(n+1), \dots, W(N)]^T \quad (2.3.7)$$

To determine an appropriate order of the model, the parsimony principle will be a very useful rule. It says that given the input and output data, if several dynamic models fit the data well, then the simplest model should be chosen, i.e., the model with the smallest number of independent parameters will be desired. Consider the situation here, we have a sequence of model structures of increasing dimensions. Given observed input and output data  $\{u(t), y(t)\}$ , a better fit will be obtained if we increase the complexity of the model structure, i.e., increasing the order  $n$ . The essential thing is to investigate whether or not the improvement will be significant in some sense .

The problem considered in this context is using  $E_n$  as the criteria. The fact is quite obvious. If the true order of the system is  $n_0$ , then for  $n < n_0$ ,  $E_n$  will decrease significantly for  $n$  increasing. When  $n$  approaches  $n_0$  . the rate of decrease of  $E_n$  will be slow and  $E_n$  will almost remain the same value for  $n > n_0$  . The typical function  $E_n$  of  $n$  looks like Fig.2.1(b).

Assuming a maximal system order is  $N_0$  . we choose  $\hat{n}$  as an estimation of  $n$  based on:

$$\hat{n} = \min\{n \mid D_n < \delta, 1 \leq n \leq N_0\}$$

$$D_n = \sum_{i=1}^{i_0} \frac{E_n - E_{n+i}}{E_1} \quad (2.3.8)$$

where  $i_0$  could be chosen as  $1 \sim 3$ , and  $\delta > 0$  is a preselected threshold.

Also for on-line identification and for decreasing computational burden, the lat-

tice filtering structure could be employed because of the Toeplitz structure of the coefficient matrix in equation (2.3.3). See [Sode89] for more detail.

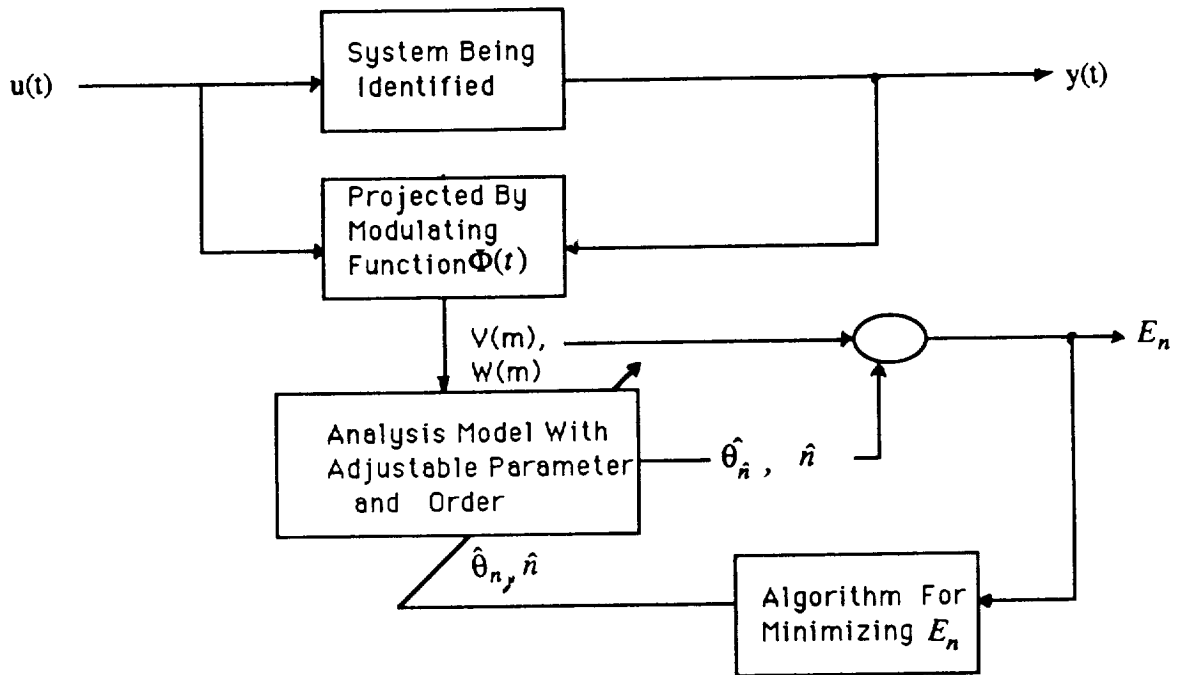


Fig.2.1(a).

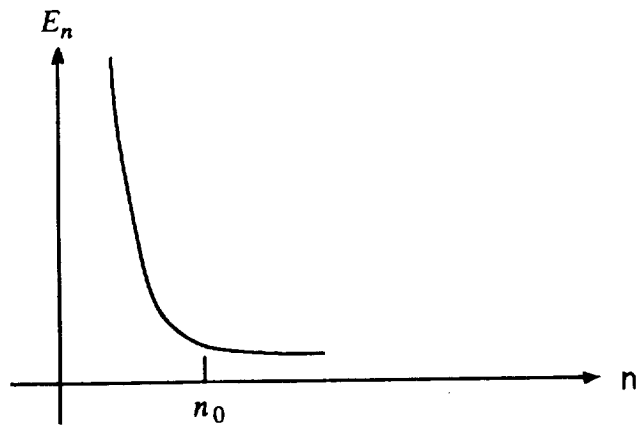


Fig.2.1(b).

## 2.4 Computer Simulation Results

### 2.4.1 Some Computational Considerations

There are several quantities associated with our identification scheme that need to be chosen before setting up the algorithm. These include  $T$ ,  $M$  and  $N$ .  $[0, T]$  is the finite time interval of observed data.  $M$  is associated with maximal frequency components of the input and output signals.  $N$  is the maximum order of the sinusoid modulating functions.

For linear systems, we understand how the choice of  $T$  and  $M$  will affect the identification procedure, thus,  $\omega_0 = 2\pi/T$  essentially plays the role of a resolution frequency. See [Pear85b]. From a heuristic notion,  $\omega_0$  should be small enough to distinguish the characteristic modes of the system. Also, if the resolution frequency  $\omega_0$  is small enough, we can choose  $M$  large without involving much high frequency measurement noise. Then the available data in our discrete autoregressive model (2.3.1) and (2.3.3) will increase and the estimation (2.3.6) will become much more robust. All this means that  $T$  should be large, i.e., we should have enough available input and output data. For linear system identification, the choice of  $T$  and  $M$  can be guided by the frequency domain consideration, i.e., the frequencies retained in the input and output signal  $(U, Y)$  should cover the system bandwidth. The highest frequency coefficient in the modulating function  $M\omega_0$  should be comparable to the system bandwidth  $W_c$ . Also, the Fourier based modulating functions act as a filter. Too large  $M\omega_0$  sometimes is not desirable because it might give undue amplification to the high frequency noise present in the input and output signals.

Assuming that we know the bandwidth of the system to be approximately  $W_c$ , a reasonable selection of  $\omega_0$  and  $M$  could be  $M\omega_0 \sim 1.25W_c$ , or a litter bit larger. For nonlinear systems, the characteristic modes and system bandwidth are not well defined concepts. But there do exist some intuitive physical meanings which relate to above discussion.

The choice of  $N$  is very flexible . Here we let  $N = 2M$  to generate a scalar discrete autoregressive model. That will simplify the calculation of the identification algorithm.

The computational cost before constructing the discrete model for parameter estimation will be the integrals of the input and output data. Using the Fourier based modulating functions not only gives us the direct frequency domain interpretation of the algorithm, but also provides us with an efficient computational tool via the FFT technique.

Let  $z(t)$  denote an observed input or output signal on the time interval  $[0, T]$ . The basic computational costs are the following integrals for  $z(t)$ :

$$\int_0^T z(t)e^{jm\omega_0 t} dt, \quad m = 0, 1, \dots, M$$

First we can sample  $z(t)$  uniformly by sampling interval  $h$  in generating the discrete signal  $z_i = z(ih)$ ,  $h = T/N_f$ ,  $i = 0, 1, \dots, N_f$  . Then the integration can be approximated by the standard parabolic rule :

$$\int_0^T z(t)e^{jm\omega_0 t} dt = \frac{h}{3}[z_0 + z_{N_f} + 4 \sum_{i=1,3,\dots}^{N_f-1} z_i W^{mi} + 2 \sum_{i=2,4,\dots}^{N_f-2} z_i W^{mi} + o(h^4)]$$

$$m = 0, 1, \dots, M$$

where  $W = e^{\frac{j2\pi}{N_f}}$  and  $o(h^4)$  is the order of the error as a function of the sampling interval  $h$ .

Choosing  $N_f$  as a power of 2, neglecting the high order error term, the right-hand side of above equation can be evaluated by using the usual FFT algorithm, yielding the Fourier series coefficients for  $m = 0, 1, 2, \dots, N_f - 1$ :

$$Z = \frac{h}{3} FFT[z_0 + z_{N_f}, 4z_1, 2z_2, \dots, 4z_{N_f-1}]$$

The computational savings of this algorithm for large  $N_f$  are significant, approximately  $\log_2 N_f / N_f$ . However, considering the fact that only  $M$  Fourier coefficients are needed and  $N_f$  should be chosen much larger than  $M$  for good accuracy in the approximation, we need a special FFT-type pruning algorithm. The efficiency of such a devised partial FFT algorithm can be demonstrated to be  $\log_2 M / M$ .

## 2.4.2 Some Numerical Examples

**Example 1.** First we consider a low pass system defined by the Chebyshev filter with bandwidth approximately 0.8[rad/sec.]. The transfer function of the system is:

$$H(s) = \frac{0.0438}{s^4 + 0.6192s^3 + 0.6140s^2 + 0.2038s + 0.0492}$$

The objective is to identify the five unknown system parameters  $\Theta = [0.0438, 0.6192, 0.6140, 0.2038, 0.0492]$  and to estimate the order of the system.

Fig.2.2(a,b) show the input/output data on a 40 sec time interval with output signal contaminated by 10% RMS additive white noise. The Fourier series coefficients for the first  $M$  modes are calculated using the first  $M$  components of the parabolic approximation with  $N_f = 1024$ .



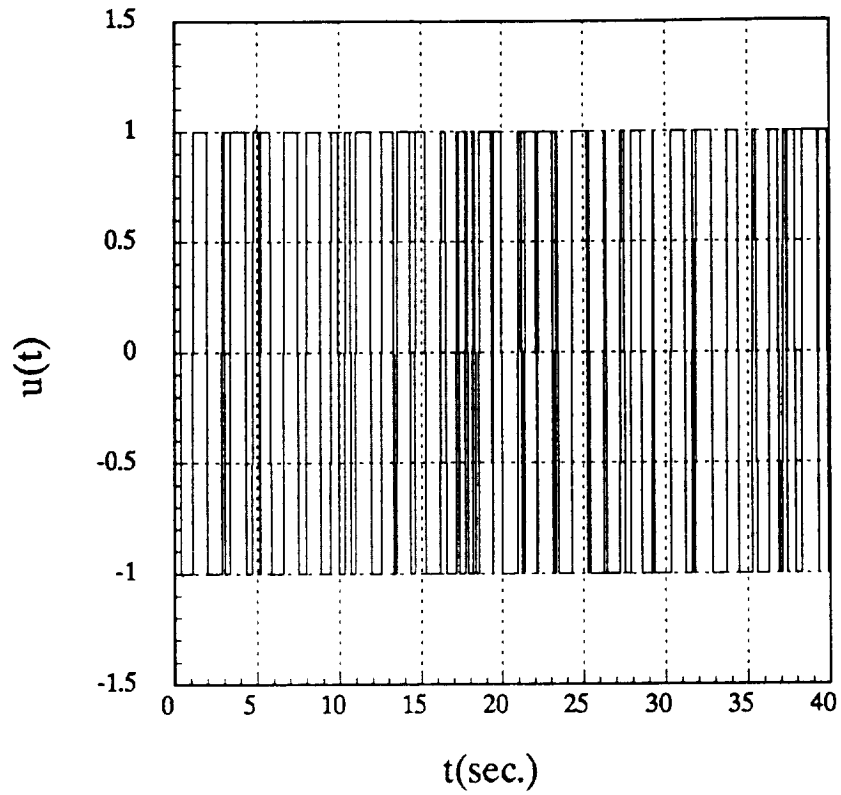


Fig.2.2(a) Input signal  $u(t)$  collected in 40 sec.

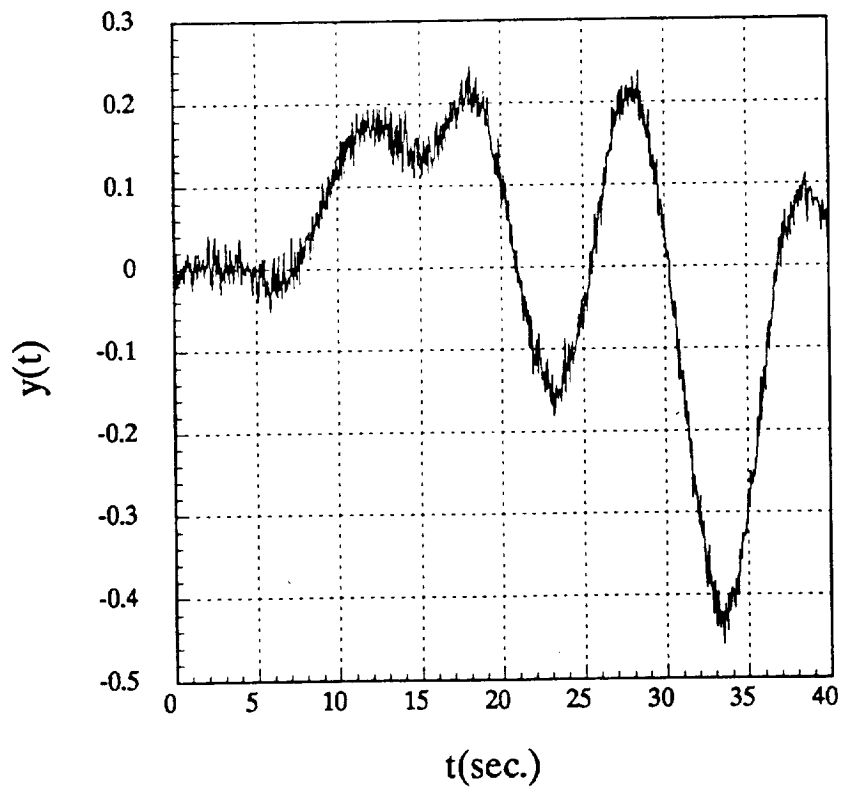


Fig.2.2(b) Output signal  $y(t)$  contaminated by 10% white noise.

For comparing the estimated parameters to the true values and checking the performance of the algorithm, we define the following normalized error criterion:

$$|\Delta\theta| = \left[ \frac{1}{K} \sum_{i=1}^K \left( \frac{\theta_i - \hat{\theta}_i}{\theta_i} \right)^2 \right]^{\frac{1}{2}} 100\%$$

where  $K$  is the number of parameters of the system and  $\theta_i, \hat{\theta}_i$  are the true and estimated parameters. Choosing  $M = 15$  and the threshold  $\delta = 0.1$ , a plot of  $D_n$  versus  $n$ , and plots comparing the frequency response of the original system and estimated system are presented in Fig.2.3 and Fig.2.4. The identified system is shown below:

$$\hat{H}(s) = \frac{0.0451}{s^4 + 0.6122s^3 + 0.6210s^2 + 0.2167s + 0.0501}$$

In the low SNR situations, the algorithm will not work as good as in the previous case. But if we can get more information about input and output signal, i.e., choosing a larger measuring time interval  $T$ , the algorithm will give good results as well. For the Chebyshev system, Table 2.1 shows the performance measured by  $|\Delta\theta|$  with the different white noise percentage involved in the output signal and two different time intervals. From the table we can see that increasing the time interval can improve the accuracy of the estimates.

TABLE 2.1

LEAST SQUARES ESTIMATION OF THE CHEVBYSHEV SYSTEM

White noise percentage	Measuring time interval T	Normalized error $ \Delta\theta $
0	[0, 40]	1.245%
5	[0, 80]	1.835%
10	[0, 40]	3.245%
20	[0, 40]	9.378%
20	[0, 80]	4.113%

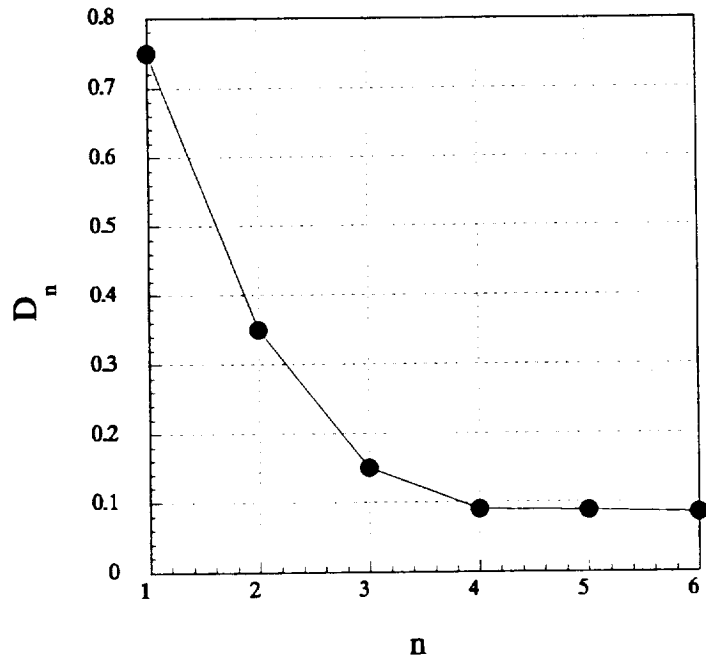


Fig.2.3.  $D_n$  verses n.

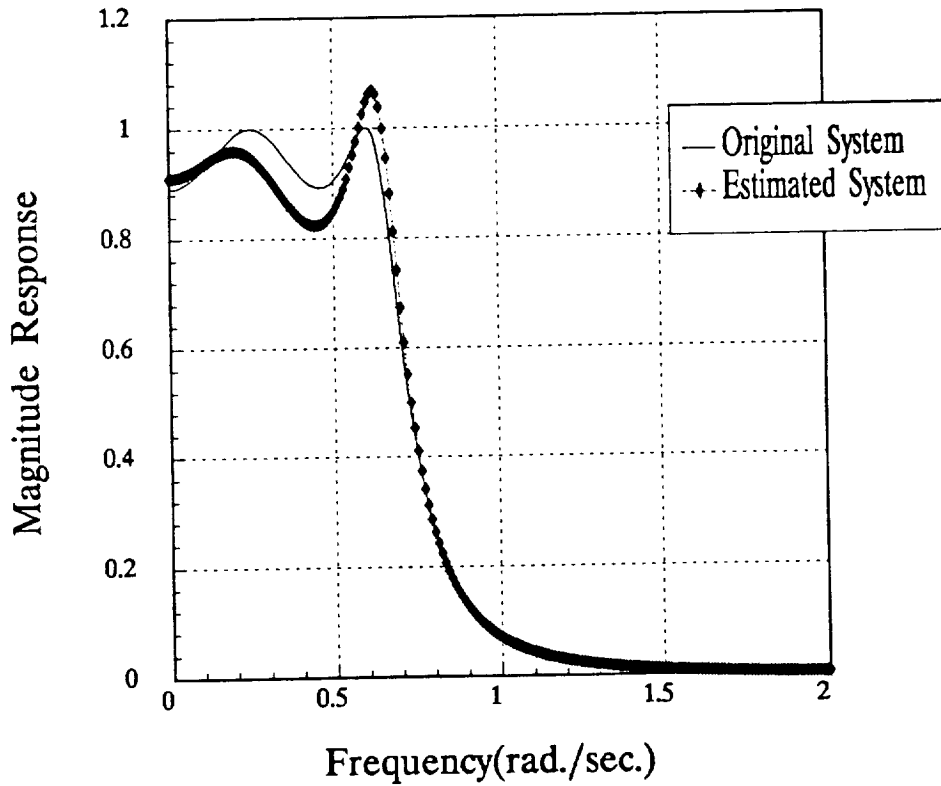


Fig.2.4. Magnitude response of the original system as well as estimated system.

**Example 2.**

Consider a bandpass system with the transfer function:

$$H(s) = \frac{s^5 + 0.994s^4 + 0.650s^3 + 0.210s^2 + 0.0446s + 0.004}{s^7 + 3.238s^6 + 5.0456s^5 + 4.9335s^4 + 3.1943s^3 + 1.3146s^2 + 0.3063s + 0.0304}$$

We use the same binary input signal as used in example one to excite the system, the output signal with 10% additive white noise is shown in Fig.2.4. Choosing  $M = 20$ ,  $N_f = 1024$  and  $N = 2M$ . The quantity  $D_n$  as a function of  $n$  is illustrated in Fig.2.5. In this case, if we select  $\delta = 5\%$ , we can obtain the correct estimate  $\hat{n} = 7$ , the exact order of the system. Fig.2.6 gives the comparison of the magnitude response of the original system and estimated system. The identified system is presented below:

$$\hat{H}(s) = \frac{1.056s^5 + 0.921s^4 + 0.621s^3 + 0.243s^2 + 0.0452s + 0.0043}{s^7 + 3.4501s^6 + 5.0903s^5 + 5.100s^4 + 3.067s^3 + 1.3406s^2 + 0.3281s + 0.031}$$

For the band pass system, Table 2.2 presents the normalized estimation error with various noise to signal percentages and two different time intervals.

TABLE 2.2  
LEAST SQUARES ESTIMATION OF THE BAND PASS SYSTEM

White noise percentage	Measuring time interval T	Normalized error $ \Delta\theta $
0	[0, 40]	2.567%
5	[0, 80]	3.223%
10	[0, 40]	6.297%
20	[0, 40]	19.473%
20	[0, 80]	11.468%

As in example one, increasing the time interval can improve the estimation accuracy and reduce noise effects. Also, based on several simulations, we have found that the best selection of  $\delta$  is around  $0.05 \sim 0.1$  which gives quite good order estimation.

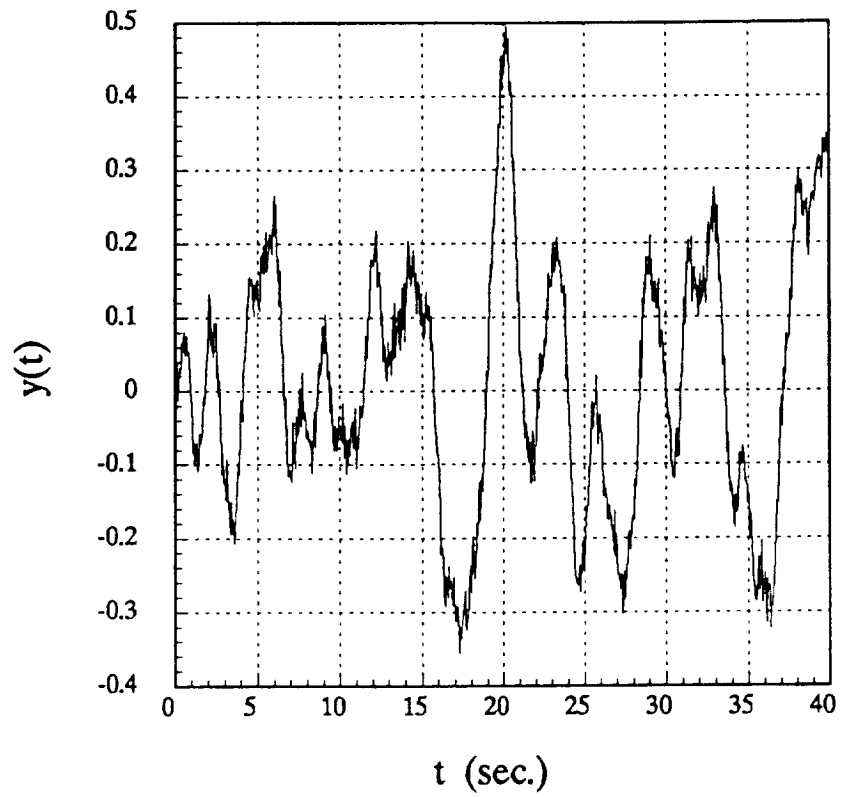


Fig.2.5(a) Output signal  $y(t)$  contaminated by 10% white noise.

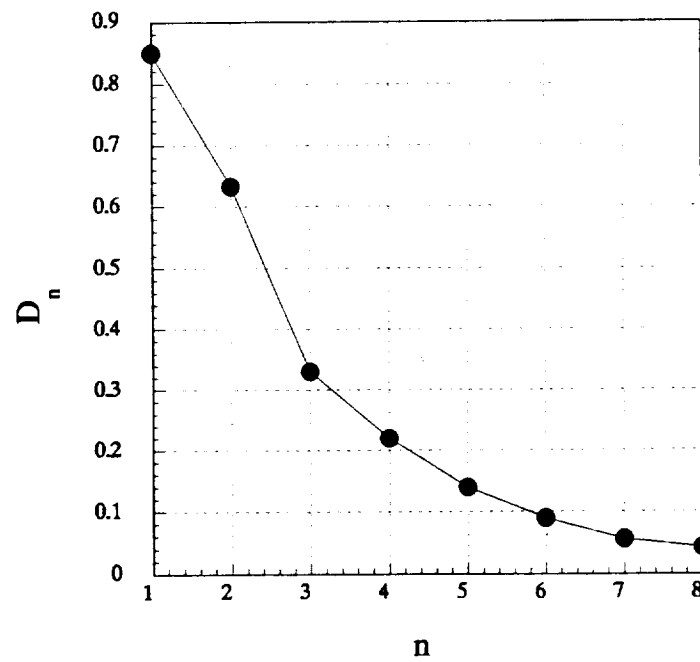


Fig.2.5(b)  $D_n$  verses  $n$ .

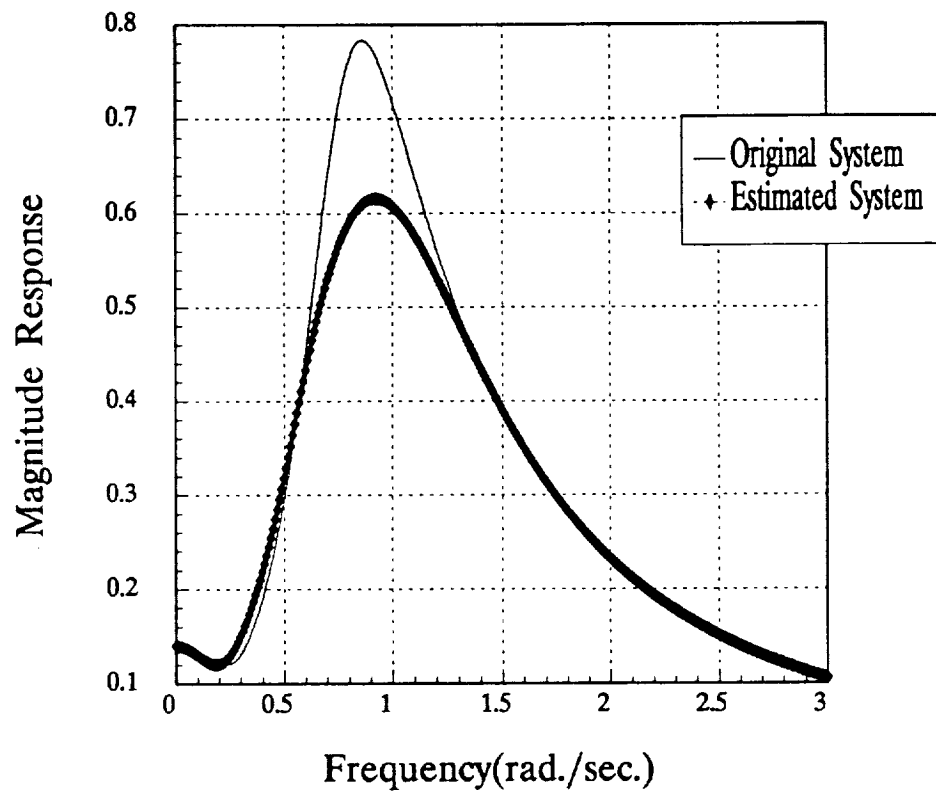


Fig.2.5(c) Magnitude response of original system as well as estimated system.

## Chapter 3

# Frequency Analysis Using Short Time Transient Data

### 3.1 Introduction

In this chapter, we present some algorithms for frequency response estimation by using short time transient input-output data. The development of the complex sinusoidal modulating functions from section 3.2 to section 3.5 follows [PearAE, Pear91], and some of A. E. Pearson's unpublished notes.

In addition to direct sinusoidal steady state measurements, available algorithms for frequency response determination are the direct DFT ratio, and the classical cross correlation method[Astr75, Ljun87, Sode89]. If a system is in the rest status initially, the length of available input and output data is long enough , and the tail part of the system impulse response vanishes dramatically, then the frequency response of the

process can be estimated by the discrete Fourier analysis:

$$G(j\omega_k) = \frac{Y(j\omega_k)}{U(j\omega_k)}, k = 1, 2, \dots, M \quad (3.1.1)$$

where,

$$\begin{aligned} Y(j\frac{2\pi k}{L}) &\approx \Delta t \sum_{i=0}^{L-1} y(i\Delta t) e^{-j\frac{2\pi i k \Delta t}{L}} \\ U(j\frac{2\pi k}{L}) &\approx \Delta t \sum_{i=0}^{L-1} u(i\Delta t) e^{-j\frac{2\pi i k \Delta t}{L}} \\ k &= 1, 2, \dots, M \end{aligned} \quad (3.1.2)$$

$\Delta t$  is a sampling interval,  $L$  is the length of input-output data and has to be large enough to make equation(3.1.2) approximately hold.

If input-output data satisfies the stationarity assumption, we can use the cross correlation method to estimate the transfer function by the following formulations.

$$G(j\omega_k) = \frac{R_{yu}(j\omega_k)}{R_{uu}(j\omega_k)}, k = 1, 2, \dots, M \quad (3.1.3)$$

where,

$$\begin{aligned} \omega_k &= \frac{2\pi k}{L} \\ R_{yu}(j\frac{2\pi k}{L}) &= \sum_{\tau=-L+1}^{L-1} r_{yu}(\tau) e^{-j\frac{2\pi k \tau}{L}} \\ R_{uu}(j\frac{2\pi k}{L}) &= \sum_{\tau=-L+1}^{L-1} r_{uu}(\tau) e^{-j\frac{2\pi k \tau}{L}} \end{aligned} \quad (3.1.4)$$

and

$$\begin{aligned} r_{yu}(\tau) &= \frac{1}{L} \sum_{i=-\min(\tau,0)}^{L-1-\max(\tau,0)} y(\Delta t(i+\tau))u(\Delta ti), \quad \tau = 0, \pm 1, \pm 2, \dots \\ r_{uu}(\tau) &= \frac{1}{L} \sum_{i=0}^{L-1-\max(\tau,0)} u(\Delta t(i+\tau))u(\Delta ti), \quad \tau = 0, 1, 2, \dots \\ r_{uu}(-\tau) &= r_{uu}(\tau) \end{aligned} \quad (3.1.5)$$



Using these approaches to estimate the spectral densities sometimes will give a poor result even if noise is negligible. The problem is that the error in calculating the spectral estimates does not approach zero (in the mean square sense) as the number of data points tends to infinity.

A critical situation is that the model is not at rest initially and the available length of input and output signals is not large. Also the signals involve sensor noise. In this case, the approximations will entail an even larger error.

Here, we deal with the general situation when the system is not at rest initially and only short transient data is available. The data consists of the input and output signals over a set of finite time intervals  $\{[t_i, t_i + T], i = 1, 2, \dots, Q\}$ . The length of each time interval is  $T = 2\pi/\omega_0$  and it is not necessary that these intervals be disjoint.

[Pear91] proposed a method which used a least squares algorithm to estimate the frequency response at selected frequencies by only using short time transient data. The advantage of the approach is that there are no assumptions of statistical stationarity of the data or steady state operation. In order to get good estimates, the input and output data should contain enough energy at the selected frequencies, or a regularized algorithm might be employed. The basis of the technique is the modulating functional approach. We have constructed the complex sinusoidal modulating signals for parametric frequency response estimation. Several formulations of the standard normal regression form for the least squares estimation of frequency response related parameters have been developed.

Here a review of the MFFM (Modulating Function Frequency Method) is presented. An algorithm of applying the MFFM to MIMO systems frequency analysis is also

proposed. Some computer simulation results will demonstrate the performance.

## 3.2 Complex Modulating Signal Construction and the Modulating Property

We consider a stable linear system with a single input  $u(t)$  and single output  $y(t)$ . The system will be expressed in the differential operator format involving some modeling errors and noise:

$$A(p)y(t) = B(p)u(t) + \epsilon(t) \quad (3.2.1)$$

where,

$$\begin{aligned} A(p) &= a_n p^n + a_{n-1} p^{n-1} + \dots + a_1 p^1 + a_0 \\ B(p) &= b_m p^m + b_{m-1} p^{m-1} + \dots + b_1 p^1 + b_0 \end{aligned} \quad (3.2.2)$$

$A(p)$  and  $B(p)$  are polynomials in the differential operator  $p = d/dt$ ,  $m \leq n$ . Modeling errors and measurement noises will constitute the term  $\epsilon(t)$ . Given the input-output data  $[u(t), y(t)]$  over the finite time intervals  $\{ [t_i, t_i + T], i = 1, 2, \dots, Q \}$ , the problem is to estimate the actual frequency response  $G(j\omega) = B(j\omega)/A(j\omega)$  at the frequency knots  $\{ k\omega_0, k = 0, 1, 2, \dots, M \}$ , where  $\omega_0 = 2\pi/T$  is a user selected “resolving” frequency and  $M$  a user chosen positive integer. The time intervals  $[t_i, t_i + T]$  need not be disjoint, but experience suggests that twenty to fifty percentage independence will be necessary in order to avoid singularity of the coefficient matrix for the normal regression equations in the LS estimation. Generally, the degeneracies in the LS estimation will not occur in normal operating records if the time intervals are more than half disjoint.

In chapter 2, we have discussed that  $\phi(t)$  is a modulating function of order  $n$  over

a fixed time interval  $[0, T]$  if  $\phi(t)$  is sufficiently smooth and satisfies the end point conditions:

$$\phi^{(i)}(0) = \phi^{(i)}(T) = 0, \quad i = 0, 1, 2, \dots, n - 1.$$

Clearly, many modulating functions could be constructed which satisfy the condition. Here a specific set of complex sinusoidal modulating signals are built which is conducive to solving the problem at hand.

Define:

$$\begin{aligned} \phi_m(t) &= e^{jm\omega_0 t}(1 - e^{j\omega_0 t})^n, \quad 0 \leq t \leq T_0 = \frac{2\pi}{\omega_0} \\ m &= 0, 1, 2, \dots, M \end{aligned} \quad (3.2.3)$$

Using the binomial expansion  $(a + b)^n = \sum_{k=0}^n C_n^k a^k b^{n-k}$  and changing the index of summation, we can equivalently rewrite (3.2.3) as

$$\phi_m(t) = \sum_{k=0}^n b_k e^{j(m+k)\omega_0 t} \quad (3.2.4)$$

where  $b_k$  relates to the binomial coefficient:

$$b_k = (-1)^k C_n^k$$

Obviously, equations(3.2.3-4) define a set of modulating functions of order  $n$  over a time interval  $[0, T]$ . One of the important motivating factors for building these complex modulating signals is that modulating the input and output data by these signals will entail calculating the Fourier series coefficients at the frequency knots  $k\omega_0, k = 0, 1, 2, \dots, M+n$  and automatically build some algebraic equations involving the estimation of the system transfer function. This is the important modulating property and will be discussed further below. Another factor is that equations(3.2.3-4) comprise linear combinations of commensurable complex sinusoids and the FFT

algorithm can be applied to compute the Fourier series coefficients of input-output data over the time intervals  $[t_i, t_i + T]$ :

$$Z_k(i) = \int_0^T z(t + t_i) e^{-jk\omega_0 t} dt \quad (3.2.5)$$

$$k = 0, 1, 2, \dots, M + n, \quad i = 1, 2, \dots, Q$$

or in terms of sine and cosine transforms:

$$Z_k^c(i) = \int_0^T z(t + t_i) \cos k\omega_0 t dt$$

$$Z_k^s(i) = \int_0^T z(t + t_i) \sin k\omega_0 t dt$$

These Fourier transform series coefficients can be computed accurately and efficiently because of the availability of the parabolic approximation and the FFT technique (see chapter 2).

## Modulation Property

Let  $P(p)$  be a differential operator of order at most  $n$ , i.e., a polynomial in  $p = d/dt$  of degree  $\leq n$ , and  $z(t)$  any sufficiently smooth function defined on  $[0, T]$ . Then the modulation of  $P(p)z(t)$  with  $\phi_m(t)$  over  $[0, T]$  will satisfy

$$\int_0^T \phi_m(t) P(p) z(t) dt = \sum_{k=m}^{m+n} b_{k-m} P(-jk\omega_0) Z_k \quad (3.2.6)$$

where  $Z_k$  is the  $k^{\text{th}}$  harmonic Fourier series coefficient of  $z(t)$ , i.e. ,

$$Z_k = \int_0^T z(t) e^{jk\omega_0 t} dt$$

**Proof:** To prove the modulation property (3.2.6), we only need to verify the special case of  $P(p) = p^i$  for a fixed integer  $i \leq n$ . Due to the superposition property of the polynomial, the result for a general  $n^{\text{th}}$  degree polynomial will follow immediately.

For sufficiently smooth function  $z(t)$  defined on  $[0, T]$ , the left side of (3.2.6) in this special case is

$$\int_0^T \phi_m(t) p^i z(t) dt = (-1)^i \int_0^T z(t) p^i \phi_m(t) dt \quad (3.2.7)$$

Equation(3.2.7) is obtained by integration by parts  $n$  times over  $[0, T]$  taking into account the end point value properties of the modulating functions. The crucial point is that none of the initial point derivatives  $z^{(i)}(0)$  and  $z^{(i)}(T)$  will appear because of the end point conditions. Substituting the expression (3.2.4) of  $\phi_m(t)$  into (3.2.6), using equation (3.2.7) and changing the index of summation, verifies the modulating property for  $P(p) = p^i$ .

In the following, we formulate several least squares algorithms to estimate the system frequency responses at the frequency knots  $k\omega_0$ ,  $k = 0, 1, 2, \dots, M + n$  using the complex sinusoidal modulating functions.

### 3.3 Least Squares Estimation ( The First Formulation)

Rewriting the linear model (3.2.1) in the equation error form, modulating both sides by the modulating signals  $\phi_m(t)$ , we can obtain:

$$\int_0^T \phi_m(t) [A(p)y(t) - B(p)u(t)] dt = \int_0^T \phi_m(t) \epsilon(t) dt \quad (3.3.1)$$

Based upon the modulation property (3.2.6), the preceding equation could be represented by the form:

$$\sum_{k=m}^{m+n} b_{k-m} [A(-jk\omega_0)Y_k - B(-jk\omega_0)U_k] = \sum_{k=m}^{m+n} b_{k-m} E_k \quad (3.3.2)$$

Define the real and imaginary parts of the polynomials  $A(jk\omega_0)$ ,  $B(jk\omega_0)$ ,  $Y_k$ ,  $U_k$  by :

$$\begin{aligned} A(jk\omega_0) &= \alpha_k + j\beta_k \\ B(jk\omega_0) &= \gamma_k + j\delta_k \end{aligned} \quad (3.3.3)$$

Also assume:

$$\begin{aligned} Y_k &= Y_k^c + jY_k^s \\ U_k &= U_k^c + jU_k^s \end{aligned} \quad (3.3.4)$$

Rewriting equation(3.3.2) in terms of the real and imaginary parts, we can obtain the following equations:

$$\begin{aligned} \sum_{k=m}^{m+n} b_{k-m} [\alpha_k Y_k^c + \beta_k Y_k^s - \gamma_k U_k^c - \delta_k U_k^s] &= \varepsilon_m^R \\ \sum_{k=m}^{m+n} b_{k-m} [-\alpha_k Y_k^s + \beta_k Y_k^c + \gamma_k U_k^c - \delta_k U_k^s] &= \varepsilon_m^I \end{aligned} \quad (3.3.5)$$

where,

$$\begin{aligned} \varepsilon_m^R &= \Re\left(\sum_{k=m}^{m+n} b_{k-m} E_k\right) \\ \varepsilon_m^I &= \Im\left(\sum_{k=m}^{m+n} b_{k-m} E_k\right) \end{aligned}$$

Computing the Fourier series coefficients  $Y_k(i)$  and  $U_k(i)$  corresponding to each time interval  $[t_i, t_i + T]$ ,  $i = 1, 2, \dots, Q$ ,  $k = 0, 1, \dots, M$  by the equations:

$$\begin{aligned} Y_k(i) &= \int_0^T y(t + t_i) e^{jk\omega_0 t} dt \\ Y_k(i) &= Y_k^c(i) + jY_k^s(i) \\ U_k(i) &= \int_0^T u(t + t_i) e^{jk\omega_0 t} dt \\ U_k(i) &= U_k^c(i) + jU_k^s(i) \end{aligned} \quad (3.3.6)$$

and define a  $2 \times 4$  data matrix  $\psi_k(i)$  in terms of these harmonic series by :

$$\psi_k(i) = \begin{bmatrix} Y_k^c(i) & Y_k^s(i) & -U_k^c(i) & -U_k^s(i) \\ -Y_k^s(i) & Y_k^c(i) & U_k^s(i) & -U_k^c(i) \end{bmatrix} \quad (3.3.7)$$

Define a  $4 \times 1$  parameter vector by :

$$\theta_k = \begin{bmatrix} \alpha_k \\ \beta_k \\ \gamma_k \\ \delta_k \end{bmatrix} \quad (3.3.8)$$

Then equation (3.3.5) could be represented by the  $2 \times 1$  vector equation form as follows:

$$\sum_{k=m}^{m+n} b_{k-m} \psi_k(i) \theta_k = \begin{bmatrix} \varepsilon_m^R(i) \\ \varepsilon_m^I(i) \end{bmatrix} = \varepsilon_m(i) \\ m = 0, 1, 2, \dots, M, \quad i = 1, 2, \dots, Q \quad (3.3.9)$$

For each fixed  $i$ , we can collect all the  $2 \times 1$  vector equations for  $m = 0, 1, 2, \dots, M$  and form the following regression equations for serving the least squares estimation:

$$\Phi(i)\theta - \xi(i) = \varepsilon(i) \\ i = 1, 2, \dots, Q \quad (3.3.10)$$

where,

$$\Phi(i) = \begin{bmatrix} U_0^c(i) & b_1\psi_1(i) & b_2\psi_2(i) & \dots & b_n\psi_n(i) & 0 & \dots & 0 \\ 0 & b_0\psi_1(i) & b_1\psi_2(i) & \dots & b_{n-1}\psi_{n+1}(i) & b_n\psi_{n+1}(i) & \dots & 0 \\ \vdots & \vdots & \vdots & & \vdots & \vdots & & \vdots \\ 0 & 0 & 0 & \dots & b_0\psi_M(i) & b_1\psi_{M+1}(i) & \dots & b_n\psi_{n+M}(i) \end{bmatrix} \quad (3.3.11)$$

$$\theta = \begin{bmatrix} -\gamma_0 \\ \theta_1 \\ \theta_2 \\ \vdots \\ \theta_{n+M} \end{bmatrix}, \quad \xi(i) = \begin{bmatrix} \eta(i) \\ 0 \\ \vdots \\ 0 \end{bmatrix}$$

and

$$\eta(i) = Y_0^c(i)$$

Here we assume that  $\alpha_0 = 1$  without loss of generality.

Collecting these equations for  $i = 1, 2, \dots, Q$ , forming the standard regression equation form and choosing the  $\theta$  to minimize the least squares criterion:

$$\min_{\theta} \epsilon = \min_{\theta} (\Phi\theta - \xi)^T (\Phi\theta - \xi) \quad (3.3.12)$$

where,

$$\Phi = \begin{bmatrix} \Phi(1) \\ \Phi(2) \\ \vdots \\ \Phi(M) \end{bmatrix} \quad \text{and} \quad \xi = \begin{bmatrix} \xi(1) \\ \xi(2) \\ \vdots \\ \xi(M) \end{bmatrix}$$

There are no disjoint requirements to these finite time intervals  $\{[t_i, t_i + T], i = 1, 2, \dots, Q\}$ . Of course a certain degree of independence in the input and output data over these time intervals is needed. The input and output data must contain a sufficient energy at these frequency knots in order to avoid the degeneracy of solving the least squares estimation (3.3.12), i.e., the matrix  $\Phi$  being composed of the harmonic Fourier series coefficients of the input and output data should have full rank.

Also, one kind of “bootstrapping” least squares algorithm can be developed by



stages according to the values assigned to  $m$  in order to avoid degeneracies of the LS algorithm due to the large number of unknown parameters.

**Initial Stage ( $m = 0$ ):**

$$\begin{aligned} \tilde{Y}_0(i) &= \sum_{k=0}^n b_k \psi_k(i) \theta_k & (3.3.13) \\ i &= 1, 2, 3, \dots, N \end{aligned}$$

where the data-related quantities are defined by the following vector-matrix equations:

$$\tilde{Y}_0(i) = \begin{pmatrix} -Y_0^c(i) \\ 0 \end{pmatrix} \quad \psi_0(i) = \begin{pmatrix} -U_0^c(i) \\ 0 \end{pmatrix} \quad (3.3.14)$$

The definitions of  $\psi_k(i)$  and  $\theta_k$  for  $k \geq 1$  are exactly the same as (3.3.7) and (3.3.8).

$\theta_0 = \gamma_0$ .

**Stage  $m$  ( $m = 1, 2, \dots, M$ ):**

Again a set of 2 dimensional vector equations are derived using (3.3.9) for the case of  $m \geq 1$ :

$$\hat{Y}_m(i) = b_n \psi_{n+m}(i) \theta_{n+m} + \epsilon_m(i) \quad (3.3.15)$$

$$i = 1, 2, \dots, Q, \quad m = 1, 2, \dots, M$$

where  $\hat{Y}_m(i)$  is defined in terms of the parameters and data of the preceding stages by:

$$\hat{Y}_m(i) = - \sum_{k=m}^{n+m-1} b_{k-m} \psi_k(i) \theta_k \quad (3.3.16)$$

The residuals for all stages are given by:

$$\epsilon_m(i) = \sum_{k=m}^{n+m} b_{k-m} \begin{pmatrix} E_k^c(i) \\ E_k^s(i) \end{pmatrix} \quad (3.3.17)$$

From the equations(3.3.3) and (3.3.8), it is easy to see that the transfer funtion  $G(jk\omega_0) = B(jk\omega_0)/A(jk\omega_0)$  relating to the parameter vector  $\theta_k$  is given by:

$$\Re(G(jk\omega_0)) = \frac{\alpha_k\gamma_k - \beta_k\delta_k}{\alpha_k^2 + \beta_k^2} \quad (3.3.18)$$

$$\Im(G(jk\omega_0)) = \frac{\alpha_k\delta_k - \beta_k\gamma_k}{\alpha_k^2 + \beta_k^2} \quad (3.3.19)$$

or equivalently by the magnitude-phase relation:

$$|G(jk\omega_0)|^2 = \frac{\gamma_k^2 + \delta_k^2}{\alpha_k^2 + \beta_k^2} \quad (3.3.20)$$

$$\angle G(jk\omega_0) = \tan^{-1} \frac{\delta_k}{\gamma_k} - \tan^{-1} \frac{\beta_k}{\alpha_k} \quad (3.3.21)$$

Investigating this least squares estimation procedure leads to the following remarks:

1. The frequency knots  $k\omega_0, k = 0, 1, 2, \dots, M + n$  scatter in the frequency range from 0 to  $(M + n)\omega_0$ . Hence, if we know the bandwidth  $W_c$  of the system, then a reasonable selection of  $\omega_0$  and  $M$  should satisfy  $M\omega_0 \sim 1.25W_c$ , or a little bit larger if it is desired that the estimation of the system frequency response cover a range 25% larger than the bandwidth  $W_c$ .
2. For bandpass or high pass systems,  $\phi_m(t)$  could be modified by:

$$\phi_m(t) = e^{j(m+m_0)\omega_0 t} (1 - e^{j\omega_0 t})^n$$

$$m = 0, 1, 2, \dots, M$$

In this case, the transfer function estimate covers the frequency range from  $m_0\omega_0$  to  $(M + n + m_0)\omega_0$ . We are only interested in the frequency band above the frequency  $m_0\omega_0$ . The available information about the system cutoff frequency and bandwidth could be utilized to determine the choice of  $m_0$  and  $M$ .

3. The total number of unknown parameters, i.e., the size of  $\theta$  is  $4(M + n)$ . Since the dimension of each  $\Phi$  is  $2Q(M + 1) \times 4(n + M)$ , the total number of time intervals  $[t_i, t_i + T]$  should satisfy  $Q \geq \frac{2(M+n)}{M+1}$ . For good accuracy, the number of equations should be double the total unknown parameters, i.e.,  $Q \geq \frac{4(M+n)}{(M+1)}$ .
4. If the resolving frequency  $\omega_0$  has to be small for some special practical applications,  $M$  should be large in order to cover the system bandwidth. In this case, the total number of unknown parameters  $\theta_k$  is incremented. The matrix  $\Phi^T \Phi$  tends to be singular and the least squares solution for the eqn.(3.3.12) will be degenerate. There are two methods to solve this problem. One is to try obtaining extra available data, i.e., increasing the total number of time intervals. Sometimes this is expensive. Another one is to exploit a numerical advantage of solving eqn.(3.3.12) which is based upon the fact that the equations(3.3.9) and (3.3.10) are partially decoupled with respect to the index  $m$ . Parameter  $\theta_k$  only depends on the  $\theta_i$  for  $i < k$ . Therefore, one kind of “bootstrapping” of the least squares algorithm could be utilized to divide estimating the parameter  $\theta$  into  $M + 1$  stages.  $(\theta_1, \theta_2, \dots, \theta_n)$  can be identified at the first stage, corresponding to  $m = 0$ , which requires  $Q$  satisfying  $N \geq 2n$  for  $4n$  unknown parameters. For good estimation,  $Q$  should be larger than  $4n$ . For each succeeding stage ( $m = 1, 2, \dots, M$ ), only  $\theta_{n+m}$  (4 unknowns) needs to be estimated, which only requires  $Q \geq 2$ . By this way, the number of unknowns at each stage is kept to the lowest level and most likely the degeneracy problem will be prevented during the least squares procedure.
5. Noting the fact that  $|\theta_k|$  goes as  $k^n$  as  $k$  increases for  $k = 1, 2, \dots, M + n$ , a nonlinear transformation might be necessary to scale  $\theta$  appropriately for good numerical accuracy, or we can normalize all parameters by  $\rho W_c^n$ , where  $\rho$  is

a scalar constant and  $W_c$  is the system bandwidth.

We have developed a scheme to estimate the original transfer function  $G(jk\omega_0)$  at frequency knots  $k\omega_0, k = 1, 2, \dots, M + n$ . The system does not have to be in the rest status initially and the input and output data could be time limited and transient. The data matrix  $\phi_k(i)$  in equation(3.3.7) comprising the  $k^{th}$  harmonic frequency series in the  $i^{th}$  time interval,  $k = 1, 2, \dots, M + n, i = 1, 2, \dots, Q$ , is mutually orthogonal. This reveals the maximum utilization of information contained in the input and output data for our least squares procedure. Clearly it is a direct result of the Fourier nature of the underlying formulation.

One numerical problem in our scheme might arise due to the highly nonlinear relations in the equations(3.3.18-21) which involves the difference between the estimated parameters whose values may be large for large frequencies. In the next section, we will develop other schemes, which have different structure from this one and will alleviate the potential numerical error source mentioned above.

### 3.4 Least Squares Estimation ( The Second Formulation)

For the original model described by equation(3.2.1), multiplying both sides by  $A(-p)$ , we can see that the input and output data also obey the following relation:

$$A(-p)A(p)y(t) = A(-p)B(p)u(t) + A(-p)e(t) \quad (3.4.1)$$

Utilizing the complex sinusoidal modulating signals of order  $2n$  defined by:

$$\begin{aligned}\phi_m(t) &= e^{jm\omega_0 t}(1 - e^{j\omega_0 t})^{2n} \\ &= \sum_{k=m}^{m+2n} C_{k-m}^{2n} (-1)^{k-m} e^{jk\omega_0 t}\end{aligned}\quad (3.4.2)$$

to project the model into the algebraic equations, we get the result:

$$\sum_{k=m}^{m+2n} \bar{b}_{k-m} A(jk\omega_0) [A(-jk\omega_0)Y_k - B(-jk\omega_0)U_k] = \varepsilon_m \quad (3.4.3)$$

where,

$$\begin{aligned}\bar{b}_k &= (-1)^k C_{2n}^k \\ \varepsilon_m &= \sum_{k=m}^{m+2n} \bar{b}_{k-m} A(jk\omega_0) E_k\end{aligned}$$

Define:

$$\begin{aligned}A(jk\omega_0)A(-jk\omega_0) &= a_k \\ A(jk\omega_0)B(-jk\omega_0) &= \alpha_k + j\beta_k\end{aligned}\quad (3.4.4)$$

$(a_k, \alpha_k, \beta_k)$  are real numbers.

Rewriting (3.4.3) in terms of real and imaginary parts of the equations, we obtain:

$$\begin{aligned}\sum_{k=m}^{m+2n} \bar{b}_{k-m} [a_m Y_k^c - \alpha_k U_k^c - \beta_k U_k^s] &= \bar{\varepsilon}_m^R \\ \sum_{k=m}^{m+2n} \bar{b}_{k-m} [a_k Y_k^s - \alpha_k U_k^s - \beta_k U_k^c] &= \bar{\varepsilon}_m^I\end{aligned}\quad (3.4.5)$$

Define a  $2 \times 3$  data matrix  $\bar{\Psi}_k(i)$  involving the  $k^{\text{th}}$  harmonic series of input output data in the  $i^{\text{th}}$  time interval  $[t_i, t_i + T]$  by :

$$\bar{\Psi}_k(i) = \begin{bmatrix} Y_k^c(i) & -U_k^c(i) & U_k^s(i) \\ Y_k^s(i) & -U_k^s(i) & -U_k^c(i) \end{bmatrix} \quad (3.4.6)$$

Define a  $3 \times 1$  parameter vector by:

$$\bar{\theta}_k = \begin{bmatrix} a_k \\ \alpha_k \\ \beta_k \end{bmatrix} \quad (3.4.7)$$

Then we combine the real and imaginary parts of equation(3.4.5) into a  $2 \times 1$  vector equation as follows:

$$\sum_{k=m}^{m+2n} \bar{b}_{k-m} \bar{\Psi}_k \bar{\theta}_k = \bar{\varepsilon}_m(i) \\ m = 0, 1, \dots, M, \quad i = 1, 2, \dots, Q \quad (3.4.8)$$

Collecting all these equation and rewriting it into a standard regression format, which is analogous to eqn.(3.3.12), the least squares algorithm can be employed to estimate the parameters  $(\bar{\theta}_1, \bar{\theta}_2, \dots, \bar{\theta}_{M+2n})$ . In this case, the relation between the estimates of the parameters and the real and imaginary parts of the original transfer function are:

$$\Re(G(jk\omega_0)) = \frac{\alpha_k}{a_k} \\ \Im(G(jk\omega_0)) = -\frac{\beta_k}{a_k} \quad (3.4.9)$$

or equivalently by the magnitude and phase relations:

$$|G(jk\omega_0)| = \frac{\sqrt{\alpha_k^2 + \beta_k^2}}{a_k} \\ \angle G(jk\omega_0) = -\tan^{-1} \frac{\beta_k}{\alpha_k} \quad (3.4.10)$$

We make the following remarks by considering the implementation of this scheme:

1. The estimates of the frequency response of the original system cover the frequency band from 0 to  $(M + 2n)\omega_0$ . An appropriate choice of the parameter

$M$  and  $\omega_0$  should satisfy the relation:

$$(M + 2n)\omega_0 \sim 1.25W_c$$

2. The total number of unknown parameters in this case is  $3(M + 2n)$ . Hence, the number of time intervals  $Q$  should satisfy  $2Q(M + 1) \geq 3(M + 2n)$ . However, in order to avoid the degeneracy of the least squares estimation, the number of equations should be double the unknown parameters, i.e.,  $Q \geq \frac{3(M+2n)}{M+1}$ .
3. Employing the partially decoupled nature of equation (3.4.8) might be necessary to solve the least squares solution if a large number of unknown parameters need to be estimated. In this case, the number  $6n$  of unknown parameters  $(\bar{\theta}_1, \bar{\theta}_2, \dots, \bar{\theta}_{2n})$  are involved in the first stage corresponding to  $m = 0$ . The choice of  $Q$  should satisfy  $Q \geq 6n$ . For each succeeding stage ( $m = 1, 2, \dots, M$ ), only 3 unknowns need to be estimated assuming the use of the preceding estimate of the parameters. Comparing to the first formulation presented before, the total number of unknowns at the first stage is  $6n$ , verses  $4n$  unknowns. But only 3 unknowns are required to be estimated in the succeeding stages, verses 4 unknowns for the first formulation.

One point we should mention is that the equations(3.4.9-10) avoids differencing the large quantities associated with the estimated parameters to calculate the frequency responses at high frequencies. This is a numerical advantage of the second formulation.

### 3.5 Least Squares Estimation ( The Third Formulation )

We can develop a dual formulation to the previous one. Multiply the original model (3.2.1) by  $B(-p)$  shows that input output data also should satisfy the relation:

$$B(-p)A(p)y(t) = B(-p)B(p)u(t) + B(-p)e(t) \quad (3.5.1)$$

Again using the complex sinusoidal modulating functions of order  $2n$  to project model (3.5.1) into the algebraic equation:

$$\sum_{k=m}^{m+2n} \bar{b}_{k,m} B(jk\omega_0) [A(-jk\omega_0)Y_k - B(-jk\omega_0)U_k] = \varepsilon_m \quad (3.5.2)$$

$$m = 1, 2, 3, \dots, M$$

where,

$$\varepsilon_m = \sum_{k=m}^{m+2n} \bar{b}_{k-m} B(jk\omega_0) E_k$$

Similarly, define:

$$B(jk\omega_0)B(-jk\omega_0) = b_k \geq 0$$

$$A(jk\omega_0)B(-jk\omega_0) = \alpha_k + j\beta_k$$

$$\theta_k = \begin{bmatrix} b_k \\ \alpha_k \\ -\beta_k \end{bmatrix} \quad (3.5.3)$$

Define a  $2 \times 3$  data matrix  $\tilde{\Psi}_k(i)$  for the  $i^{th}$  time interval by:

$$\tilde{\Psi}_k(i) = \begin{bmatrix} U_k^c(i) & -Y_k^c(i) & Y_k^s(i) \\ U_k^s(i) & -Y_k^s(i) & -Y_k^c(i) \end{bmatrix} \quad (3.5.4)$$



Then equation (3.5.2) can be rewritten into a  $2 \times 1$  vector equation which is analogous to eqn.(3.4.8):

$$\sum_{k=m}^{m+2n} \bar{b}_{k-m} \hat{\Psi}_k(i) \theta_k = \varepsilon_m(i)$$

$$m = 0, 1, \dots, M, \quad i = 1, 2, \dots, Q \quad (3.5.5)$$

A standard regression from could be constructed for setting up the least squares estimation for the unknown parameters  $(\theta_1, \theta_2, \dots, \theta_{M+2n})$ .

Calculating the frequency responses in terms of the estimated parameters reveals the following relation for the real and imaginary parts:

$$\Re(G(jk\omega_0)) = \frac{\alpha_k b_k}{\alpha_k^2 + \beta_k^2}$$

$$\Im(G(jk\omega_0)) = -\frac{\beta_k b_k}{\alpha_k^2 + \beta_k^2} \quad (3.5.6)$$

or, equivalently for the magnitude and phase relation:

$$|G(jk\omega_0)| = \frac{b_k}{\sqrt{\alpha_k^2 + \beta_k^2}}$$

$$\angle G(jk\omega_0) = -\tan^{-1} \frac{\beta_k}{\alpha_k} \quad (3.5.7)$$

The data matrices defined in equations (3.4.6,3.5.4) have the same structures by interchanging the direction of input and output flow. This reveals the dual property between these two formulations.

## 3.6 Computer Simulation Results

Here some typical numerical results are presented to demonstrate the performance of the algorithm. We employ the first formulation for the following two simulations.

**Example 1.** First we consider a low pass system with a bandwidth approximately 12[rad/sec.]. The transfer function of the system is

$$H_1(s) = \frac{1.7s^2 + 1736.8}{s^3 + 19.1s^2 + 257.48s + 1700.0}$$

A random binary process was utilized as an input signal to excite the system because it contains sufficient energy in a broad frequency band. Data was collected in 8 seconds. The plots of input signal and contaminated output signal with SNR=15(dB) are shown in Fig.3.1(a) and Fig.3.1(b). The whole data set was divided into the six time intervals  $[t_i, t_i + 3]$  for  $i = 0, 1, \dots, 5$ . The sampling frequency  $f_s$  was 200(Hz). A 1024-FFT was utilized in calculating the Fourier series coefficients on each time interval. We estimated the frequency response  $H_1(j\omega)$  at frequency knots  $\{k\omega_0, k = 0, 1, 2, \dots, 18\}$ ,  $\omega_0 = 2.09$ . The frequency knots cover the passband, transition band and a part of the stop band of the system.

Fig.3.2(a-b) shows the results of the frequency response estimation for a noise-free case, along with the results obtained by applying the direct ratio of the Fourier transforms and the standard cross correlation approaches to the same data.

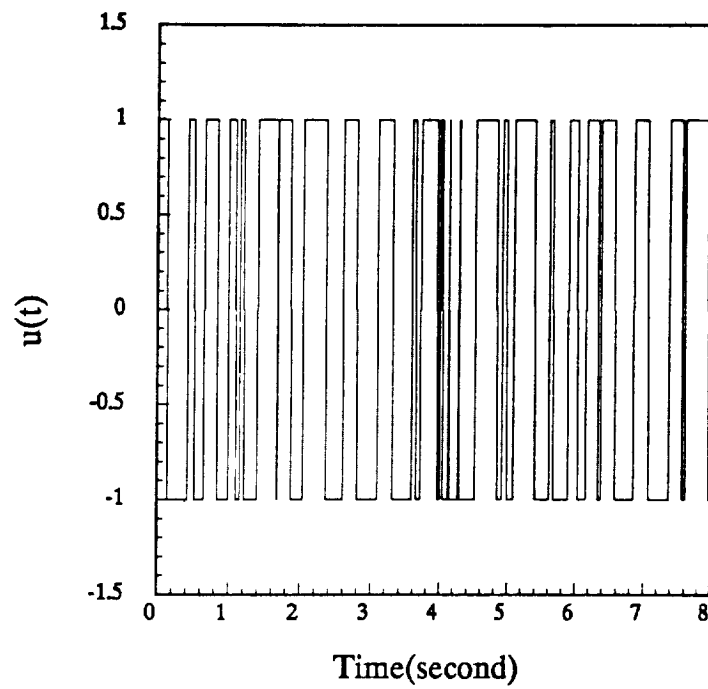


Fig.3.1(a) A random binary input signal collected in 8 seconds.

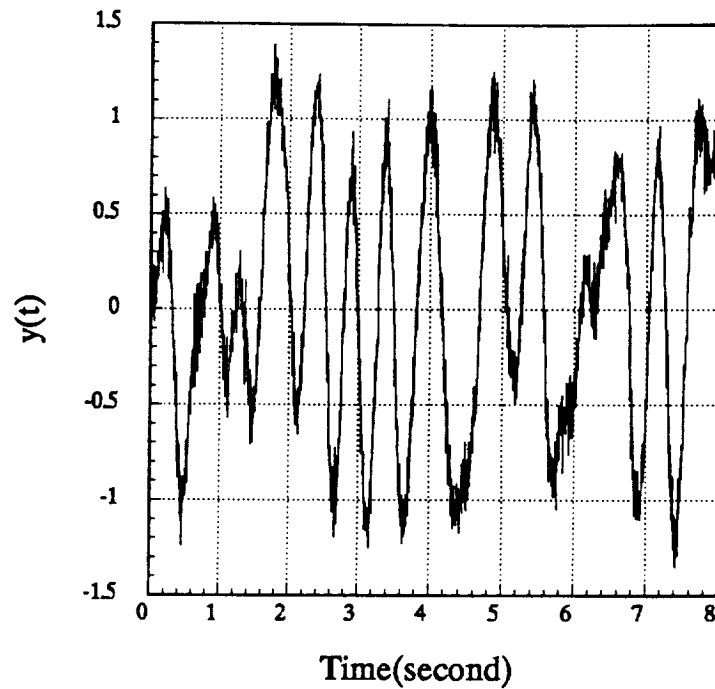


Fig.3.1(b) Output signal contaminated by white gaussian noise with SNR=15(dB) and collected in 8 seconds.

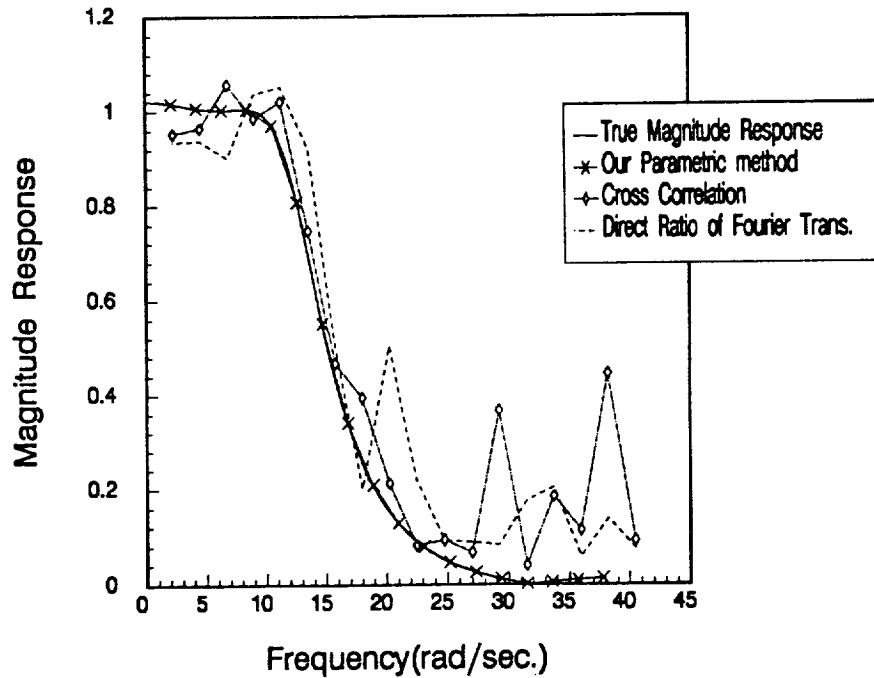


Fig.3.2(a) Estimated magnitude response at the frequency knots  $\{k\omega_0, k = 0, 1, 2, \dots, 18\}$  in the noise-free case.

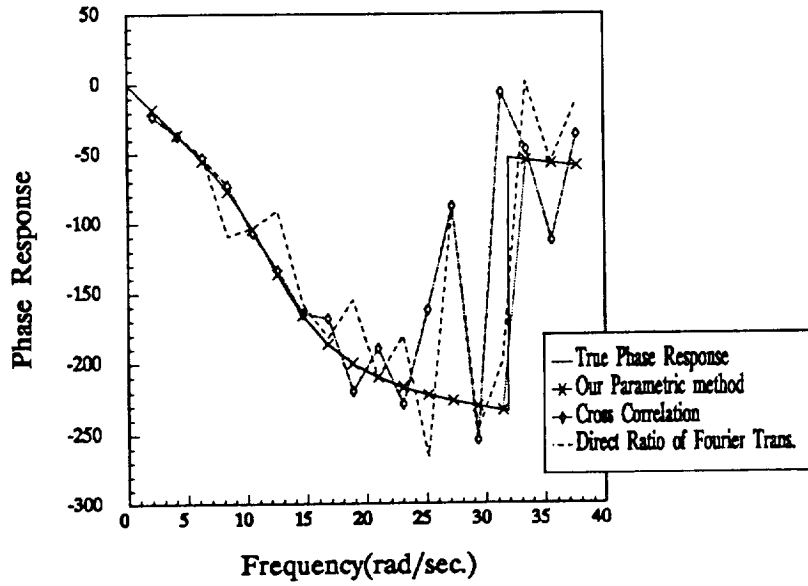


Fig.3.2(b) Estimated phase response at selected frequency knots in the noise-free case.

Also the simulation results are shown in Fig.3.3(a) and Fig.3.3(b) for the output signal contaminated by white gaussian noise with SNR=15(dB).

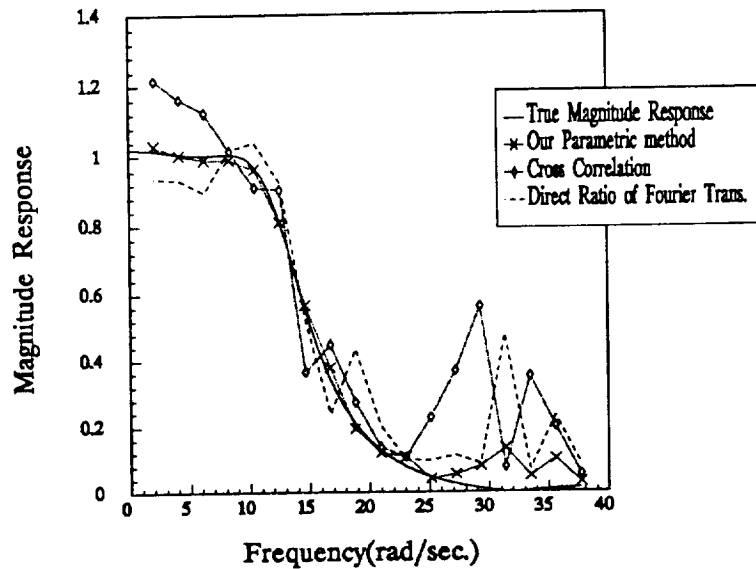


Fig.3.3(a) Estimated magnitude response at selected frequency knots for SNR=15(dB) case.

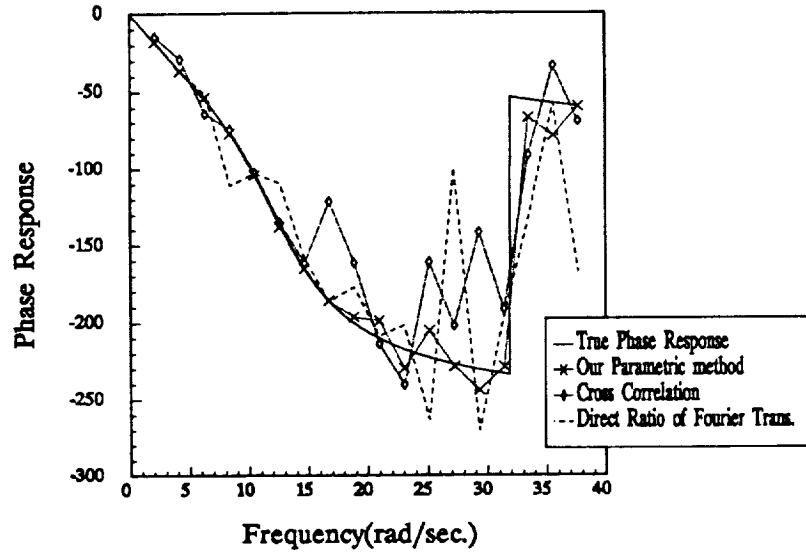


Fig.3.3(b) Estimated phase response at selected frequency knots for SNR=15(dB) case.

From the graphs we can see that noise will not affect the algorithm at low frequencies. But it does increase the estimation bias for high frequencies. The cross correlation and direct ratio methods produce large oscillations.

**Example 2.** The second example we considered was a high pass system with the transfer function:

$$H_2(s) = \frac{s^3 + 22.02s}{s^3 + 22.24s^2 + 247.44s + 1943.23}$$

The same random binary signal was used to excite the system. Again the data was collected in eight seconds. Fig.3.4 shows the output signal contaminated by white gaussian noise with SNR=20(dB). As in example 1, the whole eight second data was divided into the six time intervals  $[t_i, t_i + 3]$ ,  $t_i = 0, 1, \dots, 5$ . The sampling time interval  $\Delta t$  was 0.005. A 1024-FFT was used to calculate the Fourier series coefficients. Again we estimated the frequency response  $H_2(j\omega)$  at frequency knots

$\{k\omega_0, k = 0, 1, 2, \dots, 18\}$ ,  $\omega_0 = 2.094$ . Fig.3.5(a)(b) present the estimates of the magnitude response as well as the phase response for the noise-free case along with the results in applying the direct ratio and cross correlation methods to the same data. Also the results are shown in Fig.3.6(a)(b) for the SNR=20(dB) case.

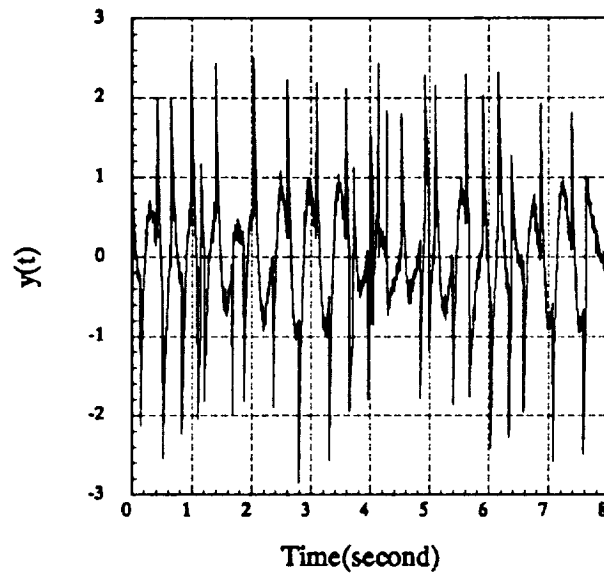


Fig.3.4 Output signal contaminated by white gaussian noise with SNR=20(dB) and collected in 8 seconds.

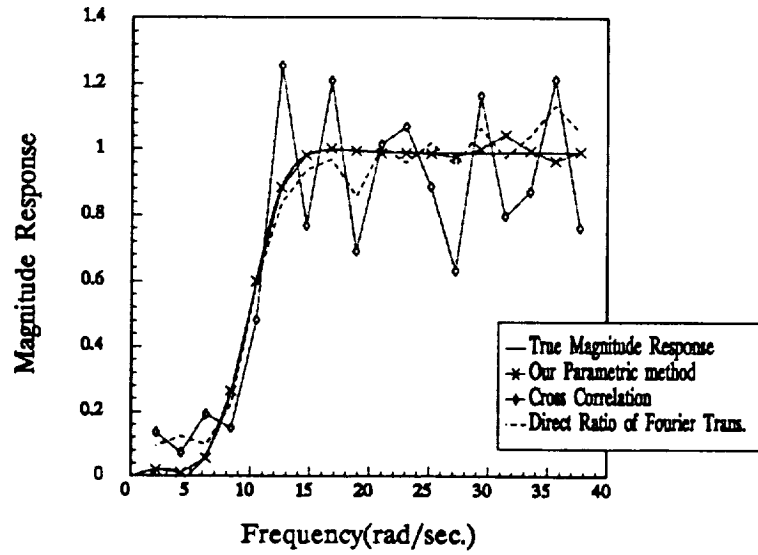


Fig.3.5(a) Estimated magnitude response at selected frequency knots in the noise-free case.

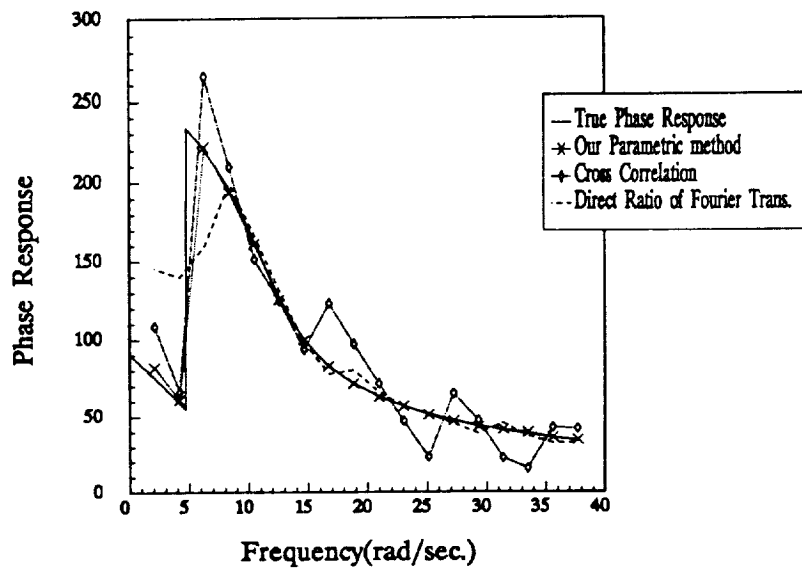


Fig.3.5(b) Estimated phase response at selected frequency knots in the noise-free case.



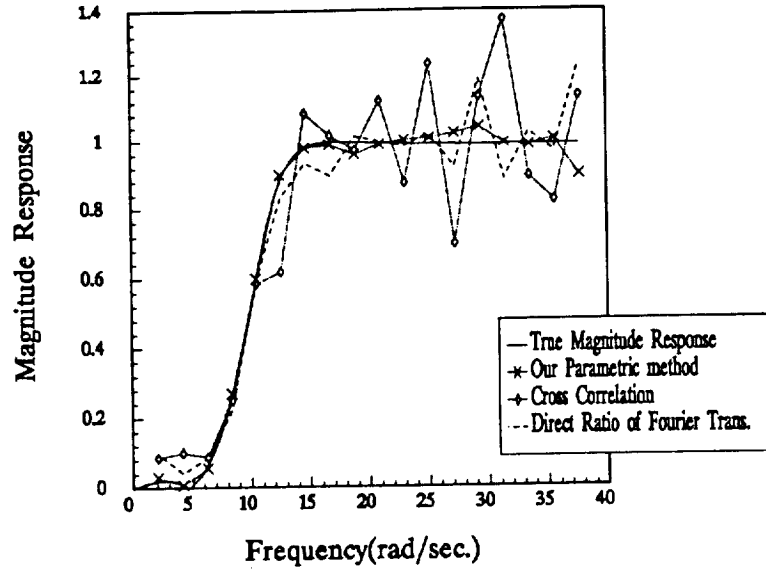


Fig.3.6(a) Estimated magnitude response at selected frequency knots for SNR=20(dB) case.

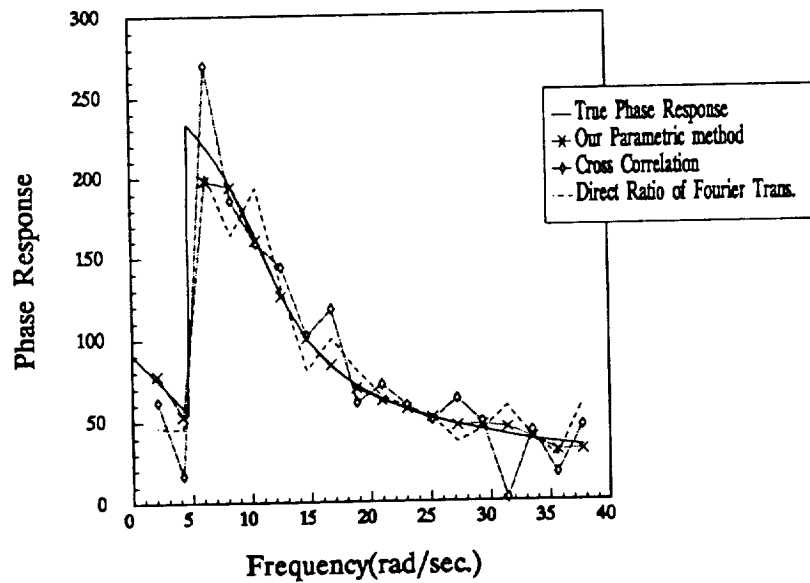


Fig.3.6(b) Estimated phase response at selected frequency knots for SNR=20(dB) case.

In the noise-free case, our algorithm gives almost exact results. The direct ratio

shows better performance than the cross correlation. Again, noise will not affect the estimates for low frequencies, but it increases the estimation error for high frequencies. The cross correlation and direct ratio gave large biases at high frequency knots.

From the above numerical simulations, we can see that if only short time transient data is available, our parametric sinusoidal modulating functional method works better than the classical cross correlation and direct ratio methods. If the system is not at rest initially, our method will present much better performance. Here one thing we need to point out is that if the order of modulating signal is larger than the order of the actual system, our algorithm works well. But if the order of modulating signal is less than the actual order of the system, our algorithm will fail to give good results.

### 3.7 Frequency Analysis for MIMO Systems

Assume a MIMO model is given by the following transfer function:

$$\mathbf{y}(s) = \mathbf{H}(s)\mathbf{u}(s) \quad (3.7.1)$$

where  $\mathbf{u}$  is a  $p_1$  input vector signal,  $\mathbf{y}$  is a  $p_2$  output vector signal,  $\mathbf{H} = (h_{i,l})$  is a  $p_2 \times p_1$  transfer function matrix.

Each transfer function element  $h_{i,l}(s)$  is given by:

$$h_{i,l}(s) = \frac{B_{i,l}(s)}{A_{i,l}(s)} \quad (3.7.2)$$

$B_{i,l}(s)$  and  $A_{i,l}(s)$  are coprime polynomials in  $s$ .

Given input-output data  $[\mathbf{u}(t), \mathbf{y}(t)]$  over the finite time intervals  $\{ [t_i, t_i + T], i = 1, 2, \dots, Q \}$ , the problem is to estimate the actual frequency response  $\mathbf{H}(j\omega) =$

$(h_{i,l}(j\omega))$  at the frequency knots  $\{k\omega_0, k = 0, 1, 2, \dots, M\}$  for each  $(i, l)$ th transfer function, where  $\omega_0 = 2\pi/T$ .

Based upon the transfer function structure (3.7.1), the problem can be decomposed into  $p_2$  subproblems by processing each row individually. The  $i^{\text{th}}$  element of output  $\mathbf{y}$  corresponds to the MISO system:

$$y_i(s) = [h_{i,1}(s), \dots, h_{i,p_1}(s)] \begin{pmatrix} u_1(s) \\ \vdots \\ u_{p_1}(s) \end{pmatrix} = \sum_{l=1}^{p_1} \frac{B_{i,l}(s)}{A_{i,l}(s)} u_l(s) \quad (3.7.3a)$$

Let  $A_i(s)$  be the least common multiple of  $\{A_{i,1}(s), \dots, A_{i,p_1}(s)\}$  and assume

$$\tilde{B}_{i,l}(s) = \frac{B_{i,l}(s)}{A_{i,l}(s)} A_i(s)$$

Then, adding some modeling errors and measurement noise, the subsystem (3.7.3a) can be rewritten as a differential operator equation form:

$$A_i(p)y_i(t) = \sum_{l=1}^{p_1} \tilde{B}_{i,l}(p)u_l(t) + e_i(t) \quad (3.7.3b)$$

Therefore, from now on we only consider the MISO systems without loss of generality. We also drop the subscript  $i$  for easy notation.

Hence, consider a stable linear MISO system:

$$A(p)y(t) = \sum_{l=1}^r B_l(p)u_l(t) + e(t) \quad (3.7.4a)$$

where,

$$A(p) = a_n p^n + a_{n-1} p^{n-1} + \dots + a_1 p^1 + a_0$$

$$B_l(p) = b_{l,m_l} p^{m_l} + b_{l,m_l-1} p^{m_l-1} + \dots + b_{l,1} p^1 + b_{l,0}, \quad m_l \leq n$$

$$l = 1, 2, 3, \dots, r$$

It is to be acknowledged that the pairs  $(A(p), B_l(p))$ ,  $l = 1, 2, \dots, r$  will not generally be coprime. However, this is not an issue for us because it is the ratios  $B_l(j\omega)/A(j\omega)$  that we seek to determine for knots  $k\omega_0$ ,  $k = 0, 1, \dots, M$ , rather than the polynomial value  $(A(j\omega), B_l(j\omega))$ . This avoids a difficult issue of sufficient parametrization and minimality for state space models which in our context is a separate issue.

Let  $\{\phi_m(t)\}$  be the set of  $n^{\text{th}}$  order modulating functions defined by (3.2.3). Rewriting the linear model (3.7.4a) as the equation error form, modulating both sides by the signal  $\phi_m(t)$ , we can obtain:

$$\sum_{k=m}^{m+n} b_{k-m} [A(-jk\omega_0)Y_k - \sum_{l=1}^r B_l(-jk\omega_0)U_{l,k}] = \sum_{k=m}^{m+n} b_{k-m} E_k \quad (3.7.4b)$$

Define the real and imaginary parts of the polynomials  $A(jk\omega_0)$ ,  $B_l(jk\omega_0)$ ,  $Y_k$ ,  $U_{l,k}$  as:

$$\begin{aligned} A(jk\omega_0) &= \alpha_k + j\beta_k \\ B_l(jk\omega_0) &= \gamma_{l,k} + j\delta_{l,k} \\ Y_k &= Y_k^c + jY_k^s = \int_0^T y(t)e^{jk\omega_0 t} dt \\ U_{l,k} &= U_{l,k}^c + jU_{l,k}^s = \int_0^T u_l(t)e^{jk\omega_0 t} dt \end{aligned} \quad (3.7.5)$$

Rewriting the equation (3.7.4b) in terms of the real and imaginary parts, we can obtain the following equations:

$$\begin{aligned} \sum_{k=m}^{m+n} b_{k-m} [\alpha_k Y_k^c + \beta_k Y_k^s - \sum_{l=1}^r (\gamma_{l,k} U_{l,k}^c + \delta_{l,k} U_{l,k}^s)] &= \epsilon_m^R \\ \sum_{k=m}^{m+n} b_{k-m} [-\alpha_k Y_k^s + \beta_k Y_k^c + \sum_{l=1}^r (\gamma_{l,k} U_{l,k}^s - \delta_{l,k} U_{l,k}^c)] &= \epsilon_m^I \end{aligned} \quad (3.7.6)$$

where,

$$\begin{aligned}\varepsilon_m^R &= \Re\left(\sum_{k=m}^{m+n} b_{k-m} E_k\right) \\ \varepsilon_m^I &= \Im\left(\sum_{k=m}^{m+n} b_{k-m} E_k\right)\end{aligned}$$

Compute the Fourier series coefficients  $Y_k(i)$  and  $U_{l,k}(i)$  corresponding to each time interval  $[t_i, t_i + T]$ ,  $i = 1, 2, \dots, Q$ ,  $k = 0, 1, \dots, M$ , by the equations:

$$\begin{aligned}Y_k(i) &= \int_0^T y(t + t_i) e^{jk\omega_0 t} dt \\ Y_k(i) &= Y_k^c(i) + jY_k^s(i) \\ U_{l,k}(i) &= \int_0^T u_l(t + t_i) e^{jk\omega_0 t} dt \\ U_{l,k}(i) &= U_{l,k}^c(i) + jU_{l,k}^s(i)\end{aligned}\tag{3.7.7}$$

and define a  $2 \times (2 + 2r)$  data matrix  $\psi_k(i)$  in terms of these harmonic series by :

$$\psi_k(i) = \begin{bmatrix} Y_k^c(i) & Y_k^s(i) & -U_{1,k}^c(i) & -U_{1,k}^s(i) & \dots & -U_{r,k}^c(i) & -U_{r,k}^s(i) \\ -Y_k^s(i) & Y_k^c(i) & U_{1,k}^s(i) & -U_{1,k}^c(i) & \dots & U_{r,k}^s(i) & -U_{r,k}^c(i) \end{bmatrix}\tag{3.7.8}$$

Define a  $2(r + 1)$  parameter vector by :

$$\theta_k = [\alpha_k, \beta_k, \gamma_{1,k}, \delta_{1,k}, \dots, \gamma_{r,k}, \delta_{r,k}]^T\tag{3.7.9}$$

Then equation (3.7.6) could be represented by a  $2 \times 1$  vector equation form as follows:

$$\begin{aligned}\sum_{k=m}^{m+n} b_{k-m} \psi_k(i) \theta_k &= \begin{bmatrix} \varepsilon_m^R(i) \\ \varepsilon_m^I(i) \end{bmatrix} = \varepsilon_m(i) \\ m &= 0, 1, 2, \dots, M, \quad i = 1, 2, \dots, Q\end{aligned}\tag{3.7.10}$$

In the same way as SISO systems, we can use a bootstrapping algorithm to form a sequence of linear regressions for equation (3.7.10). We omit the algebraic detail here. After getting the estimates of  $\theta_k$ , we can employ formulae similar to (3.3.20-21) to estimate the frequency response function for each subsystem  $B_l(j\omega)/A(j\omega)$  at the frequency knots  $k\omega_0$ . Other formulations discussed in the previous sections could also be applied to MIMO systems.

## 3.8 Numerical Simulation Results

Here a numerical simulation result is presented to show the performance of the algorithm. We utilize the first formulation.

We consider a two input, one output system. The first subsystem is a low pass second order system with the transfer function given by:

$$H_1(s) = \frac{2s + 160}{s^2 + 20s + 160}$$

The second subsystem is a high pass system with the transfer function given by:

$$H_2(s) = \frac{s^2 + 50s + 54}{s^2 + 40s + 500}$$

The input-output relation in the form of (3.7.4a) is

$$A(p)y(t) = B_1(p)u_1(t) + B_2(p)u_2(t)$$

where

$$A(p) = (p^2 + 20p + 160)(p^2 + 40p + 500)$$

$$B_1(p) = (p^2 + 40p + 500)(2p + 160)$$

$$B_2(p) = (p^2 + 50p + 54)(p^2 + 20p + 160)$$

Notice that the  $(A(p), B_1(p))$  and  $(A(p), B_2(p))$  are not pairwise coprime.

A random binary process was used as an input signal  $u_1$  to excite the first subsystem. The superimposed sinusoidal signal

$$u_2 = \sin(5t^3) + \sin(20t^2) + \sin(6t) + \sin(25t + 0.9434)$$

was used as an input signal to excite the second subsystem. Data was collected in 15 seconds. The whole data set was divided into the twelve time intervals  $[t_i, t_i + 4]$

for  $t_i = 0, 1, 2, \dots, 11$ . The sampling frequency was 200(Hz). 1024-FFT was utilized for calculating the Fourier series coefficients on each time interval. We estimated the frequency response  $H_l(j\omega)$  ( $l = 1, 2$ ) at frequency knots  $\{k\omega_0, k = 0, 1, 2, \dots, 15\}$ .  $\omega_0 = 1.57$ . The frequency knots cover a part of the passband, transition band and stop band of the two subsystems.

For comparison, we use  $u_1(t)$  to excite the first subsystem while holding  $u_2$  at zero to get the output  $y_1(t)$ , and then in a separate simulation use  $u_2(t)$  to excite the second subsystem to get the output  $y_2(t)$  while holding  $u_1$  at zero. Then we apply the direct ratio of Fourier transform and the standard cross correlation approaches to the separate data  $[u_1(t), y_1(t)]$ ,  $[u_2(t), y_2(t)]$  to estimate the frequency response of the subsystems. Although this comparison is favorable to the direct ratio and cross correlation, the MFFM still gives better results.

Fig.3.7(a,c) give the magnitude response plots of the two subsystems by using the MFFM for the data  $[u_1, u_2, y]$  in the noise free case along with the results obtained by applying the direct ratio and the cross correlation approaches to the data  $[u_1, y_1]$ ,  $[u_2, y_2]$ . Fig.3.7(b,d) are the phase response plots.

Also the simulation results of the magnitude and phase responses are shown in Fig.3.8(a-d) for the output signal contaminated by white gaussian noise with SNR=15dB.

As in the SISO system case, the MFFM gives almost exact results in a noise-free situation. Again noise did not affect the estimates of the MFFM at low frequencies. Comparing to the SISO case, noise causes larger estimation biases at high frequencies for the MFFM. The direct ratio and the cross correlation estimates present a large

oscillation and have large error, especially at high frequencies.

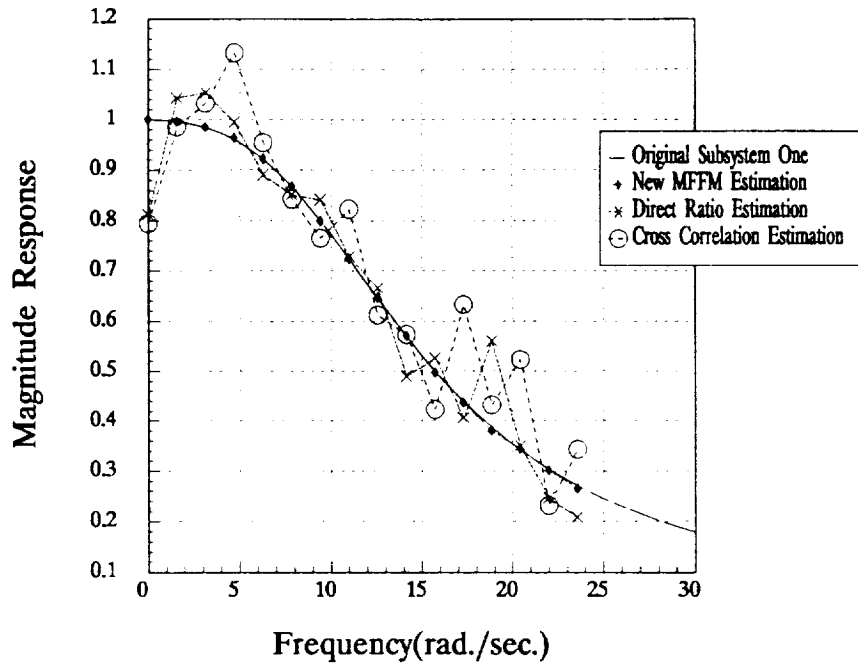


Fig.3.7(a) Estimated magnitude response of subsystem one at selected frequency knots in the noise-free case.

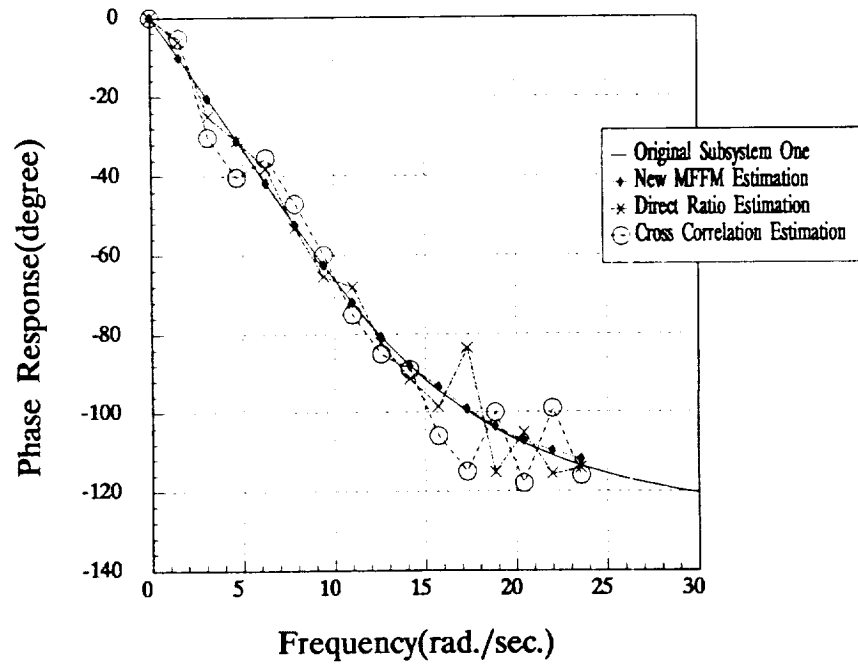


Fig.3.7(b) Estimated phase response of subsystem one at selected frequency knots in the noise-free case.



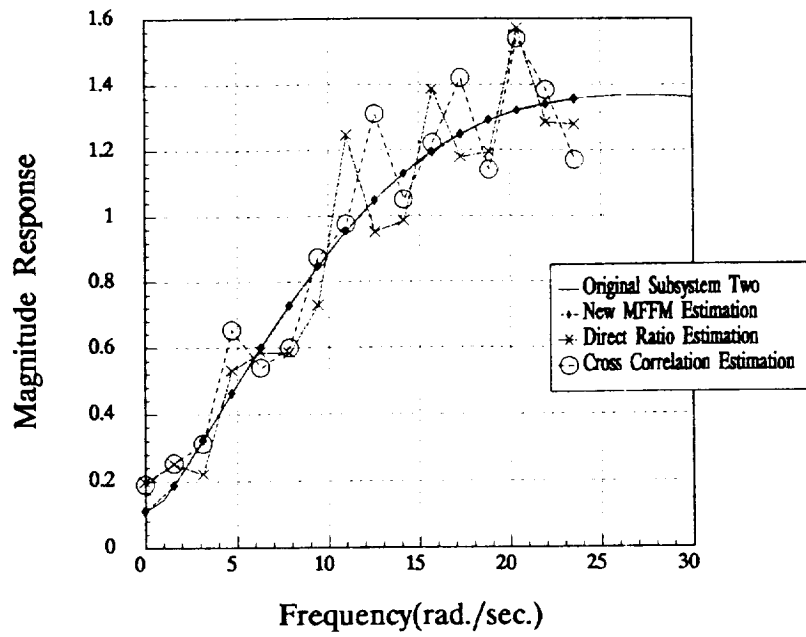


Fig.3.7(c) Estimated magnitude response of subsystem two at selected frequency knots in the noise-free case.

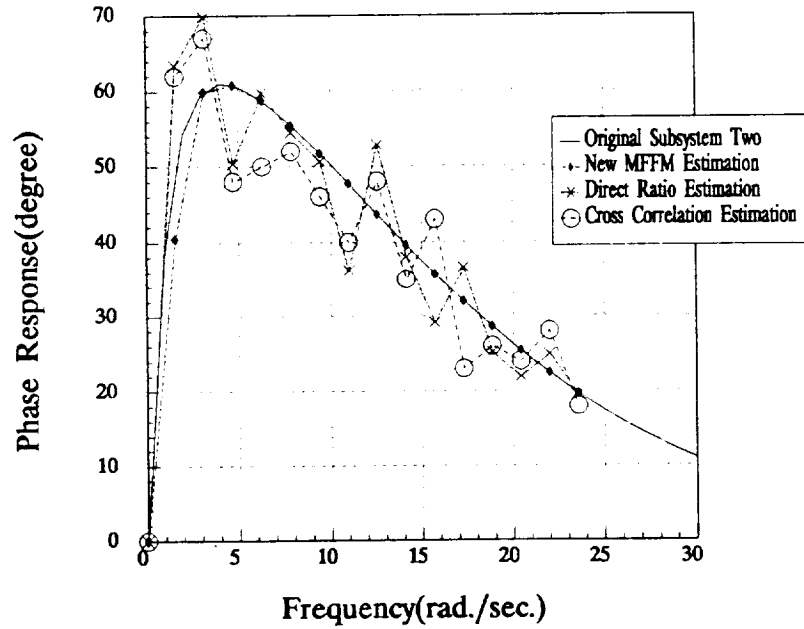


Fig.3.7(d) Estimated phase response of subsystem two at selected frequency knots in the noise-free case.

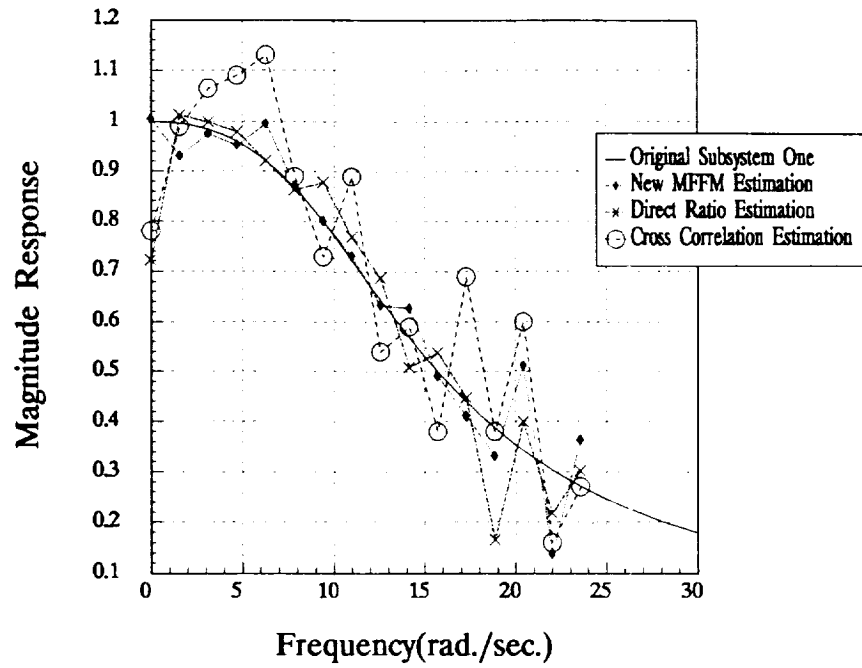


Fig.3.8(a) Estimated magnitude response of subsystem one at selected frequency knots for SNR=15(dB).

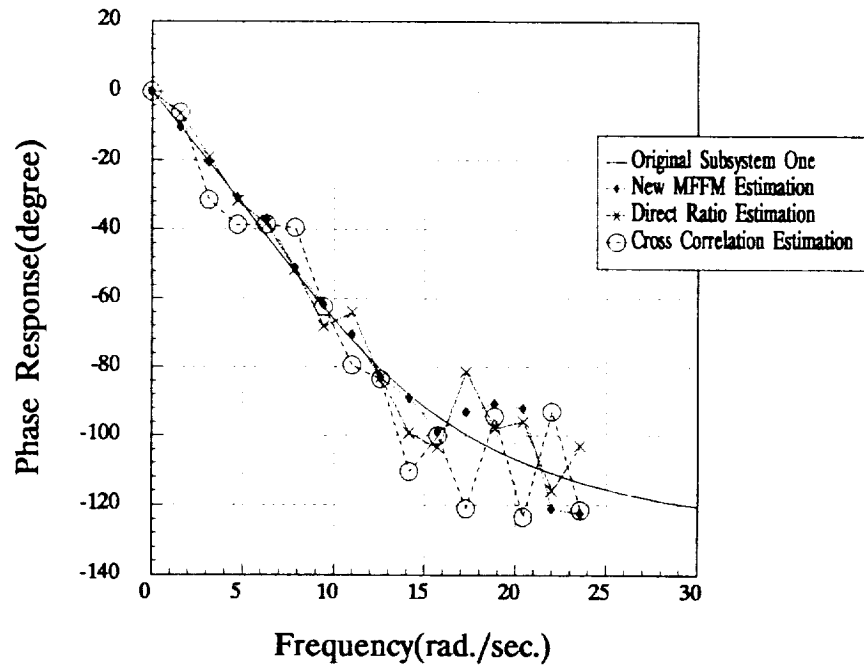


Fig.3.8(b) Estimated phase response of subsystem one at selected frequency knots for SNR=15(dB).

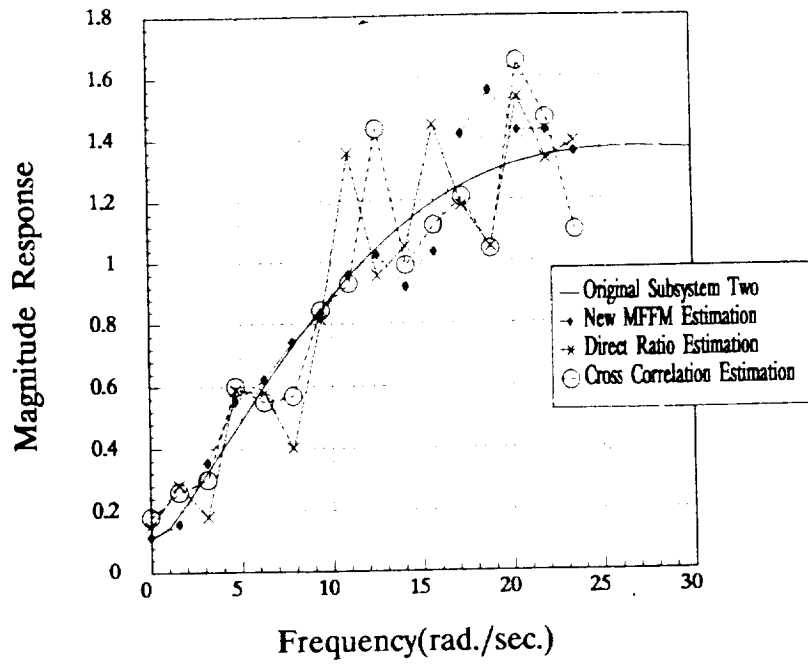


Fig.3.8(c) Estimated magnitude response of subsystem two at selected frequency knots for SNR=15(dB).

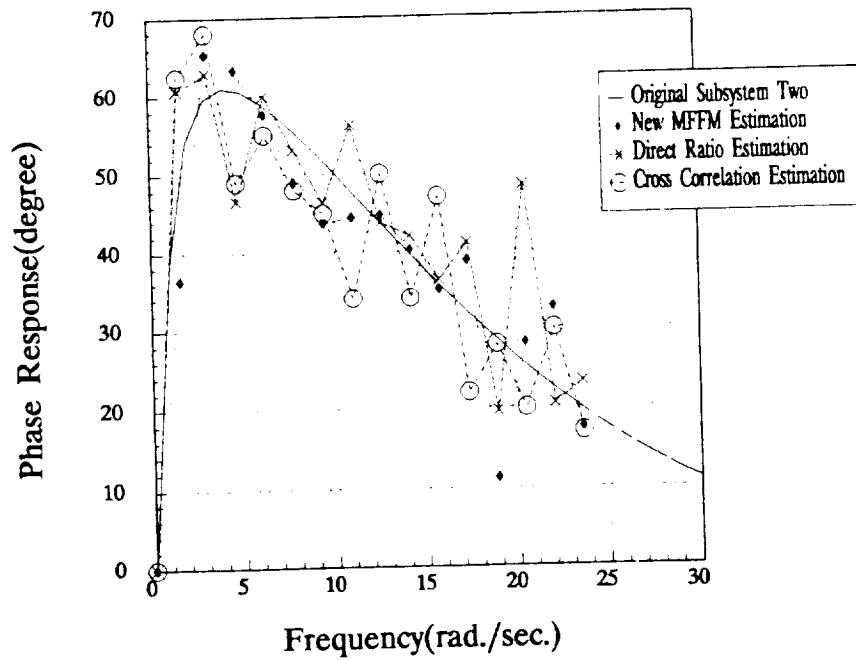


Fig.3.8(d) Estimated phase response of subsystem two at selected frequency knots for SNR=15(dB).



## Chapter 4

# Schemes for Model Reduction and Parameter Identification in the Frequency Domain

The approximation of high-order linear models by lower order systems is a very important problem involving a wide range of applications, such as signal processing and filtering, system synthesis, verification, and controller design. Many researches have been done in these and related areas [Sham75, Lari83, Mull76, Wahl90]. The main task of model reduction is to find a simple model structure characterizing the major behavior of an original high-order system and to simplify the hardware design and system analysis. The accuracy of the reduced system really depends upon the selection of the error criterion.

During the last two decades, most of the work utilized the classical approximation theory to match the state space realization, Markov parameters ( a part of the impulse response sequence ), and etc. These algorithms are based on the classical padé

approximation and continued fraction expansion which expand the original system into a Taylor series about the origin. The disadvantages of these methods are a low accuracy in the high frequency band and the possibility of losing stability for the reduced model.

In order to avoid these problems, some new approaches have been investigated. Current methods for model simplification and parameter estimation fall into two categories: deterministic and stochastic approaches, each approach adopts either a time domain or frequency domain format. Some proposed algorithms in [Mull76, Inou83, Wagi86] not only match a finite portion of the Markov parameters but also fit a finite portion of the output covariance sequence. For dealing with non-minimum phase system, [Tugn86] presented an optimization algorithm for matching the autocorrelation sequence as well as the higher order statistics. Based up the principal component analysis and singular value decomposition technique, [Moor81] gives an algorithm to transform an original system into a balanced state space realization and reduce a high-order model into a lower one. [HuXi87] combines the Padé approximation method and frequency fitting approach to acquire better accuracy in the middle and high frequency ranges.

Most of the investigations mentioned above require some assumptions about the original system, or availability of data before starting the algorithm. By deterministic means, the usual assumption is that the original model is known in advance. If this is not the case, then the first step is to identify it using the measurements of input-output signals. By stochastic means, the usual assumption is statistical stationarity, i.e., the system is working on a steady status. A long data length is required in order to get good estimates of statistical quantities of the original system for acheiving good accuracy of a reduced model, especially when the tail part of the impulse response of

the original model does not vanish significantly.

One of main advantages of using the modulating function technique is that we can attack continuous time models directly, which is much desired in classical and adaptive model reference control. By this means, it avoids the potentially significant errors in approximating derivatives from noisy input and output signals, selecting a sampling frequency, constructing a transformation for mapping a discrete time system to a continuous time system, and etc. All these processes will bring distortion to the model. Some are even much more noise sensitive. Another advantage of using the modulating function approach is that there is no necessity to deal with the complicated initial value problem.

This chapter focuses on reducing the linear continuous model using only transient input and output data and concerns with the task of combining the model identification and simplification process together. Apart from linearity, there are no assumptions of knowing the original model or presuming statistical stationarity of the input and output data which are crucial to the previous methods. The approach could be realized by two steps. The first step is to set up a least squares algorithm for estimating the frequency response of the original model at selected frequency points using short input output data records. This issue has been discussed in chapter 3. The second step, which we will develop here, is to select a lower order system to match the frequency responses at these dominant frequencies. These frequencies should cover the system bandwidth in order to characterize the behavior of the model. The original model could be minimum or nonminimum phase and our method can deal with phase and magnitude information flexibly. If the phase response is not important, we can exploit this advantage for further reducing the structure of the model utilizing an error norm criterion only depending on the magnitude.

## 4.1 Scheme 1

Let an original high-order linear stable system be represented in the transfer function form by :

$$G(s) = \frac{b_0 + b_1 s^1 + \dots + b_m s^m}{a_0 + a_1 s^1 + \dots + a_n s^n} \quad (4.1.1)$$

where  $a_n = 1, a_0, \dots, a_{n-1}, b_0, \dots, b_m$  are polynomial coefficients and are probably all unknown.

Let the corresponding reduced model be:

$$G_r(s) = \frac{c_0 + c_1 s^1 + \dots + c_{m_0} s^{m_0}}{d_0 + d_1 s^1 + \dots + d_{n_0} s^{n_0}} \quad (4.1.2)$$

where  $m_0 \leq n_0 < n$ .

The problem considered here is to set up a criterion for measuring the difference between  $G(s)$  and  $G_r(s)$ , and to select these coefficients  $c_0, c_1, \dots, c_{m_0}, d_0, \dots, d_{n_0}$  to minimize the error norm. Here, we utilize the frequency fitting approximation. Suppose  $\{\omega_1, \omega_2, \dots, \omega_J\}$  are selected as the fundamental frequency points ranging in the system bandwidth. The choice of  $c_0, c_1, \dots, c_{m_0}, d_0, \dots, d_{n_0}$  should ensure that the model frequency response  $G_r(j\omega_k) (k = 1, \dots, J)$  matches the original model frequency response  $G(j\omega_k)$  as closely as possible.

One simple approach for fitting the frequency responses at points  $(\omega_1, \omega_2, \dots, \omega_J)$  is to set up the following equation errors:

$$\begin{aligned} C(j\omega_i) - D(j\omega_i)\tilde{G}_i &= \varepsilon_i \\ i &= 1, 2, 3, \dots, J \end{aligned} \quad (4.1.3)$$



or equivalently, rewriting the (4.1.3) into the equations of real and imaginary parts:

$$\begin{aligned}
& c_0 - c_2\omega_i^2 + c_4\omega_i^4 + \dots \\
& -d_0|\tilde{G}_i| \cos(\phi_i) + d_1|\tilde{G}_i|\omega_i \sin(\phi_i) + d_2|\tilde{G}_i|\omega_i^2 \cos(\phi_i) + \dots = \varepsilon_i^R \\
& c_1\omega_i - c_3\omega_i^3 + c_5\omega_i^5 - \dots \\
& -d_0|\tilde{G}_i| \sin(\phi_i) - d_1|\tilde{G}_i|\omega_i \cos(\phi_i) + d_2|\tilde{G}_i|\omega_i^2 \sin(\phi_i) - \dots = \varepsilon_i^I \quad (4.1.4) \\
& i = 1, 2, 3, \dots, J
\end{aligned}$$

where,  $\tilde{G}_i$  is a frequency response estimation at  $\omega_i$  obtained through the algorithms developed in the last chapter.

$$\hat{G}_i = |\tilde{G}_i|e^{j\phi_i}$$

and

$$\varepsilon_i^R = \Re(\varepsilon_i), \quad \varepsilon_i^I = \Im(\varepsilon_i)$$

$\varepsilon_i$  is the frequency fitting error.

Assume  $d_{n_0} = 1$ , and

$$\begin{aligned}
\sigma_i^R &= \Re\{(j\omega_i)^{n_0} |\tilde{G}_i| (\cos(\phi_i) + j \sin(\phi_i))\} \\
\sigma_i^I &= \Im\{(j\omega_i)^{n_0} |\tilde{G}_i| (\cos(\phi_i) + j \sin(\phi_i))\} \quad (4.1.5)
\end{aligned}$$

Collecting all unknowns into the parameter vector:

$$\xi = \begin{bmatrix} c_0 \\ c_1 \\ \vdots \\ c_{m_0} \\ d_0 \\ \vdots \\ d_{n_0-1} \end{bmatrix} \quad (4.1.6)$$

and defining a dimension  $2J \times (m_0 + n_0 + 1)$  data matrix as follows:

$$\Xi = \begin{bmatrix} 1 & 0 & -\omega_1^2 & 0 & \omega_1^4 & \dots & -|\tilde{G}_1| \sin(\phi_1) & |\tilde{G}_1| \omega_1^2 \cos(\phi_1) & \dots \\ 0 & \omega_1 & 0 & -\omega_1^3 & 0 & \dots & -|\tilde{G}_1| \sin(\phi_1) & -|\tilde{G}_1| \omega_1 \cos(\phi_1) & \dots \\ \vdots & \vdots & \vdots & \vdots & \vdots & \dots & \vdots & \vdots & \dots \\ 1 & 0 & -\omega_J^2 & 0 & \omega_J^4 & \dots & -|\tilde{G}_J| \sin(\phi_J) & |\tilde{G}_J| \omega_J^2 \cos(\phi_J) & \dots \\ 0 & \omega_J & 0 & -\omega_J^3 & 0 & \dots & -|\tilde{G}_J| \sin(\phi_J) & -|\tilde{G}_J| \omega_J \cos(\phi_J) & \dots \end{bmatrix} \quad (4.1.7)$$

Define:

$$\sigma = \begin{bmatrix} \sigma_1^R \\ \sigma_1^I \\ \vdots \\ \sigma_J^R \\ \sigma_J^I \end{bmatrix} \quad \varepsilon = \begin{bmatrix} \varepsilon_1^R \\ \varepsilon_1^I \\ \vdots \\ \varepsilon_J^R \\ \varepsilon_J^I \end{bmatrix} \quad (4.1.8)$$

Then we can combine the real and imaginary parts of equation(4.1.4) into a standard regression format for setting up the least squares estimation:

$$\min_{\xi} \varepsilon = \min_{\xi} (\Xi \xi - \sigma)^T (\Xi \xi - \sigma) \quad (4.1.9)$$

A consideration of this procedure leads to the following remarks:

1. Estimating the unknown parameter set of the reduced model only involves constructing and solving linear equations. Hence, the algorithm is simple and the computational cost is low.
2. The reduced model may have large distortion in some frequency bands comparing with the original system because the selected error norm (4.1.3) differs somewhat from fitting the true frequency response. Actually, (4.1.3) can be

regarded as the true error criterion weighted by the denominator polynomial  $D(j\omega)$ . Thus there is a trade-off between the model accuracy and simplicity of the algorithm.

3. The algorithm cannot guarantee the stability of the reduced system although the original system is stable. The possibility of getting a reduced stable model will be enhanced by picking up more middle and high frequencies in the system bandwidth.

## 4.2 Scheme 2

Scheme 1 presents a biased result because it is equivalent to weighting the match criterion by the reduced denominator  $D(j\omega)$ . Here, the following iterative algorithm can be employed to asymptotically remove the bias if it converges. The error criterion at the  $k^{th}$  iteration is defined as:

$$E_k = \sum_{i=1}^J \left| \frac{W_i}{D_{k-1}(j\omega_i)} [C_k(j\omega_i) - \tilde{G}_i D_k(j\omega_i)] \right|^2 \quad (4.2.1)$$

where  $D_{k-1}(j\omega_i)$ ,  $i = 1, 2, \dots, J$ , are the estimates of  $D(j\omega)$  at the  $(k-1)^{th}$  iteration.

Another similar scheme is to utilize the following error criterion:

$$E_k = \sum_{i=1}^J W_i^2 |e_{k,i}|^2$$

$$e_{k,i} = C_k(j\omega_i) - \frac{C_{k-1}(j\omega_i)}{D_{k-1}(j\omega_i)} [D_k(j\omega_i) - 1] - \tilde{G}_i \quad (4.2.2)$$

These recursive least squares algorithms update the estimates of the reduced system at each iteration. If  $C_k(j\omega) \rightarrow C(j\omega)$  and  $D_k(j\omega) \rightarrow D(j\omega)$ , the iterative

algorithms will asymptotically produce a reduced order system which matches the frequency response data without any bias.

One advantage of using equ.(4.2.1-2) as an error fitting criterion is that we can use a linear least squares algorithm to update the estimation at each iteration because each error term is linearly related to the unknown parameters. Thus, nonlinear optimization algorithms are not needed.

From the error criterion (4.2.1-2) we can see that at the  $k^{\text{th}}$  stage of iteration the error term  $e_{k,i}$  has the general form:

$$e_{k,i} = \lambda_{k,i}C_k(j\omega_i) + \rho_{k,i}D_k(j\omega_i) - \zeta_{k,i} \quad (4.2.3)$$

where for the error norm (4.2.1),

$$\begin{aligned} \lambda_{k,i} &= \frac{W_i}{D_{k-1}(j\omega_i)} \\ \rho_{k,i} &= -\frac{W_i}{D_{k-1}(j\omega_i)}\tilde{G}_i \\ \zeta_{k,i} &= 0 \end{aligned} \quad (4.2.4)$$

For the error norm (4.2.2), we have:

$$\begin{aligned} \lambda_{k,i} &= W_i \\ \rho_{k,i} &= -\frac{C_{k-1}(j\omega_i)}{D_{k-1}(j\omega_i)}W_i \\ \zeta_{k,i} &= W_i\left[\frac{C_{k-1}(j\omega_i)}{D_{k-1}(j\omega_i)} - \tilde{G}_i\right] \end{aligned} \quad (4.2.5)$$

Define:

$$\mathbf{c}_c^T = [c_{0k} \ c_{2k} \ c_{4k} \ \dots]$$

$$\mathbf{c}_s^T = [c_{1k} \ c_{3k} \ c_{5k} \ \dots]$$

$$\begin{aligned}
\mathbf{d}_c^T &= [d_{0k} \ d_{2k} \ d_{4k} \ \dots] \\
\mathbf{d}_s^T &= [d_{1k} \ d_{3k} \ d_{5k} \ \dots] \\
\Omega_{c,i}^T &= [1 \ 0 \ -\omega_i^2 \ 0 \ \omega_i^4 \ 0 \ \dots] \\
\Omega_{s,i}^T &= [0 \ -\omega_i^1 \ 0 \ -\omega_i^3 \ 0 \ \omega_i^5 \ \dots]
\end{aligned} \tag{4.2.6}$$

Rewrite  $\lambda_{k,i}$ ,  $\rho_{k,i}$ ,  $\zeta_{k,i}$ ,  $C_k(j\omega_i)$ ,  $D_k(j\omega_i)$  as the real and imaginary parts as:

$$\begin{aligned}
\lambda_{k,i} &= \lambda_{k,i}^{(R)} + j\lambda_{k,i}^{(I)} \\
\rho_{k,i} &= \rho_{k,i}^{(R)} + j\rho_{k,i}^{(I)} \\
\zeta_{k,i} &= \zeta_{k,i}^{(R)} + j\zeta_{k,i}^{(I)} \\
C_k(j\omega_i) &= \Omega_{c,i}^T \mathbf{c}_c + j\Omega_{s,i}^T \mathbf{c}_s \\
D_k(j\omega_i) &= \Omega_{c,i}^T \mathbf{d}_c + j\Omega_{s,i}^T \mathbf{d}_s
\end{aligned} \tag{4.2.7}$$

Therefore, at the  $k^{th}$  stage of iteration and at each frequency  $\omega_i$ , we can represent the error  $e_{k,i}$  linearly in terms of unknown parameters:

$$\begin{aligned}
\Re(e_{k,i}) &= \lambda_{k,i}^{(R)} \Omega_{c,i}^T \mathbf{c}_c - \lambda_{k,i}^{(I)} \Omega_{s,i}^T \mathbf{c}_s + \rho_{k,i}^{(R)} \Omega_{c,i}^T \mathbf{d}_c - \rho_{k,i}^{(I)} \Omega_{s,i}^T \mathbf{d}_s - \zeta_{k,i}^{(R)} \\
\Im(e_{k,i}) &= \lambda_{k,i}^{(I)} \Omega_{s,i}^T \mathbf{c}_s + \lambda_{k,i}^{(R)} \Omega_{c,i}^T \mathbf{c}_c + \rho_{k,i}^{(I)} \Omega_{s,i}^T \mathbf{d}_s + \rho_{k,i}^{(R)} \Omega_{c,i}^T \mathbf{d}_c - \zeta_{k,i}^{(I)}
\end{aligned} \tag{4.2.8}$$

Express the equations (4.2.8) as a matrix form:

$$\begin{pmatrix}
\lambda_{k,i}^{(R)} \Omega_{c,i}^T & -\lambda_{k,i}^{(I)} \Omega_{s,i}^T & \rho_{k,i}^{(R)} \Omega_{c,i}^T & -\rho_{k,i}^{(I)} \Omega_{s,i}^T \\
\lambda_{k,i}^{(I)} \Omega_{s,i}^T & \lambda_{k,i}^{(R)} \Omega_{c,i}^T & \rho_{k,i}^{(I)} \Omega_{s,i}^T & \rho_{k,i}^{(R)} \Omega_{c,i}^T
\end{pmatrix}
\begin{pmatrix}
\mathbf{c}_c^T \\
\mathbf{c}_s^T \\
\mathbf{d}_c^T \\
\mathbf{d}_s^T
\end{pmatrix}
=
\begin{pmatrix}
\zeta_{k,i}^{(R)} \\
\zeta_{k,i}^{(I)}
\end{pmatrix}$$

$$i = 1, 2, 3, \dots, J \tag{4.2.9}$$

Collecting all these equations, we can construct a standard linear regression form for the least squares solution. Without loss of generality we can assume  $d_{n_0} = 1$ . If  $\zeta_k = 0$ , we will get a trivial solution. In this case equation (4.2.9) can be modified slightly to overcome this problem.

The following observation can be made for this scheme:

1. As in scheme 1, this procedure can be implemented via the linear least squares algorithm, thus it is easy to realize. Also it might asymptotically eliminate the matching bias if it converges.
2. Numerical simulation and analysis have shown that sometimes the matrix adaptation (4.2.9) will be divergent. Also when noise is not neglectable, it will not guarantee convergence to a desired reduced model.
3. At each iteration, we have to solve an overdetermined set of equations. The computation cost is larger comparing to the first scheme.

In addition, the above algorithm lacks the flexibility of dealing with magnitude and phase information. In the following, we develop a procedure matching a reduced model and the frequency response data directly. The expense we will pay is by employing a nonlinear optimization technique.

### 4.3 Scheme 3

We assume that the simplified model (4.1.2) is specified in terms of second order cascade connections and a scalar constant, which is determined by a parameter set  $P$ .

$(\tilde{G}_1, \tilde{G}_2, \dots, \tilde{G}_J)$  are treated as the original frequency responses at selected frequencies  $(\omega_1, \omega_2, \dots, \omega_J)$ . We choose the  $r^{th}$  norm error criterion by:

$$E = \left[ \sum_{i=1}^J W_i |G_{r,i} - \tilde{G}_i|^r \right]^{\frac{1}{r}}$$

where,

$$G_{r,i} = G_r(j\omega_i) \quad i = 1, 2, \dots, J \quad (4.3.1)$$

Our goal is to find optimal parameters  $P$  to minimize  $E$ , or equivalently  $E^r$ . For utilizing a nonlinear optimization algorithm, we need a formula for calculating the gradient. Suppose  $q \in P$  is a parameter, then it is easy to prove that the derivative of  $E^r$  with respect to  $q$  is given by the following equation:

$$\frac{\partial E^r}{\partial q} = \sum_{i=1}^J r |G_{r,i} - \tilde{G}_i|^{r-2} W_i \Re \left[ \frac{\partial G_{r,i}^*}{\partial q} (G_{r,i} - \tilde{G}_i) \right] \quad (4.3.2)$$

where,

$$\frac{\partial G_{r,i}^*}{\partial q} = \frac{\partial G_r^*(j\omega)}{\partial q} \Big|_{\omega=\omega_i} \quad (4.3.3)$$

$G_r^*$  is the complex conjugate of  $G_r$ .

For the second order cascade connection form of a reduced model  $G_r$ , we have the following:

$$G_r(s) = C \prod_{k=1}^L \frac{1 + q_{k,1}s + q_{k,2}s^2}{1 + q_{k,3}s + q_{k,4}s^2} = CF(s) \quad (4.3.4)$$

The advantages of choosing the form (4.3.4) are its relative lower parameter sensitivity and direct relationships between the parameters and the location of zeros as well as poles. Based upon (4.3.4), for each parameter  $q \in P$  we can represent the model  $G_r(j\omega)$  as a product of the two terms:

$$G_r(j\omega) = G_{r,s}(\omega)g(q, \omega) \quad (4.3.5)$$

where only  $g(q, \omega)$  involves the parameter  $q$ ,  $G_{r,s}(\omega)$  does not depend on  $q$ . Parameter  $q$  could be associated with the value of a real pole, a real zero, or complex conjugate poles and complex conjugate zeros.

By substituting equation(4.3.5) into (4.3.3), a simple calculation will lead to the following equation:

$$\frac{\partial E^r}{\partial q} = \sum_{i=1}^J r |G_{r,i} - \tilde{G}_i|^{r-2} W_i \Re[G_{r,i}^* (G_{r,i} - \tilde{G}_i) \frac{\partial \ln g_i(q)}{\partial q}] \quad (4.3.6)$$

where,

$$g_i(q) = g(q, \omega) |_{\omega=\omega_i} \quad (4.3.7)$$

If we select  $r$  to be 2, and take the derivative of  $E^2$  with respect to the scalar parameter  $C$  and set the equation to zero, then the parameter  $C$  can be easily estimated in terms of the other remaining parameters.

In fact, using (4.3.2) we can obtain:

$$\frac{\partial E^2}{\partial C} = 2 \sum_{i=1}^J W_i \Re[F_i^* (G_{r,i} - \tilde{G}_i)] = 2 \sum_{i=1}^J W_i [C |F_i|^2 - \Re(F_i^* \tilde{G}_i)] = 0 \quad (4.3.8)$$

where,

$$F_i = F(j\omega) |_{\omega=\omega_i}$$

Solving the equation for  $C$ , we get:

$$C = \frac{\sum_{i=1}^J W_i \Re(F_i^* \tilde{G}_i)}{\sum_{i=1}^J W_i |F_i|^2} \quad (4.3.9)$$

In this way, we can reduce by one the total number of unknown parameters.

Another alternative is to represent the reduced model by taking the partial fraction expansion. For each parameter  $q \in P$  we can represent the model  $G_r(s)$  as a sum of



two terms:

$$G_r(j\omega) = G_{r,s}(\omega) + g_1(\omega)g_2(q, \omega) \quad (4.3.10)$$

where  $G_{r,s}(\omega)$  and  $g_1(\omega)$  do not depend on the parameter  $q$ , only  $g_2(q, \omega)$  involves the  $q$ . Similar to the previous case,  $q$  can associate with a real pole, a real zero, or complex conjugate poles and complex conjugate zeros.  $g_2(q, \omega)$  could be expressed explicitly for all these different cases.

It is clear to see that the error norm criterion defined in equ.(4.3.1) takes care of both magnitude and phase information of the original system. If only the magnitude is important, we can further simplify the model structure and keep the quality of matching magnitude response as good as the previous one. The error norm criterion we can use is:

$$\tilde{E} = \left[ \sum_{i=1}^J W_i ||G_{r,i}| - |\tilde{G}_i||^r \right]^{\frac{1}{r}} \quad (4.3.11)$$

It is easy to show in this case that the formula for calculating the differentiation is given as follows:

$$\frac{\partial \tilde{E}^r}{\partial q} = \frac{1}{2} \sum_{i=1}^J r W_i \text{sign}(|G_{r,i}| - |\tilde{G}_i|) ||G_{r,i}| - |\tilde{G}_i||^{r-1} |G_{r,i}| \Re\left(\frac{\partial \ln g_i(q)}{\partial q}\right) \quad (4.3.12)$$

here, all the variables have the same meaning as the former equations.

It is well understood that it is not guaranteed for a nonlinear optimization scheme to achieve the global minimum in the general case. Actually, it is most likely for the algorithm to get into a local minimum if the initial value is arbitrarily selected. Therefore, in order to get a good estimate of the optimal reduced model, it is necessary to have a fairly accurate initial estimate. In the next section, we will present a quite reasonable algorithm to estimate the initial value for the reduced system  $G_r(j\omega)$  which will help the optimal algorithm obtain excellent results.

The algorithm shown here could be utilized to weight different frequency bands, and force the system to satisfy a stability constraint. Usually, the deviation  $|G_{r,i} - \tilde{G}_i|$  or  $||G_{r,i}| - |\tilde{G}_i||$  differs significantly in different frequency ranges. The error at the middle frequency band tends to be larger. Hence, utilizing adaptive weighting factors  $W_i$  is preferred instead of using constant values. Corresponding to the criterion (4.3.1), the usual selection of adaptive weighting factor is:

$$W_i = \frac{|G_{r,i} - \tilde{G}_i|}{\sum_{i=1}^J |G_{r,i} - \tilde{G}_i|} \quad (4.3.13)$$

For the error norm (4.3.11), we choose:

$$W_i = \frac{||G_{r,i}| - |\tilde{G}_i||}{\sum_{i=1}^J ||G_{r,i}| - |\tilde{G}_i||} \quad (4.3.14)$$

During the search,  $W_i$  will be modified adaptively according to (4.3.13-14) with the updating of all the parameters  $q \in P$  and  $G_{r,i}$  in each iteration.

It should be mentioned that the selection of the fitting frequencies is very important. Any inappropriate selection of dominate fitting frequency points will lead to a bad accuracy in some frequency bands which might be crucial to the reduced model. One thing obvious is that the selected frequency points should cover the system bandwidth and the total number of fitting frequencies  $L_f$  should satisfy :

$$L_f \geq n_0 + m_0 + 1$$

Assuming that the estimated frequency response  $\hat{G}_i$  is exact, a larger  $L_f$  implies the reduced model will be more accurate. The expense we pay is to increase the computation cost.

## 4.4 An Algorithm for Initial Value Estimation

In this section, a least squares algorithm is suggested to estimate the initial value  $(c_0, c_1, \dots, c_{m_0}, d_0, \dots, d_{n_0-1})$  of the reduced system.

Construct the following equation error based upon the complex sinusoidal modulating signals:

$$\sum_{k=m}^{m+n} b_{k-m} [D(-jk\omega_0)Y_k - C(-jk\omega_0)U_k] = \varepsilon_m \quad (4.4.1)$$

where,

$$C(-jk\omega_0) = c_0 + c_1(-jk\omega_0) + c_2(-jk\omega_0)^2 + \dots + c_{m_0}(-jk\omega_0)^{m_0}$$

$$D(-jk\omega_0) = d_0 + d_1(-jk\omega_0) + d_2(-jk\omega_0)^2 + \dots + d_{n_0}(-jk\omega_0)^{n_0} \quad (4.4.2)$$

Rearranging equation (4.4.1) into real and imaginary parts, we get the forms:

$$\begin{aligned} & d_0 \sum_{k=m}^{m+n} b_{k-m} Y_k^c + d_1 \sum_{k=m}^{m+n} b_{k-m} (k\omega_0) Y_k^s - d_2 \sum_{k=m}^{m+n} b_{k-m} (k\omega_0)^2 Y_k^c + \dots \\ & - c_0 \sum_{k=m}^{m+n} b_{k-m} U_k^c - c_1 \sum_{k=m}^{m+n} b_{k-m} (k\omega_0) U_k^s + c_2 \sum_{k=m}^{m+n} b_{k-m} (k\omega_0)^2 U_k^c + \dots = \varepsilon_m^R \\ & d_0 \sum_{k=m}^{m+n} b_{k-m} Y_k^s - d_1 \sum_{k=m}^{m+n} b_{k-m} (k\omega_0) Y_k^c - d_2 \sum_{k=m}^{m+n} b_{k-m} (k\omega_0)^2 Y_k^s + \dots \\ & - c_0 \sum_{k=m}^{m+n} b_{k-m} U_k^s + c_1 \sum_{k=m}^{m+n} b_{k-m} (k\omega_0) U_k^c + c_2 \sum_{k=m}^{m+n} b_{k-m} (k\omega_0)^2 U_k^s + \dots = \varepsilon_m^I \end{aligned} \quad (4.4.3)$$

$$m = 0, 1, 2, 3, \dots, M$$

Define:

$$\theta_p = \begin{bmatrix} d_0 \\ d_1 \\ \vdots \\ d_{n_0-1} \\ c_0 \\ c_1 \\ \vdots \\ c_{m_0} \end{bmatrix} \quad (4.4.4)$$

For each time interval  $[t_i, t_i + T]$ , we assume that:

$$\Gamma_0^y(i) = \begin{bmatrix} \sum_{k=0}^n b_k Y_k^c(i) \\ \sum_{k=0}^n b_k Y_k^s(i) \\ \sum_{k=1}^{n+1} b_{k-1} Y_k^c(i) \\ \sum_{k=1}^{n+1} b_{k-1} Y_k^s(i) \\ \vdots \end{bmatrix}_{2(M+1)} \quad \Gamma_1^y(i) = \begin{bmatrix} \sum_{k=0}^n b_k(k\omega_0) Y_k^s(i) \\ -\sum_{k=0}^n b_k(k\omega_0) Y_k^c(i) \\ \sum_{k=1}^{n+1} b_{k-1}(k\omega_0) Y_k^s(i) \\ -\sum_{k=1}^{n+1} b_{k-1}(k\omega_0) Y_k^c(i) \\ \vdots \end{bmatrix}_{2(M+1)} \quad \dots$$

$$\Gamma_0^u(i) = \begin{bmatrix} -\sum_{k=0}^n b_k U_k^c(i) \\ -\sum_{k=0}^n b_k U_k^s(i) \\ -\sum_{k=1}^{n+1} b_{k-1} U_k^c(i) \\ -\sum_{k=1}^{n+1} b_{k-1} U_k^s(i) \\ \vdots \end{bmatrix}_{2(M+1)} \quad \Gamma_1^u(i) = \begin{bmatrix} -\sum_{k=0}^n b_k(k\omega_0) U_k^s(i) \\ +\sum_{k=0}^n b_k(k\omega_0) U_k^c(i) \\ -\sum_{k=1}^{n+1} b_{k-1}(k\omega_0) U_k^s(i) \\ +\sum_{k=1}^{n+1} b_{k-1}(k\omega_0) U_k^c(i) \\ \vdots \end{bmatrix}_{2(M+1)} \quad \dots$$

Define:

$$\Gamma(i) = [\Gamma_0^y(i), \Gamma_1^y(i), \dots, \Gamma_{n_0-1}^y(i), \Gamma_0^u(i), \dots, \Gamma_{m_0}^u(i)] \quad (4.4.5)$$

Assume:

$$\mu_m^R = \Re \left\{ \sum_{k=m}^{m+n} b_{k-m} (-jk\omega_0)^{n_0} (Y_k^c(i) + jY_k^s(i)) \right\}$$

$$\mu_m^I = \Im \left\{ \sum_{k=m}^{m+n} b_{k-m} (-jk\omega_0)^{n_0} (Y_k^c(i) + jY_k^s(i)) \right\}$$

$$m = 0, 1, 2, 3, \dots, M \quad (4.4.6)$$

and denote:

$$\zeta(i) = \begin{bmatrix} \mu_0^R(i) \\ \mu_0^I(i) \\ \vdots \\ \mu_M^R(i) \\ \mu_M^I(i) \end{bmatrix}_{2(M+1)} \quad (4.4.7)$$

Collecting all the equations for  $m = 0, 1, 2, \dots, M$ , we form the following matrix equation for each time interval  $[t_i, t_i + T]$ :

$$\varepsilon(i) = \Gamma(i)\theta_p - \zeta(i)$$

$$i = 1, 2, 3, \dots, N \quad (4.4.8)$$

Make the following definition:

$$\Gamma = \begin{bmatrix} \Gamma(1) \\ \Gamma(2) \\ \vdots \\ \Gamma(N) \end{bmatrix} \quad \zeta = \begin{bmatrix} \zeta(1) \\ \zeta(2) \\ \vdots \\ \zeta(N) \end{bmatrix} \quad (4.4.9)$$

Collecting all matrix equations (4.4.8) for each time interval  $[t_i, t_i + T]$ , we construct a standard linear regression equation for the least squares estimation:

$$\min_{\theta_p} \varepsilon = \min_{\theta_p} (\Gamma\theta_p - \zeta)^T (\Gamma\theta_p - \zeta) \quad (4.4.10)$$

Equation (4.4.10) can be used to estimate an initial value for a reduced system. Again there is no promise for these initial values to satisfy the stability constraint.

The initial reduced system matches the harmonic Fourier series coefficients of the input and output data. The estimated initial values are fairly accuracy. These values will be updated to satisfy the optimal criterion.

## 4.5 Some Numerical Examples

In this section we present some numerical examples to demonstrate the performance of the algorithm by comparing with the existing approaches. Here we apply the scheme 3 for model reduction. For the MFFM algorithm, there is no requirement of knowing the actual high order system a priori. But we do need an input-output pair generated from the original model. These data can be obtained from the real process. If the original model is known, these data can also be produced by simulating the system.

**Example 1.** Co and Ydsti[CoTB90] compared a Frequency Fitting Padé algorithm and the P-L Modulating Function method in reducing some high order models into lower order systems. For easy comparison, we took the first example from [Xihe87]:

$$H_1(s) = \frac{(s + 2)^2(s + 5)^2(s + 1000)}{(s + 1)^2(s + 10)^2(s + 100)^2}$$

The PL method which matches the Fourier series coefficients of input-output data is quite similar to our scheme 1. An input signal for exciting the system used by [CoTB90] consists of a positive unit step function followed by a negative step function. Data was collected in five seconds. The reduced third order model is:

$$H_1^{PL}(s) = \frac{3.8111s^2 + 21.7853s + 38.7277}{s^3 + 49.9836s^2 + 548.5900s + 381.0047}$$

They found that the PL method works better than the FFP algorithm.

For the purpose of comparison, we also utilized the classical balanced realization method to reduce the system. Using functions provided by MATLAB, we obtain a reduced model:

$$H_1^{Bin}(s) = \frac{5.4156s^2 + 30.9466s + 58.5745}{s^3 + 65.4461s^2 + 793.1840s + 585.7454}$$

For simulating our MFFM algorithm, we selected the same random binary input signal as used in chapter 3 to excite the system. Data is collected in 8 seconds. The whole data set is divided into the six time intervals  $[t_i, t_i + 3]$  for  $t_i = 0, 1, \dots, 5$ . The sampling time interval  $\Delta t$  is 0.005. 1024-FFT is utilized in calculating the Fourier series coefficients on each time interval. We first estimated the frequency response  $H_1(j\omega)$  at frequency knots  $\{k\omega_0, k = 0, 1, 2, \dots, 30\}$ ,  $\omega_0 = 2.094$ .

The reduced third order system by matching the first twelve frequency knots is:

$$H_1^{MFFM} = \frac{4.5233s^2 + 30.6739s + 45.2871}{s^3 + 51.2456s^2 + 710.2395s + 453.6771}$$

Fig.4.1(a)(b) present the Bode plots of above system along with the simulation results obtained by applying the balanced realization method and PL procedure. Fig.4.1(c) shows the corresponding Nichols plot.

The low order model achieved by matching the last fifteen frequency knots is:

$$\hat{H}_1^{MFFM}(s) = \frac{1.4952s^2 + 863.1844s + 5334.4197}{s^3 + 187.4456s^2 + 11304.2301s + 141250.0129}$$

The Bode plots of the above system along with other results are shown in Fig.4.2(a)(b). Fig.4.2(c) gives the corresponding Nichols plot.

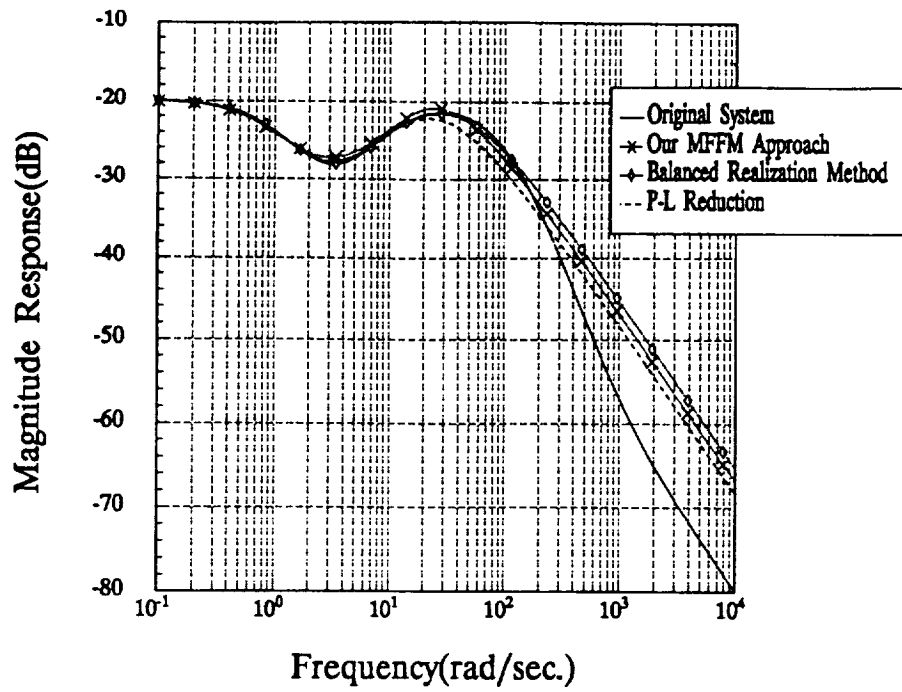


Fig.4.1(a) Magnitude response vs. frequency. The MFFM uses the low frequency matching.

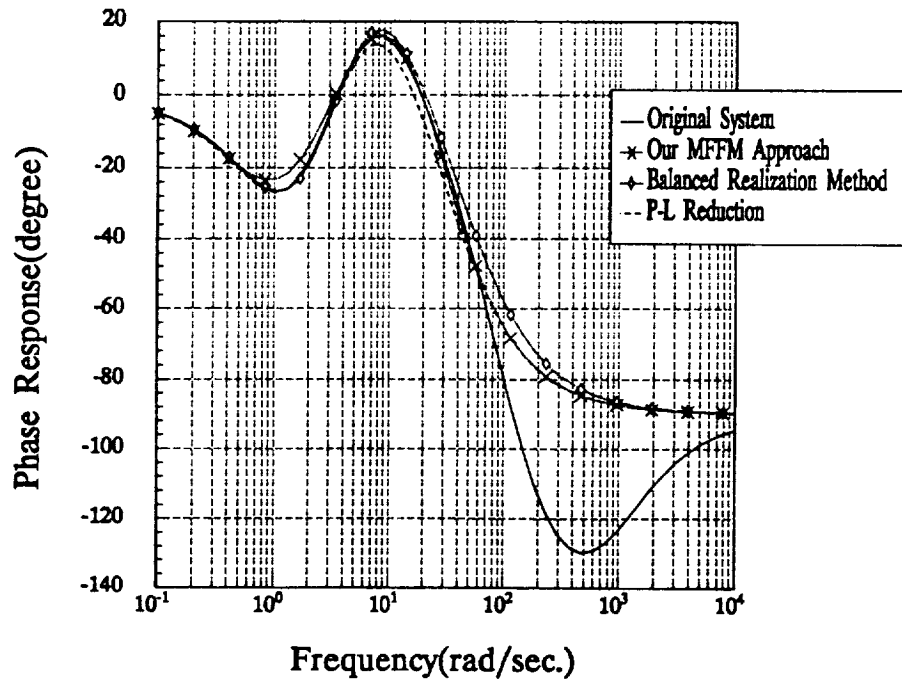


Fig.4.1(b) Phase response vs. frequency. The MFFM uses the low frequency matching.



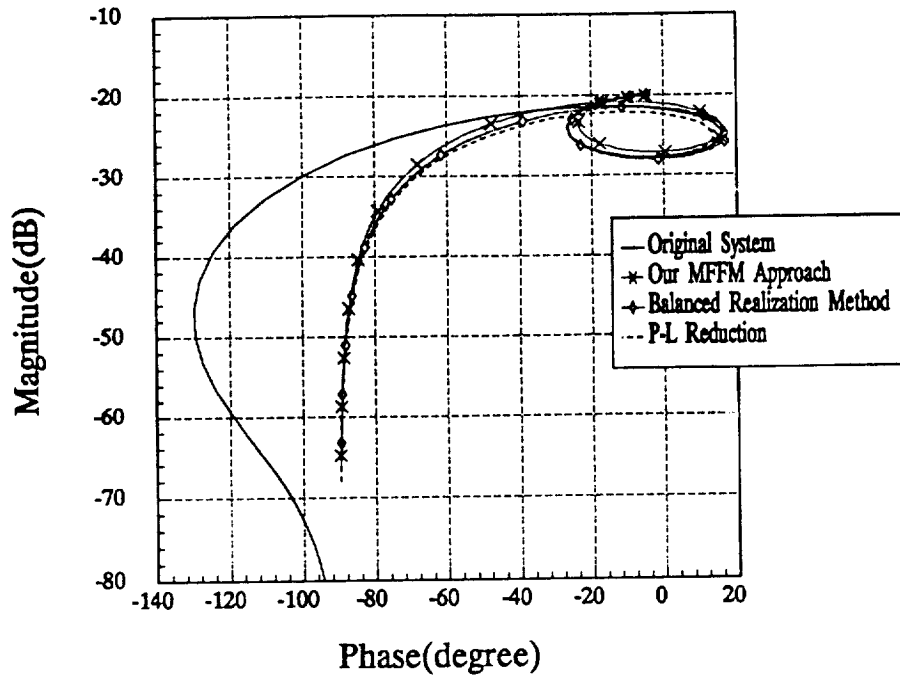


Fig.4.1(c) Nichols plots. The MFFM uses the low frequency matching.

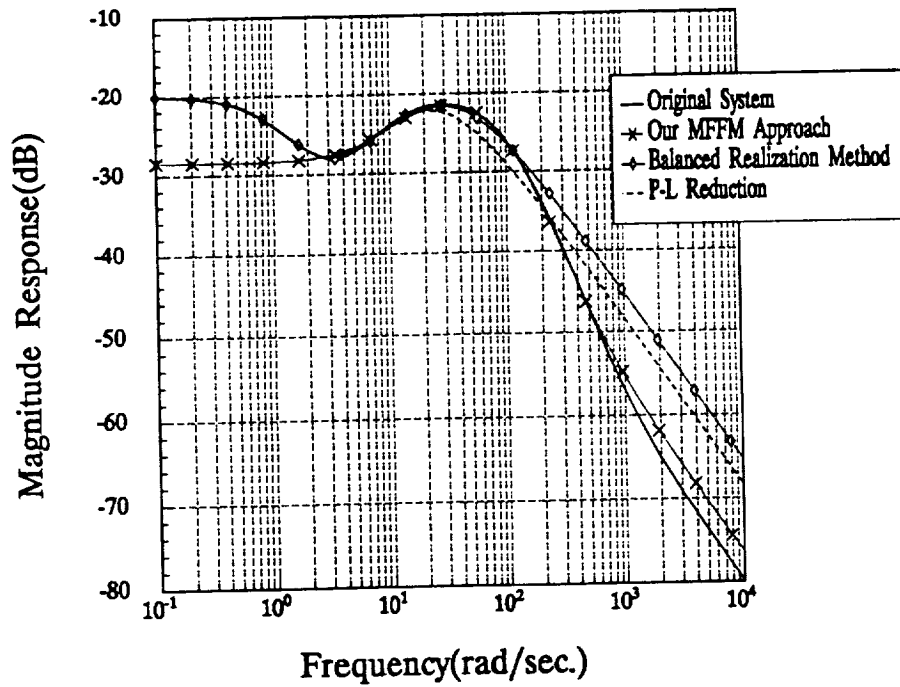


Fig.4.2(a) Magnitude response vs. frequency. The MFFM uses the high frequency matching.

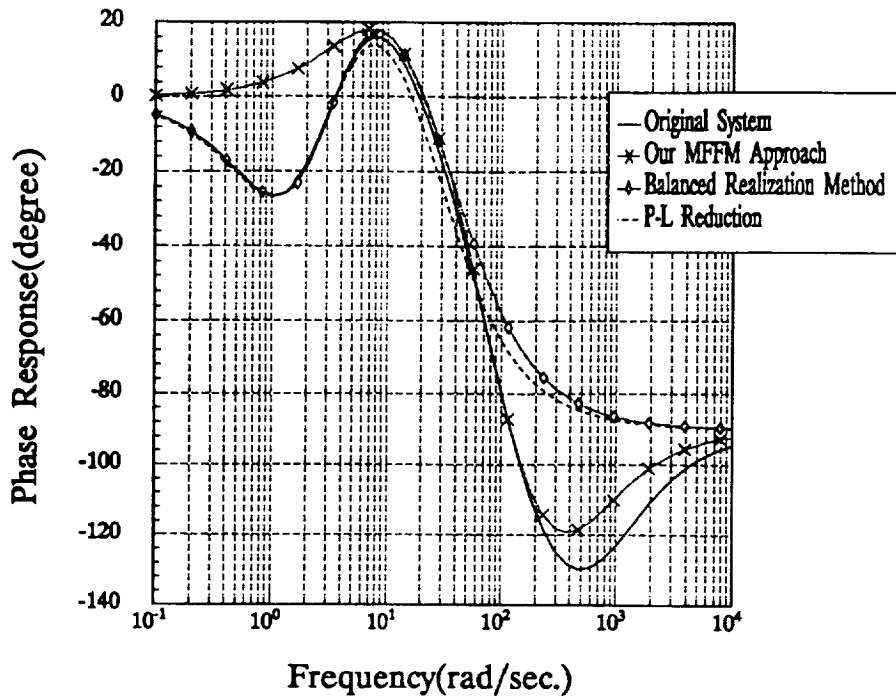


Fig.4.2(b) Phase response vs. frequency. The MFFM uses the high frequency matching.

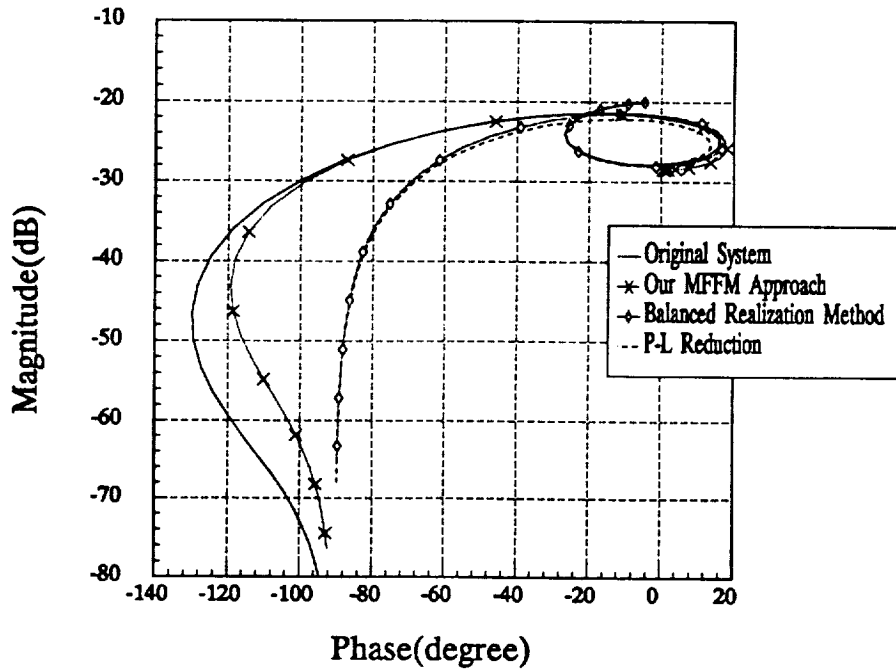


Fig.4.2(c) Nichols plots. The MFFM uses the low frequency matching.

Simulation results indicate that the PL method and the balanced realization technique weight the low frequency modes more heavily. The MFFM algorithm gives results similar to the PL and balanced realization by picking more low frequency knots. If we sacrifice the DC response and the frequency band lower than 10(Hz), then the MFFM algorithm gives a reduced model which approximates the original system much better in the frequency band larger than 10(Hz). The tradeoff depends upon real applications. The MFFM has this flexibility.

**Example 2.** The second example we considered here is a six order model:

$$H_2(s) = \frac{4.5000s^5 + 16.8750s^4 + 1.2474 \times 10^4 s^2 + 8.0454 \times 10^6 s + 3.6556 \times 10^7}{s^6 + 66.85s^5 + 2778.9s^4 + 7.1963 \times 10^4 s^3 + 1.0168 \times 10^6 s^2 + 9.8011 \times 10^6 s + 4.7306 \times 10^7}$$

The same random binary signal is used to excite the system as in Example 1. Data was collected in 8 seconds. The whole data set is divided into two disjoint time intervals for using the PL reduction. The parameter  $L$  was selected as 12. The reduced system is:

$$H_2^{PL}(s) = \frac{0.1372s^2 + 124.0337s + 345.1078}{s^3 + 10.6977s^2 + 145.0830s + 453.2253}$$

Using the balanced realization, we obtained:

$$H_2^{Bln}(s) = \frac{-5.5419s^2 + 170.4683s + 872.5521}{s^3 + 15.4064s^2 + 207.4581s + 1129.1082}$$

For using the MFFM method, we divided the whole data set into the six time intervals  $[t_i, t_i + 3]$ ,  $t_i = 0, 1, \dots, 5$ . We first estimated the frequency response  $H_2(j\omega)$  at knots  $\{k\omega_0, k = 0, 1, 2, \dots, 30\}$ ,  $\omega_0 = 2.094$ . We picked five low frequencies, five

middle frequencies near the valley and five high frequency knots. We put a slightly heavier weight on the middle frequencies. The reduced third order system is:

$$H_2^{MFFM}(s) = \frac{3.8121s^2 - 59.6845s + 6913.6012}{s^3 + 42.7534s^2 + 389.3838s + 8388.2031}$$

Fig.4.3(a)(b) present the Bode plots of obtained results. Fig.4.3(c) is the corresponding Nichols plot.

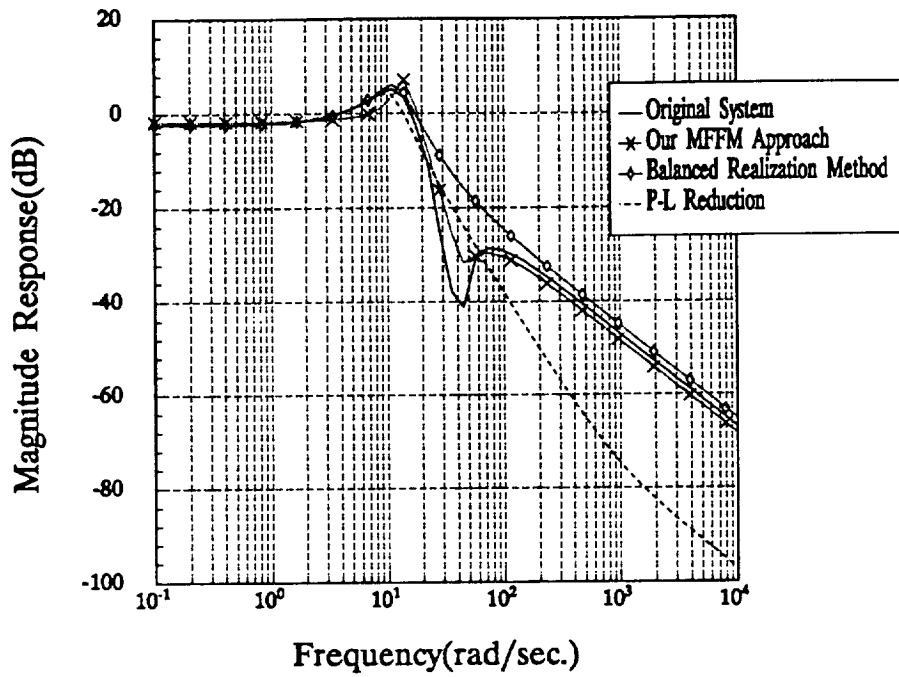


Fig.4.3(a) Magnitude response vs. frequency.

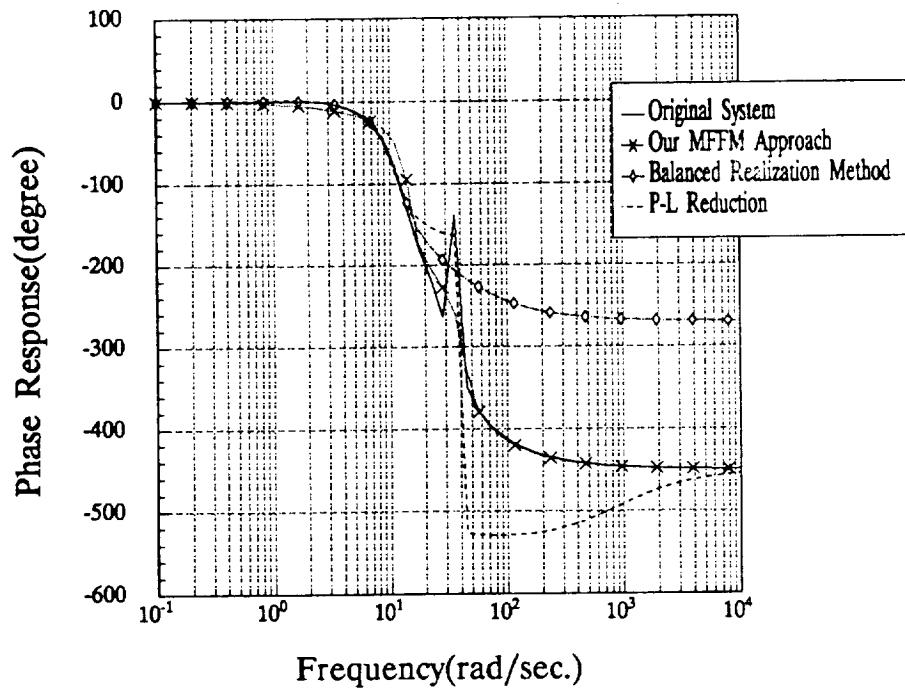


Fig.4.3(b) Phase response vs. frequency.

The MFFM achieves considerably better results in this example. The PL algorithm produces a large bias in the high frequency band. The balanced realization cannot track the valley. Only the MFFM gives almost an exact match for low frequency and high frequency modes, as well as tracks the rapid change in the frequency band near the valley.

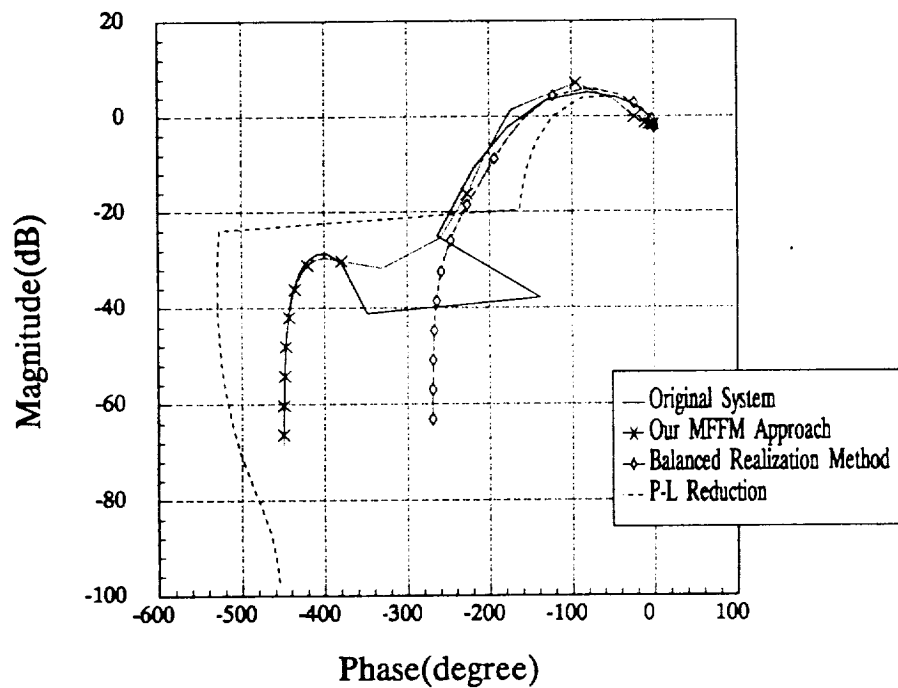


Fig.4.3(c) Nichols plots.

## Chapter 5

# High Resolution Frequency Estimation in the Presence of Noise Using Complex Sinusoidal Modulating Signals

### 5.1 Introduction

In this chapter, we focus on the problem of estimating the angular frequencies  $\omega_1, \omega_2, \dots, \omega_K$  for given superimposed harmonic signals over a set of finite time intervals  $\{[t_i, t_i + T], i = 1, 2, \dots, Q\}$  :

$$y(t) = y_d(t) + e(t) \quad (5.1.1)$$

where,

$$y_d(t) = \sum_{i=1}^K A_i \sin(\omega_i t + \phi_i) \quad (5.1.2)$$

In equations(5.1.1-2),  $e(t)$  is a stationary white Gaussian noise,  $K$  is the number of superimposed sinusoids and is not necessarily known.  $A_i$  and  $\phi_i$  are unknown am-

plitudes and phases of the signal  $y_d(t)$ .  $T$ , the length of the time intervals, is actually a frequency resolution related parameter. The time intervals need not necessarily be disjoint.

The problem has many practical applications and has received considerable attention[Kay84, OhSG91, Sher91]. Although traditional FFT and periodogram methods work well in a high signal-to-noise ratio case, they are nonparametric algorithms and the resolution is not high enough for small data sets, nor for low SNR's.

This has spurred interest in developing high resolution parametric algorithms. Some approaches, like the maximum likelihood estimation, nonlinear optimization algorithms, etc., work well in the low SNR situation[Fraz88, Scha91, Tuft82]. However, they require either long data lengths or sophisticated computing and time costly algorithms. MUSIC is a typical algorithm for frequency estimation and direction finding. But it is quite computationally demanding[Stoi91, LeeH91]. The Yule-Walker equation approach has been widely utilized for frequency estimation and spectrum analysis because of its effectiveness and the availability of fast lattice algorithms. Recently, some researchers have proposed a HOYW algorithm for improving the frequency resolution [Chan82, Mose88, Stoi91]. But the problem is that sometimes it is difficult to separate " spurious zeros " from signal frequencies.

In contrast to the previous methods, here we focus on the problem of high resolution frequency estimation employing a simple linear least squares algorithm. We use a continuous time model for the analysis. The method we utilize is to construct an autoregressive differential equation model to fit the received signal. Then complex sinusoidal modulating signals are utilized to convert the differential equation into simple algebraic equations. The parametric least squares algorithm can be de-



signed to detect the frequencies. One advantage of our method is that there is no requirement of a long data length record, i.e., the algorithm works well for short time observation data. Numerical simulation results will demonstrate the performance of the algorithm.

## 5.2 Overview of the High Order Yule-Walker

### Estimation

The HOYW estimation utilizes the discrete time samples of the sinusoidal signal (5.1.1) for  $t = 0, 1, \dots, N - 1$ . Assume  $\omega_i \neq \omega_j$ , and the phases  $\phi_i$ ,  $i = 1, 2, \dots, K$  are mutually independent random variables obeying a uniform distribution on  $[0, 2\pi]$ , with frequency  $\omega_k \in [0, 2\pi]$ . It is assumed that the signal  $y_d(t)$  and the white Gaussian noise  $e(\tilde{t})$  are uncorrelated for all  $t, \tilde{t}$ , i.e.,  $E\{y_d(t)e(\tilde{t})\} = 0$ .

Define a whitening filter as:

$$\begin{aligned} A(z^{-1}) &= \prod_{k=1}^K (1 - z^{-1}e^{j\omega_k})(1 - z^{-1}e^{-j\omega_k}) \\ &= \prod_{k=1}^K (1 - 2z^{-1}\cos(\omega_k) + z^{-2}) \end{aligned} \quad (5.2.1)$$

Then it is easy to verify that the received sinusoidal signal  $y(t)$  obeys the following discrete ARMA model:

$$A(z^{-1})y(t) = A(z^{-1})e(t) \quad (5.2.2)$$

The filter has zeros on the unit circle  $e^{\pm j\omega_k}$ ,  $k = 1, 2, \dots, K$ , from which we can get the frequency estimates of the signal once the zeros of  $A(z^{-1})$  have been estimated.

It is easy to verify from equation (5.2.2) that the signal  $y(t)$  also satisfies the

following high order ARMA model:

$$C(z^{-1})y(t) = C(z^{-1})e(t) \quad (5.2.3a)$$

where,

$$C(z^{-1}) = \sum_{i=0}^L c_i z^{-i} = B(z^{-1})A(z^{-1}) \quad (5.2.3b)$$

and where  $B(z^{-1})$  is a polynomial of degree  $L - 2K$ :

$$B(z^{-1}) = \sum_{i=0}^{L-2K} b_i z^{-i} \quad (5.2.3c)$$

It has been shown from theoretical analyses and numerical experiments that using the high order ARMA equation (5.3.3a) for frequency estimation can decrease the variance of the estimator and improve the frequency resolution. But the problem is that sometimes it is not easy to separate the “ spurious zeros ” of  $B(z^{-1})$  from the signal frequency zeros of  $A(z^{-1})$ .

Define  $\{r(k)\}$  to be the autocorrelation sequence of the signal, i.e.,

$$r(k) = E\{y(t)y(t+k)\} \quad (5.2.4)$$

Without loss of generality,  $c_0$  can be constrained to be 1. It is well known that the following high order Yule-Walker equation holds for solving the coefficients of the whitening filter:

$$\begin{pmatrix} r(L+1) & r(L) & \dots & r(1) \\ r(L+2) & r(L+1) & \dots & r(2) \\ \vdots & \vdots & \ddots & \vdots \\ r(L+L_1) & r(L+L_1-1) & \dots & r(L_1) \end{pmatrix} \begin{pmatrix} c_0 \\ c_1 \\ \vdots \\ c_L \end{pmatrix} = 0, \quad L, L_1 \geq 2K \quad (5.2.5)$$

The number of equations  $L_1$ , and the order  $L$  of the polynomial  $C(z)$  can be selected flexibly for improving the resolution and accuracy of the frequency estimates.

But the larger  $L$  is to be chosen, the more difficult it is to separate the roots of  $B(z)$  and  $A(z)$ .

Rewrite (5.2.5) into the following standard linear regression equation ( $c_0 = 1$ ):

$$(c_1 \quad c_2 \quad \dots \quad c_n) R(L, L_1) = - (r(L+1) \quad r(L+2) \quad \dots \quad r(L+L_1)) \quad (5.2.6)$$

where,

$$R(L, L_1) = \begin{pmatrix} r(L) & \dots & r(L+L_1-1) \\ \vdots & \ddots & \vdots \\ r(1) & \dots & r(L_1) \end{pmatrix}$$

Numerical experiments have shown that the covariance matrix  $R(L, L_1)$  is very likely to be ill conditioned, especially for large  $(L, L_1)$ . For achieving a good robust estimator, some regularization procedures have to be taken. It has been proven that a much better frequency estimate can be obtained by first approximating  $R(L, L_1)$  in the subspace of rank  $2K$  in the Frobenius norm sense, and then taking the Moore-Penrose pseudoinverse. See [Stoi91, Chan82] for more details.

The HOYW equation has some advantages. The efficient lattice Levinson algorithm can be utilized to solve equation(5.2.5), and computation time can be saved. The selection of  $(L, L_1)$  is flexible. In the next section we present a method of using complex sinusoidal modulating signals to estimate the frequencies. Comparing with the YW equation method, our approach gives high frequency resolution estimates, especially for short data lengths. The proposed algorithm is very robust and shows outstanding performance in high SNR circumstances. Conversely, it also works well in the low SNR case.

### 5.3 The Parametric Least Squares Estimation

For the received signal (5.1.1-2), we assume  $e(t)$  is a real stationary Gaussian white noise with zero mean, and variance  $\sigma^2$ . Our estimation algorithm is based upon the fact that the signal  $y_d(t) = \sum_{i=1}^K \sin(\omega_i t + \phi)$  satisfies a differential continuous time autoregressive model of order  $2K$ . The coefficients of this model only depend on the angular frequencies and not on the amplitudes nor phases. More specifically,  $K$  imaginary zeros of the autoregressive model are exactly the  $K$  angular frequencies to be estimated.

Define:

$$\Pi(p) = \prod_{m=1}^K (p^2 + \omega_m^2) = p^{2K} + \alpha_1 p^{2(K-1)} + \dots + \alpha_{K-1} p^2 + \alpha_K \quad (5.3.1)$$

where,  $p = d/dt$ (differential operator),

$$\begin{aligned} \alpha_1 &= \sum_{j=1}^K \omega_j^2 \\ \alpha_2 &= \sum_{j \neq k} \omega_j^2 \omega_k^2 \\ &\vdots \\ \alpha_K &= \prod_{j=1}^K \omega_j^2 \end{aligned} \quad (5.3.2)$$

$\alpha_1, \alpha_2, \dots, \alpha_K$  are elementary symmetric functions of  $\omega_1, \omega_2, \dots, \omega_K$ .

Then it follows that on each time interval  $[t_i, t_i + T]$ , the received signal  $y(t)$  satisfies the differential equation model:

$$\Pi(p)y(t) = y^{2K} + \alpha_1 y^{2(K-1)} + \dots + \alpha_{K-1} y^2 + \alpha_K = \epsilon(t) \quad (5.3.3)$$

where,

$$\epsilon(t) = \Pi(p)e(t)$$

and  $\epsilon(t)$  is the noise term. From (5.3.1) we can see that  $\Pi(p)$  has imaginary zeros at  $\pm j\omega_m, m = 1, 2, \dots, K$ .

Define a set of modulating functions:

$$\phi_m(t) = e^{jm\omega_0 t}(1 - e^{j\omega_0 t})^n \quad (n \geq 2K) \quad (5.3.4)$$

$$m = m_0, m_1, m_2, \dots, m_M$$

where  $\omega_0 = 2\pi/T$ . The appropriate selection of these  $m_i$  will make the modulating signals more flexible and work in different situations. Taking the binomial expansion of (5.3.4) and changing the index of summation,  $\phi_m(t)$  can be written as the form:

$$\begin{aligned} \phi_m(t) &= \sum_{k=0}^n b_k e^{j(m+k)\omega_0 t} \\ b_k &= (-1)^k C_n^k \end{aligned} \quad (5.3.5)$$

where  $C_n^k$  is the binomial coefficient.

Multiplying both sides of equation(5.3.3) by  $\phi_m(t)$  and using the modulating property, we can construct the following equation format for the observed signal on each time interval  $[t_i, t_i + T]$ ,  $i = 1, 2, \dots, Q$ :

$$\sum_{k=m}^{m+n} b_{k-m} \Pi(-jk\omega_0) Y_k(i) = \epsilon_m(i) \quad (5.3.6)$$

$$m = m_0, m_1, \dots, m_M.$$

where

$$\begin{aligned} Y_k(i) &= \int_0^T y(t_i + t) e^{jk\omega_0 t} dt \\ \epsilon_m(i) &= \sum_{k=m}^{m+n} b_{k-m} E_k(i) \\ E_k(i) &= \int_0^T e(t_i + t) \phi_m(t) dt \end{aligned} \quad (5.3.7)$$

The best selection of  $m_0, m_1, \dots, m_M$  is to make  $[m_j\omega_0, (m_j + n)\omega_0]$  cover, or at least be close to, the signal frequencies. In this way eqn.(5.3.6) will most reveal and utilize the signal information.

From equation (5.3.1), we have:

$$\Pi(-jk\omega_0) = \alpha_K - (k\omega_0)^2\alpha_{K-1} + \dots + (jk\omega_0)^{2(K-1)}\alpha_1 + (jk\omega_0)^{2K} \quad (5.3.8)$$

and hence rearranging equation (5.3.6) into a linear form relating the unknown parameters  $\alpha_i$ , we obtain:

$$\begin{aligned} & \alpha_K \sum_{k=m}^{m+n} b_{k-m} Y_k(i) - \alpha_{K-1} \sum_{k=m}^{m+n} b_{k-m} (k\omega_0)^2 Y_k(i) + \dots \\ & + (-1)^{K-1} \alpha_1 \sum_{k=m}^{m+n} b_{k-m} (k\omega_0)^{2(K-1)} Y_k(i) + \sum_{k=m}^{m+n} b_{k-m} (-1)^K (k\omega_0)^{2K} Y_k(i) = \epsilon_m(i) \\ & m = m_0, m_1, m_2, \dots, m_M \\ & i = 1, 2, \dots, Q \end{aligned} \quad (5.3.9)$$

Define:

$$\begin{aligned} \alpha &= \begin{pmatrix} \alpha_K \\ \alpha_{K-1} \\ \vdots \\ \alpha_2 \\ \alpha_1 \end{pmatrix} \\ \Xi_m(i) &= \left[ \sum_{k=m}^{m+n} b_{k-m} Y_k(i), - \sum_{k=m}^{m+n} b_{k-m} (k\omega_0)^2 Y_k(i) \dots \right] \\ \rho_m(i) &= (-1)^K \sum_{k=m}^{m+n} b_{k-m} (k\omega_0)^{2K} \begin{pmatrix} Y_k^c(i) \\ Y_k^s(i) \end{pmatrix} \end{aligned} \quad (5.3.10)$$

Collecting all equations for  $m = m_0, m_1, \dots, m_M$  and constructing a standard

regression matrix-vector format for least squares estimation:

$$\begin{pmatrix} \Xi_0(i) \\ \Xi_1(i) \\ \vdots \\ \Xi_M(i) \end{pmatrix} \alpha + \begin{pmatrix} \rho_0(i) \\ \rho_1(i) \\ \vdots \\ \rho_M(i) \end{pmatrix} = \epsilon(i)$$

$$i = 1, 2, \dots, Q \quad (5.3.11)$$

where

$$\epsilon(i) = \begin{pmatrix} \epsilon_0(i) \\ \epsilon_1(i) \\ \vdots \\ \epsilon_M(i) \end{pmatrix}$$

Using standard least squares estimation, we can get estimates of the coefficients  $\hat{\alpha}_1, \hat{\alpha}_2, \dots, \hat{\alpha}_K$  for the autoregression model. Then we can easily obtain the frequency estimates using the following procedure: Construct the polynomial equation:

$$x^K - \hat{\alpha}_1 x^{K-1} + \hat{\alpha}_2 x^{K-2} - \dots + (-1)^K \hat{\alpha}_K = 0 \quad (5.3.12)$$

and solve this equation to get  $K$  roots, say  $x_1, x_2, \dots, x_K$ . Then we obtain the frequency estimates by taking the square root of these roots:  $\hat{\omega}_i = \sqrt{x_i}$  ( $i = 1, 2, \dots, K$ ).

The polynomial (5.3.12) is called the Prony polynomial in numerical analysis. The accuracy of the frequency estimates will depend upon the estimates of the model coefficient  $\hat{\alpha}_i$  and the root estimates of equation (5.3.12). The former is more essential. If any roots of (5.3.12) are negative or complex, they are regarded as outliers. In this case, the whole procedure fails to give the good results. In the next section we prove that the variance of the estimation error goes to zero as the signal-to-noise ratio goes to infinity.

## 5.4 Performance Analysis for Large SNR Circumstances

In the last section, we have proposed a parametric least squares algorithm for estimating frequencies of a received signal. Here, we will give the performance analysis for the parametric least squares method in large SNR cases. For large SNR assumption, we mean  $A_k \gg \sigma$  for each  $k$ . So, the noise term  $e(t)$  in the received signal  $y(t) = y_d(t) + e(t)$  is a very small component. Also, we make an assumption here that there is no numerical calculation error involved. Estimation bias is only caused by noise. In our analysis, we will approximate the original autoregression model and discard some high order small terms relating to noise  $e(t)$  whenever appropriate.

If there is no noise, i.e.,  $e(t) = 0$ , the received signal  $y(t)$  will obey the autoregressive model  $\Pi(p)$  exactly. When a noise  $e(t)$  exists, but the SNR is very large, the linear regression equation will give a coefficient estimate  $\hat{\alpha}$ , and  $\alpha - \hat{\alpha}$  is a small term due to the least squares estimation property. Solving the roots  $\hat{x}$  of the polynomial equation (5.3.12) and taking the squares root of  $\hat{x}$  will give the frequency estimates  $\hat{\omega}_k, k = 1, 2, \dots, K$ . The estimates will involve a small error  $\delta_k = \omega_k^2 - \hat{x}_k, k = 1, 2, \dots, K$ . Thus in the general case we can say that the estimation errors  $\delta_k$  are random variables depending upon the noise and are small terms comparing to the signal.

In the following analysis we define:

$$\hat{\Pi}(p) = \prod_{m=1}^K (p^2 + \hat{\omega}_m^2) = \prod_{m=1}^K (p^2 + \omega_m^2 + \delta_m) \quad (5.4.1)$$

Based upon the above argument, we can claim that the following equation approx-



imately holds:

$$\hat{\Pi}(p)[y(t)] \simeq 0 \quad (5.4.2)$$

Taking the Taylor expansion of (5.4.1) and neglecting the high order small terms, we have:

$$\hat{\Pi}(p) = \Pi(p) + \sum_{k=1}^K \delta_k \Pi_k(p) \quad (5.4.3)$$

where,

$$\Pi_k(p) = \prod_{\substack{j=1 \\ j \neq k}}^K (p^2 + \omega_j^2)$$

Discarding the high order small terms relating to  $\epsilon$  and  $\delta_k$ , we obtain the following equation:

$$\hat{\Pi}(p)[y(t)] = \sum_{k=1}^K \delta_k \Pi_k(p)[y_d] + \Pi(p)[\epsilon] = 0 \quad (5.4.4)$$

Using the parametric least squares method, we multiply both sides of (5.4.4) by the modulating function  $\phi_m(t)$  and employ the modulating property:

$$\sum_{l=1}^K \left[ \sum_{k=m}^{m+n} b_{k-m} \Pi_l(-jk\omega_0) \beta_k \right] \delta_k + \int \Pi[\epsilon(t)] \phi_m(t) = 0 \quad (5.4.5)$$

where

$$\beta_k = \int_0^T \sum_{i=1}^K A_i \sin(\omega_i t + \phi_i) e^{jk\omega_0 t} dt = \sum_{i=1}^K A_i f_{i,k}$$

Define:

$$\Pi_l(-jk\omega_0) = \prod_{\substack{r=1 \\ r \neq l}}^K (\omega_r^2 - k^2 \omega_0^2) \stackrel{\text{def}}{=} \eta_{k,l} \quad (5.4.6)$$

$$E_k = \int_0^T e(t) e^{jk\omega_0 t} dt \quad (5.4.7)$$

We can see that the  $E_k$  are complex Gaussian random variables with  $E(E_k) = 0$ ,  $\text{Var}(E_k) = \sigma^2 T$ .

Assume:

$$e_m = \sum_{k=m}^{m+n} b_{k-m} \Pi(-jk\omega_0) E_k$$

Utilizing these notations, equation (5.4.5) can be expressed by the format:

$$\sum_{l=1}^K \left[ \sum_{k=m}^{m+n} b_{k-m} \eta_{k,l} \beta_k \right] \delta_l = -e_m$$

$$m = m_0, m_1, m_2, \dots, m_M \quad (5.4.8)$$

We can represent the equation(5.4.8) as a standard linear vector-matrix form. If we choose  $m_i = i$ , then the regression form is very simple.

Define:

$$B \stackrel{\text{def}}{=} \begin{pmatrix} b_0\beta_0 & b_1\beta_1 & \dots & b_n\beta_n & & & \\ & b_0\beta_1 & \dots & b_{n-1}\beta_n & b_n\beta_{n+1} & & \\ & & \ddots & & & \ddots & \\ & & & b_0\beta_M & \dots & b_n\beta_{M+n} & \end{pmatrix}$$

$$\Gamma \stackrel{\text{def}}{=} \begin{pmatrix} \eta_{0,1} & \eta_{0,2} & \dots & \eta_{0,K} \\ \eta_{1,1} & \eta_{1,2} & \dots & \eta_{1,K} \\ \vdots & \vdots & \ddots & \vdots \\ \eta_{M+n,1} & \eta_{M+n,2} & \dots & \eta_{M+n,K} \end{pmatrix}$$

$$\epsilon = \begin{pmatrix} E_0 \\ E_1 \\ \vdots \\ E_{M+n} \end{pmatrix}$$

and assume:

$$\Psi \stackrel{\text{def}}{=} \begin{pmatrix} b_0\Psi_0 & b_1\Psi_1 & \dots & b_n\Psi_n & & & \\ & b_0\Psi_1 & \dots & b_{n-1}\Psi_n & b_n\Psi_{n+1} & & \\ & & \ddots & & & \ddots & \\ & & & b_0\Psi_M & \dots & b_n\Psi_{M+n} & \end{pmatrix} \quad (5.4.9)$$

where

$$\begin{aligned}\Psi_m &= \Pi(-jm\omega_0) \\ m &= 0, 1, 2, \dots, M\end{aligned}$$

Thus, equation (5.4.8) can be written as a standard matrix-vector regression form:

$$B\Gamma\delta = -\Psi\epsilon \quad (5.4.10)$$

Here,

$$\delta = \begin{pmatrix} \delta_1 \\ \delta_2 \\ \vdots \\ \delta_K \end{pmatrix}$$

It is easy to prove that  $B$  has full rank. So if  $\Gamma$  has full rank, we can solve for  $\delta$  explicitly:

$$\delta = -[(B\Gamma)^T(B\Gamma)]^{-1}(B\gamma\Psi)\epsilon \quad (5.4.11)$$

$\delta$  is a frequency estimation error and Equation (5.4.11) reveals an approximate relationship between the estimation error and the noise. It is easy to see that  $E(\delta) = 0$ . Thus our estimation algorithm gives unbiased estimates.

Also from above analysis we can see that  $\Gamma$  is a constant matrix. The elements of  $B$  depend upon the amplitudes  $A_i$ . The variance of  $\epsilon$  is  $O(\sigma^2)$ . Thus, for large SNR, i.e.,  $A_k/\sigma \rightarrow \infty$  for  $k = 1, 2, \dots, K$ , the variance of  $\delta$  will approach the zero matrix, i.e.,  $Var(\delta) \rightarrow 0$ .

The analysis up to now demonstrates that the frequency estimation errors are random variables depending upon the noise  $\epsilon$ . The SNR will determine the variance

of  $\delta$ . When the SNR is very large and approaches infinity, the variance of  $\delta$  is small and goes to zero.

## 5.5 Some Numerical Examples

Here we present some numerical examples which compare the modulating signal approach with the HOYW equation method, and evaluate the utility of the proposed algorithm for improving frequency estimation in various SNR circumstances.

**Example .** In this example, the analog angular frequencies, amplitudes and phases are given by:  $\omega_{a,1} = 50, \omega_{a,2} = 55, \omega_{a,3} = 100$ ;  $A_1 = A_2 = A_3 = 6$ ;  $\phi_1 = 0.123, \phi_2 = 0.541, \phi_3 = 0$ . The sampling frequency  $f_s$  is 100(Hz), measuring time  $T = 0.64$  seconds. So we have a total of  $N = 64$  points. The normalized frequencies are  $f_1 = 0.079Hz, f_2 = 0.0875Hz, f_3 = 0.1592Hz$  respectively. The  $\omega_i$  represent the normalized angular frequencies, i.e.,  $\omega_1 = 0.5, \omega_2 = 0.55, \omega_3 = 1.0$ . For testing and comparing the performance of the algorithms, we select the noise variance  $\sigma^2$  for producing the different signal-to-noise ratios.  $SNR_i$  is defined for each frequency component  $f_i$  as  $SNR_i = 10 \log_{10}(A_i^2/2\sigma^2)$ .

$K$  is chosen to be 3.  $\omega_0 = 2\pi/T = 9.82$ . We use one short time estimation and make the very common selection  $m_i = i$ . The integration(3.7) is approximated by the standard parabolic rule. Each  $m_i$  corresponds to a complex equation. Real and imaginary equations basically reveal similar frequency information of the data. So we can think them as one equation. The number of unknowns is 3. The minimum  $M$  needed is 3. The selection of  $M$  is important. Based upon the numerical experiments and our experience in using the modulating signal approach, we have found that the

optimal choice of  $M$  is around 6, i.e., making the number of equations double the total unknown parameters. This can be explained by the fact that as  $M$  increases from the minimum value needed for solving the equations, more data information is utilized until up to a certain frequency value beyond which frequency more noise will be involved in the data causing a deterioration of the LS estimator, see[Pear85]. The algorithm gives unbiased estimates in the case of  $SNR = +\infty$ .

The normalized error criterion for the frequency estimates is defined as:

$$VOE_j(dB) = 10 \log_{10} \left( \frac{N}{I_0} \sum_{i=1}^{I_0} (\omega_j^* - \hat{\omega}_{i,j})^2 \right)$$

where  $N$  is the total number of sampling points,  $j$  indicates the  $j^{th}$  frequency,  $\omega_j^*$  is the true frequency and  $\hat{\omega}_{i,j}$  is the estimate for the  $i^{th}$  Monte-Carlo run.  $I_0$  is the total number of runs. Based upon the theoretical analysis, the asymptotic normalized Cramèr-Rao lower bound(CRLB) is governed by the equation  $(24\sigma^2)/(A_i^2 N^2)$ , see [Stoi91]. The CRLB can be utilized to test the performance of the proposed algorithms.

Tables 5.1 and 5.2 show the normalized variance of  $\hat{\omega}_1$ ,  $\hat{\omega}_3$  estimates for several selected values of  $M$  and SNR based upon the total of 50 Monte-Carlo runs. From the tables we can see that the optimal selection of  $M$  is 6. As  $M$  becomes larger than 9, the  $VOE_i$  increases dramatically. For large SNR cases, the sensitivity in choosing the different  $M$  is low. From the tables, we can see that there is less than a 10(dB) difference in picking  $M = 6$  and  $M = 9$  for the SNR=30(dB) or SNR=40(dB) cases.

TABLE 5.1

NORMALIZED VARIANCE OF  $\hat{\omega}_1$  (IN DECIBELS)

M	$SNR_1 = 0(\text{dB})$	10(dB)	20(dB)	30(dB)	40(dB)
3	-5.7335	-7.9588	-21.9382	-28.4797	-49.9441
6	-11.4818	-23.3867	-27.5682	-35.8743	-54.6284
9	-11.3892	-15.9320	-19.3961	-30.4661	-48.8173
12	-9.8970	-13.9034	-16.6418	-27.7312	-46.661
14	-6.3752	-12.7231	-16.0842	-27.6992	-45.551

TABLE 5.2

NORMALIZED VARIANCE OF  $\hat{\omega}_3$  (IN DECIBELS)

M	$SNR_1 = 0(\text{dB})$	10(dB)	20(dB)	30(dB)	40(dB)
3	7.6042	4.9103	2.5681	-6.3952	-10.7561
6	-11.3122	-26.1734	-32.8596	-38.6037	-57.4839
9	4.0824	-12.3958	-20.6769	-30.2958	-48.5842
12	10.5268	7.4328	-14.5609	-20.5128	-39.4813
14	13.6248	12.9028	9.5663	-3.9128	-21.4812

Regarding the HOYW algorithm, the fact that we only have 64 points and 3 unknown frequencies will lead to a poor autocorrelation estimate and increase the difficulty in attaining frequency root separation if  $L$  and  $L_1$  are too large. We selected  $L = 18$ ,  $L_1 = 20$  in using the HOYW equations. This is a fairly good selection in this case. Fig.5.1(a-c) and Fig.5.2(a-c) present the normalized variance and bias of  $\hat{\omega}_1$ ,  $\hat{\omega}_2$ ,  $\hat{\omega}_3$ , using the proposed modulating signal approach and HOYW equations based upon the total of 50 Monte-Carlo runs. The theoretical Cramèr-Rao lower bound is also shown for easy comparison. From the simulations we can see that our algorithm is much more robust and gives reasonable results even for negative

SNR(dB). Comparing to the HOYW equation method, the variance of the frequency estimates of our modulating signal approach is much close to the CRLB in most cases. For the case of SNR=-10(dB), approximately one out of eight runs failed because of complex or negative roots. These were regarded as outliers and were removed from the least squares estimation. For SNR=-5(dB), roughly one out of fifteen runs failed to give a good result. For SNR=0(dB), only one run broke up.

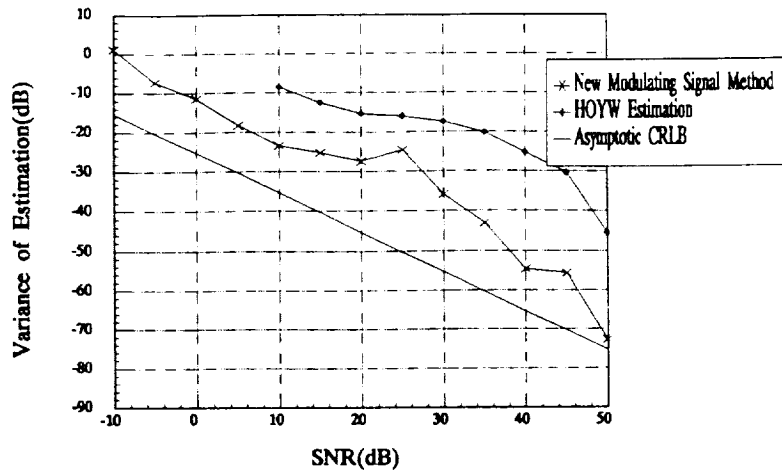


Fig.5.1(a) The variance of estimation of  $\omega_1$  in different SNR cases.

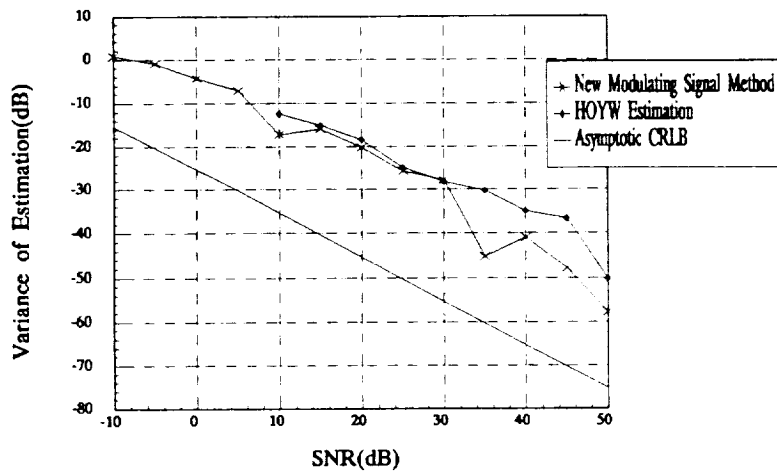


Fig.5.1(b) The variance of estimation of  $\omega_2$  in different SNR cases.

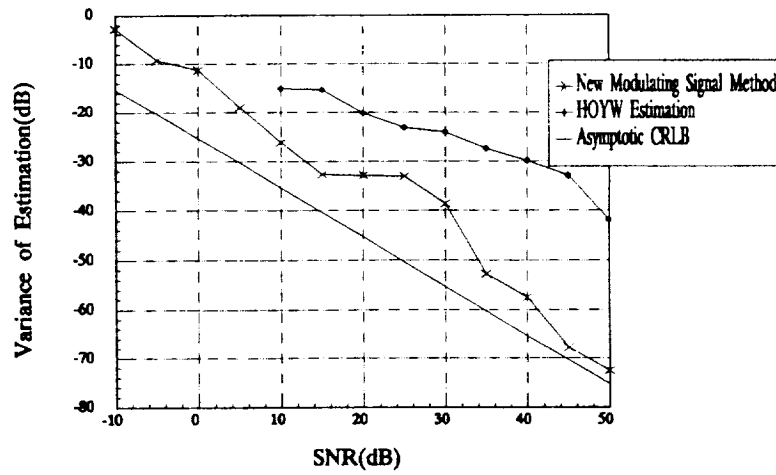


Fig.5.1(c) The variance of estimation of  $\omega_3$  in different SNR cases.



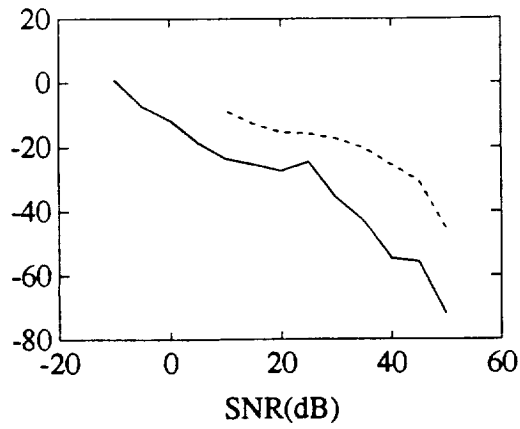


Fig.5.2(a) The estimation bias(dB) verses different SNR for  $\omega_1$ . Solid line for the modulating function method, dot line for the HOYW.

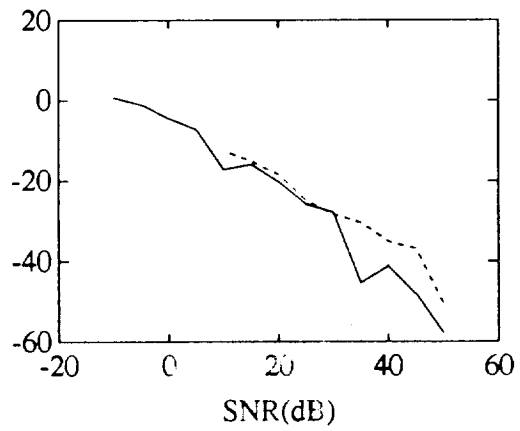


Fig.5.2(b) The estimation bias(dB) verses different SNR for  $\omega_2$ . Solid line for the modulating function method, dot line for the HOYW.

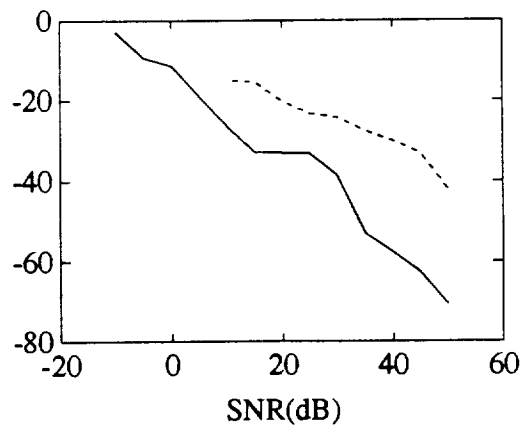


Fig.5.2(c) The estimation bias(dB) verses different SNR for  $\omega_3$ . Solid line for the modulating function method, dot line for the HOYW.

The HOYW equation method cannot identify the normalized frequencies 0.5 and 0.55 for SNR smaller than 5(dB). Fig.5.3 demonstrates the power spectrum of the identified whitening filter(mean value) for  $SNR = 0$ (dB). From the graph we can see that there is only one peak around the middle of the 0.5 and 0.55 frequencies. The HOYW algorithm mixes the two frequencies and only gives one frequency estimation. Also, there are several spurious frequencies having larger power than the true frequencies, which makes the root separation of  $A(z)$  and  $B(z)$  much more difficult and even impossible.

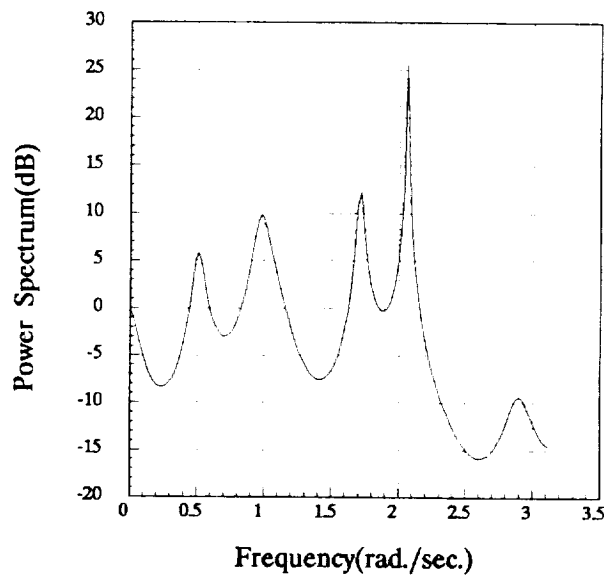


Fig.5.3. Power spectrum of the estimated filter  $1/C(z^{-1})$  using the HOYW equations for  $SNR=0$ (dB).

If the FFT or periodogram is utilized to identify the frequencies, the minimum resolving frequency is guided by the formula  $\Delta f = f_s/N$ , which is 1.56(Hz) or 9.8(rad./sec.) in our case. So the frequencies 50 and 55 will be recognized as one frequency and cannot be distinguished.

From our simulations, we have also found that the selection of  $\omega_0$  is important. As discussed earlier,  $\omega_0$  is actually a frequency resolution related parameter. Suppose we know the minimum distance between two frequencies is  $\Delta\omega$ .  $\omega_0$  should not be too much larger than  $\Delta\omega$  otherwise the resolution will not be high enough and closer frequencies may not be distinguished by the algorithm.  $\omega_0$  is related to the length of each shot. So the above argument means that the measuring time interval should not be too small. Selection of  $\omega_0$  should not be too small either. Too small  $\omega_0$  will cause the algorithm to require picking a large  $M$  for covering a sufficiently large frequency band which will not help in increasing the frequency resolution. Based upon our simulation we have found that the optimal choice of  $\omega_0$  is around the range of  $0.4\Delta\omega \sim 2.5\Delta\omega$ .

Therefore the time interval used for each shot formulation should not be too large. If we get a large measuring time interval  $T$ , the best way to utilize this large data set is to divide it into several shots for making the length of each shot appropriate. So we can construct a more robust algorithm as well as obtaining the optimal resolving frequency  $\omega_0$ .

For testing the performance of using different resolving frequencies, we sampled the signal up to  $T = 3$  seconds. We divide this three second signal into  $i$  disjoint sections.  $i = 1$  means that we use whole data set as one shot;  $i = 2$  means that we separate the whole data set into two shots, and etc. The resolving frequencies utilized for  $i$  disjoint

separations is equal to  $2\pi i/3$ . We chose  $i = 1, 2, \dots, 7$  and tested the algorithm in the different SNR circumstances. Fig.5.4(a-c) show the simulation results for frequency  $\omega_2$  and  $\omega_3$ . From the figures we can see that the best result is obtained by selecting  $\omega_0$  around 8.5(rad./sec.), i.e., dividing the whole data set into four disjoint shots. Also, the selection of  $\omega_0$  is not very sensitive, especially in high SNR cases.

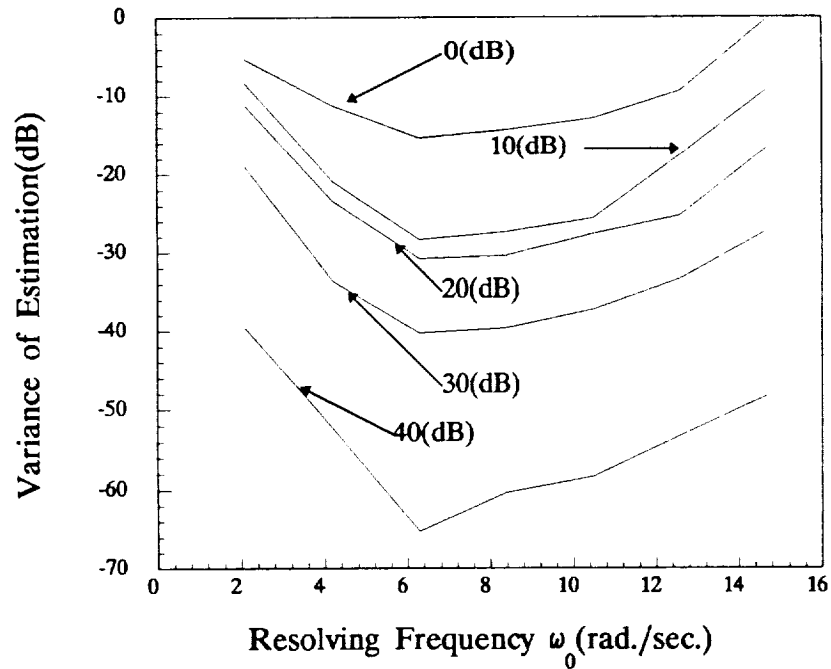


Fig.5.4(a) Variance of estimation of  $\omega_1$  against resolving frequency  $\omega_0$  in different SNR cases.

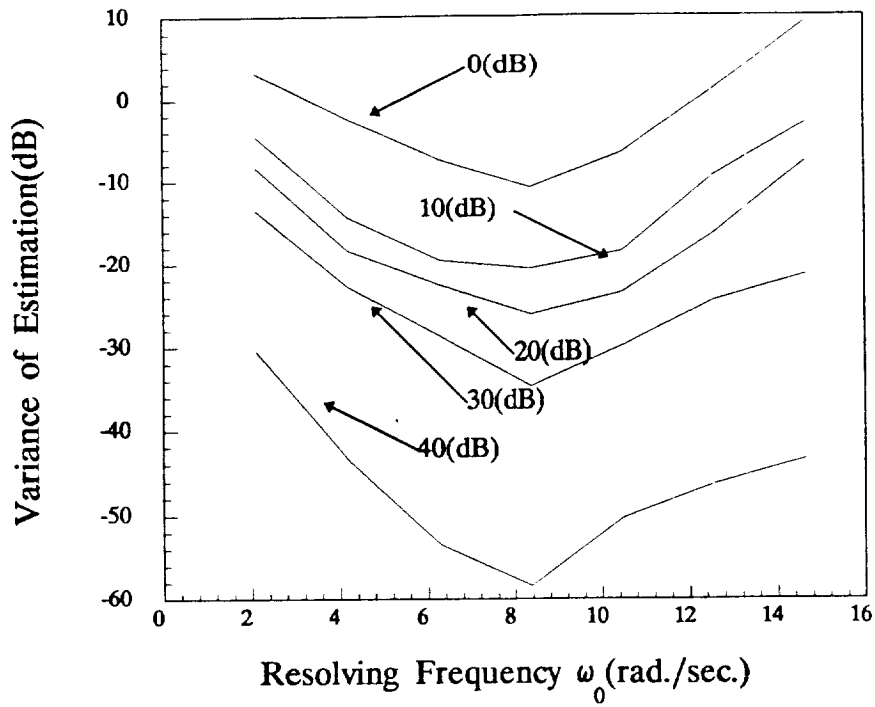


Fig.5.4(b) Variance of estimation of  $\omega_2$  against resolving frequency  $\omega_0$  in different SNR cases.

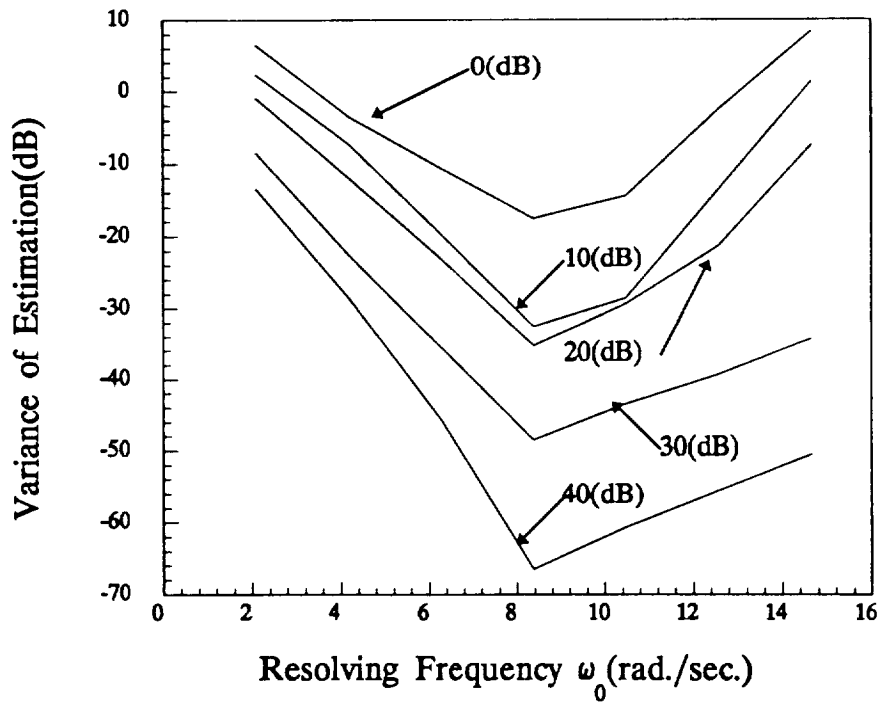


Fig.5.4(c) Variance of estimation of  $\omega_3$  against resolving frequency  $\omega_0$  in different SNR cases.

**Example 2.** In the second example, the received signal is composed of four sinusoids. The analog angular frequencies, amplitudes and phases are given by:  $\omega_{a,1} = 40$ ,  $\omega_{a,2} = 50$ ,  $\omega_{a,3} = 60$ ,  $\omega_{a,4} = 70$ ;  $A_1 = A_2 = A_3 = A_4 = 5$ ;  $\phi_1 = 0$ ,  $\phi_2 = 0.872$ ,  $\phi_3 = 1.537$ ,  $\phi_4 = 1.975$ . The sampling frequency  $f_s$  is 100(Hz). The measuring time  $T$  is 1.28 seconds. So we have total of  $N = 128$  points. The normalized frequencies are 0.06366(Hz), 0.07958(Hz), 0.09549(Hz) , 0.11141(Hz).  $K$  is selected as 4.  $\omega_0 = 2\pi/T = 4.91$ . We utilize one-shot time estimation and let  $m_i = i$  for simplicity. There are four unknown parameters.  $M$  is chosen to be 8. Reasoning the same as before, we select  $L = 20$ ,  $L_1 = 25$  for using the HOYW equations. It is very good selection for the HOYW algorithm.

Fig.5.5(a-d) give the plots of normalized variances of estimates  $\hat{\omega}_i$ ,  $i = 1, 2, 3, 4$  using the modulating signal method and the HOYW equations based upon the total of 50 Monte-Carlo runs. Also the theoretical Cramèr-Rao lower bound is presented for easy comparison. Same as example 1, the HOYW equations cannot identify the four frequencies for SNR lower than 5(dB). Fig.6 shows the power spectrum of estimated predictive filter for SNR=0(dB). From the graphs we can see that there are only two high peaks around frequencies 0.4 to 0.7. Also there are two high spurious peaks at other frequencies. These high spurious peaks will increase the difficulty in recognizing the true frequencies.

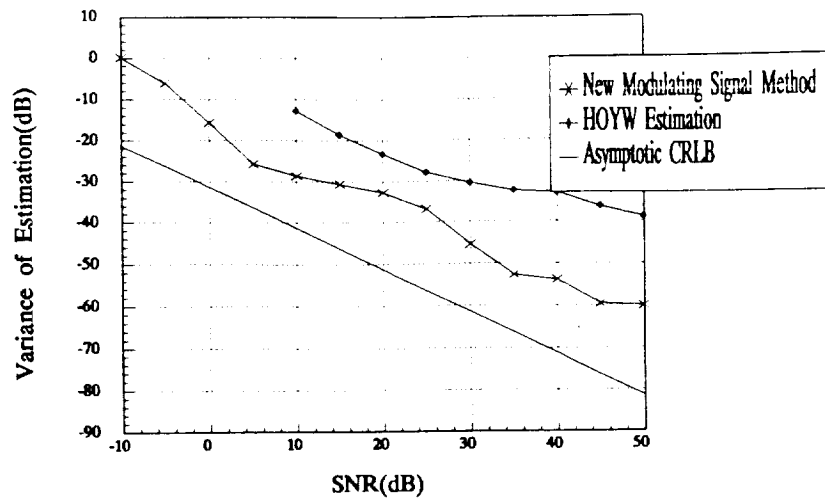


Fig.5.5(a) The variance of estimation of  $\omega_1$  in different SNR cases.

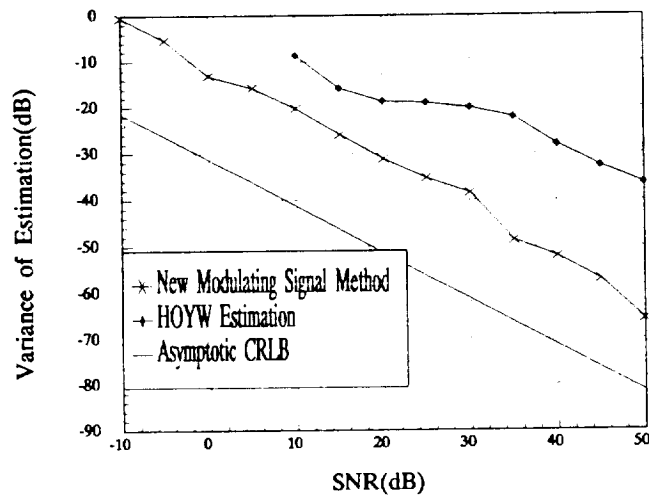


Fig.5.5(b) The variance of estimation of  $\omega_2$  in different SNR cases.

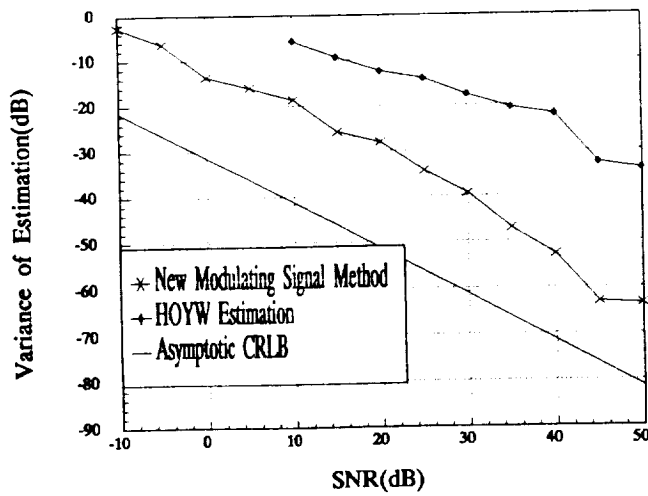


Fig.5.5(c) The variance of estimation of  $\omega_3$  in different SNR cases.

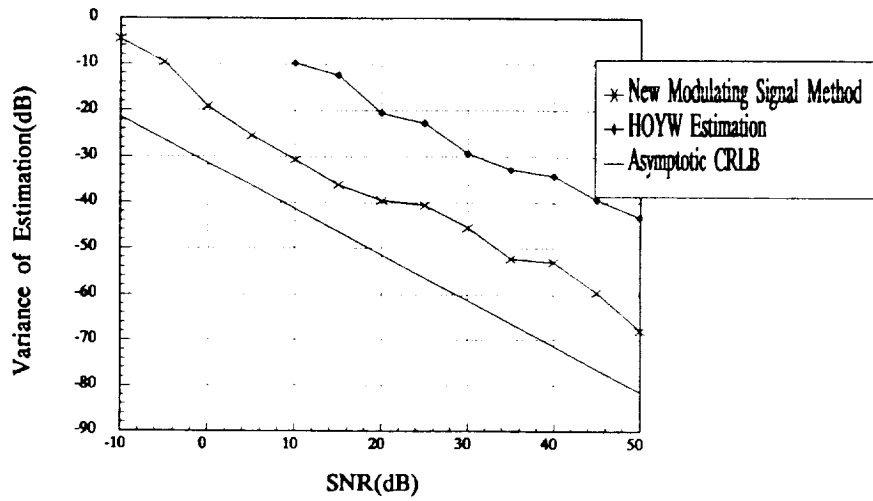


Fig.5.5(d) The variance of estimation of  $\omega_4$  in different SNR cases.

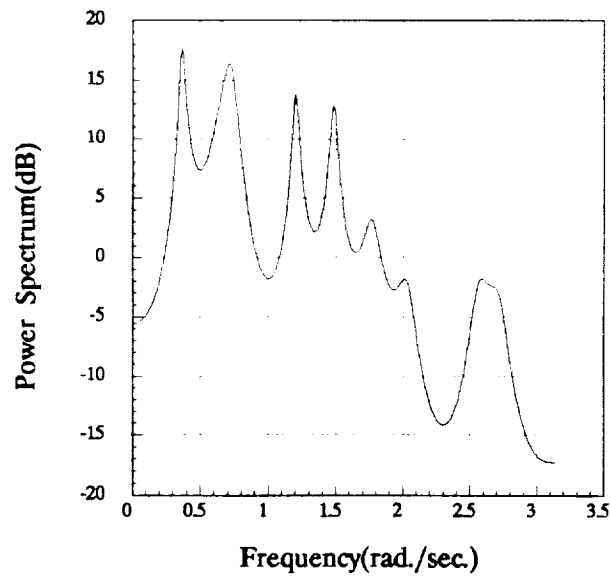


Fig.5.6 Power spectrum of the estimated filter  $1/C(z^{-1})$  using the HOYW equations for SNR=0(dB)



## 5.6 Concluding Remarks

We have proposed a new algorithm for high resolution frequency estimation using the Fourier based sinusoidal modulating function technique. A continuous autoregressive differential equation model was used for the analysis. The complex sinusoidal modulating signal was constructed for projecting the model into linear algebraic equations. Comparing with the HOYW equations, the new algorithm gave better performance, especially for short time observation and low SNR data.

## **Chapter 6**

# **Deconvolution and Parameter Identification for Noncausal Nonminimum Phase ARMA Systems Using Inverse Cumulants**

### **6.1 Introduction**

Linear time-invariant system modeling, nonminimum phase system deconvolution and identification play a very important role in adaptive process control, system theory, signal processing and data communication. Methods abound for system modeling and identification via the second order statistics, i.e., autocorrelation and power spectrum [Sode89, Ljun87, BoxG70], and inverse autocorrelations can be used to estimate the coefficients of MA models driven by random Gaussian input processes [Chat79, Clev72]. Although the first and second order statistics which characterize a random

Gaussian process are quite useful tools in many practical applications, the problem of using only second order moments is that it is phase blind. Hence only the minimum phase, power spectral equivalent modes of the system can be identified.

Recently, some researchers have used higher order statistics ( bispectrum, trispectrum, etc. ) for estimating the parameters of linear rational transfer functions [Bril67, Gian89, Niki87, Frie89] . It is well-known that high order statistics are phase sensitive, and contain information of the true phase response as well as magnitude response of the linear system. Also, the high order statistics are insensitive to Gaussian noise, which is a very important property and has many practical applications, e.g., signal detection in large Gaussian white noise background. Comparing to the second order moments, the high order statistics can be employed for identifying and reducing non-minimum phase systems, estimating the parameters of non-Gaussian processes, and modeling nonlinear systems.

In this chapter, we focus on the issues of system deconvolution and parameter identification. Currently, Chiang and Nikias [Chia90, Niki87] use a noncausal AR process to approximate a finite FIR system and construct certain linear equations with respect to the parameters of an AR process based upon the third order cumulants. They invoke some adaptive gradient-type algorithms to solve these equations in obtaining estimates of the parameters. The problem is that their method cannot be applied to infinite IIR systems.

Here we are interested in the deconvolution and parameter identification of a general SISO noncausal nonminimum phase ARMA system driven by a random non-Gaussian process. Although in system theory and signal processing, causal system modeling is commonly used, noncausal ARMA system will also be necessary for char-

acterizing many processes in practice. Except for the very special case of a symmetric noncausal system, the high order statistics will play a crucial rule in identifying the system ( phase response as well as magnitude response ).

We introduce the inverse polyspectra and inverse cumulants which are reciprocals of the polyspectra and cumulants of an original process. It is a natural generalization of the definition of inverse power spectrum and inverse autocorrelation [Chat79, Clev72]. It will be demonstrated that there is duality between cumulants and inverse cumulants which corresponds to the duality between the AR modes and MA modes of the system. For a general noncausal ARMA system, the inverse filter has been constructed by utilizing a noncausal AR model to approximate the original process. Then a relationship can be established between the inverse cumulants and the parameters of the inverse filter which is unique to within a scale factor. For achieving good numerical performance, we use a gradient type nonlinear optimization algorithm to minimize an error function for matching the inverse cumulants and the parameters of the AR model.

The algorithms are proposed to estimate the inverse cumulants using both frequency domain and time domain formulations. The advantage of estimating the inverse cumulants in the frequency domain is that the numerically efficient FFT technique is available and no equations need to be solved. But the price we pay is that the algorithm is less robust in the low signal-to-noise ratios(SNR) situation. For estimating the inverse cumulants in the time domain, some linear equations in terms of inverse cumulants have been derived for using the least squares technique. We use the forward regression orthogonal algorithm suggested in [Bill89] to solve the least squares problem because only part of the unknowns need to be estimated. The algorithm can be used to estimate a subset of the parameters, and computation time can

be saved. With adoption of the steepest gradient type optimization algorithm, the parameters of the AR filter can be identified adaptively.

This chapter is arranged as follows. In section 6.2, we review the background about cumulants and polyspectra and give the problem statements. In section 6.3, the definitions are given of the inverse polyspectra and inverse cumulants. Section 6.4 provides some algorithms for estimating these quantities, deconvolving and identifying the nonminimum phase system based on the inverse cumulants estimated both in the frequency and time domain. In section 6.5, some computer simulation results are presented. Section 6.6 is concluding remarks.

## 6.2 Background and Problem Statements

In this section, we give the problem statements and present some preliminary definition and results related to the cumulants and polyspectra before giving the definition of the inverse cumulants. For a rigorous definition of the cumulants, we recommend [Rose85] to the reader.

The scalar output signal  $\{y(t)\}$  is assumed to be a zero mean stationary, discrete time process, described by the following noncausal linear ARMA model:

$$\sum_{k=-M^-}^{M^+} a_k y(t-k) = \sum_{k=-N^-}^{N^+} b_k u(t-k) \quad (6.2.1)$$

where  $u(t)$  satisfies the condition (6.2.4) specified below.

Equation (6.2.1) can also be expressed equivalently by the impulse response ver-

sion:

$$y(t) = \sum_{k=-\infty}^{k=+\infty} h(k)u(t-k) \quad (6.2.2)$$

The third and fourth order cumulants contain sufficient information to characterize the magnitude and phase of the system. For a zero mean stationary process  $y(t)$ , the  $k$ th order cumulants of  $y(t)$ ,  $k = 1, 2, 3, 4$ , can be computed via the following equations:

$$\begin{aligned} c_1^y &= E\{y(i)\} = 0 \\ c_2^y(m) &= E\{y(i)y(i+m)\} \\ c_3^y(m_1, m_2) &= E\{y(i)y(i+m_1)y(i+m_2)\} \\ c_4^y(m_1, m_2, m_3) &= E\{y(i)y(i+m_1)y(i+m_2)y(i+m_3)\} \\ &\quad - c_2^y(m_1)c_2^y(m_2-m_3) - c_2^y(m_2)c_2^y(m_3-m_1) \\ &\quad - c_2^y(m_3)c_2^y(m_1-m_2) \end{aligned} \quad (6.2.3)$$

Suppose the system (6.2.1) satisfies the following modeling assumptions. The input driving signal  $u(t)$  is stationary, non-Gaussian, zero mean i.i.d. ,  $Eu(t)u(t+\tau) = \sigma^2\delta(\tau)$ , and with the  $k$ th order cumulants  $\gamma_k^u$ ,  $0 < |\gamma_k^u| < \infty$ ,  $k \geq 3$ :

$$c_k^u(m_1, m_2, \dots, m_{k-1}) = \gamma_k^u \delta(m_1)\delta(m_2)\dots\delta(m_{k-1}) \quad (6.2.4)$$

where  $\delta(m_i)$  is the Kronecker delta function.  $u(t)$  has a  $k$ th order flat polyspectra, and is not accessible in the identification scheme.

Also, we assume that the ARMA model (6.2.1) with parameters  $\theta = \{a_{-M-}, \dots, a_{M+}, b_{-N-}, \dots, b_{N+}\}$  is generally nonminimum phase , i.e. the system has some zeros inside and outside the unit circle, free of pole zero cancellations. The system may have some poles outside the unit circle. These poles correspond to the noncausal modes.

The transfer function of the system (6.2.1) is

$$H(z) = \sum_{k=-\infty}^{k=+\infty} h(k)z^{-k} = \frac{\sum_{k=-N^-}^{N^+} b_k z^{-k}}{\sum_{k=-M^-}^{M^+} a_k z^{-k}} = \frac{B(z)}{A(z)} \quad (6.2.5)$$

The region of convergence is a ring including the unit circle  $\rho_0 < |z| < \rho_1$ .  $\rho_0$  is the maximum amplitude of the poles inside the unit circle,  $\rho_1$  is the minimal amplitude of the poles outside of the unit circle. We assume that the system does not have any poles and zeros on the unit circle, i.e.  $A(z)B(z) \neq 0$  for  $|z| = 1$ .

The problem is to identify the system transfer function  $H(e^{j\omega})$  ( phase response as well as magnitude response ) and reconstruct the input signal  $u(t)$  using only output data  $y(t)$ . The method we utilize here is to introduce the inverse cumulants and approximate the original noncausal ARMA system via the AR model. There exists a direct relationship between the inverse cumulants and the parameters of the AR model, and the inverse cumulants can be estimated easily in the frequency domain using an FFT algorithm and in the time domain by solving a least squares problem using an efficient forward regression orthogonal algorithm. By this means, the original system can be characterized exactly by the AR model, and the input signal can be estimated by deconvolving this inverse filter with output signal  $y(t)$ . In the following, we present some basic facts about cumulants for later use.

Denoting the  $k$ th order cumulants of  $y(t)$  by  $c_k^y(m_1, m_2, \dots, m_{k-1})$ , and assuming that  $\sum_{m_1, \dots, m_{k-1}} |c_k^y(m_1, m_2, \dots, m_{k-1})| < +\infty$ , then the  $k$ th order polyspectra exists and is defined as:

$$S_k^y(\omega_1, \omega_2, \dots, \omega_{k-1}) = \sum_{m_1, \dots, m_{k-1}=-\infty}^{+\infty} c_k^y(m_1, m_2, \dots, m_{k-1}) e^{-j \sum_{i=1}^{k-1} \omega_i m_i} \quad (6.2.6)$$

Because  $u(t)$  is a  $k$ th order white, it is easy to verify from (6.2.4) that :

$$S_k^u(\omega_1, \omega_2, \dots, \omega_{k-1}) = \gamma_k^u = \text{constant} \quad (6.2.7)$$

The  $k$ th order cumulants  $c_k^y(m_1, m_2, \dots, m_{k-1})$  can be calculated in terms of the  $k$ th order polyspectra:

$$c_k^y(m_1, \dots, m_{k-1}) = \frac{1}{(2\pi)^{k-1}} \int_{-\pi}^{\pi} \dots \int_{-\pi}^{\pi} S_k^y(\omega_1, \omega_2, \dots, \omega_{k-1}) e^{j \sum_{i=1}^{k-1} \omega_i m_i} d\omega_1 d\omega_2 \dots d\omega_{k-1} \quad (6.2.8)$$

From equ.(6.2.5), the  $k$ th order cumulants can also be represented in terms of the system impulse response as :

$$c_k^y(m_1, m_2, \dots, m_{k-1}) = \gamma_k^u \sum_{i=-\infty}^{+\infty} h(i)h(i+m_1) \dots h(i+m_{k-1}) \quad (6.2.9)$$

Taking the  $Z$ -transform of equ.(6.2.9), we can get the following expression :

$$S_k^y(z_1, z_2, \dots, z_{k-1}) = \gamma_k^u H(z_1)H(z_2) \dots H(z_{k-1})H((z_1 z_2 \dots z_{k-1})^{-1}) \quad (6.2.10)$$

So,

$$S_k^y(z_1, z_2, \dots, z_{k-1}) = \gamma_k^u \frac{B(z_1)B(z_2) \dots B(z_{k-1})B((z_1 z_2 \dots z_{k-1})^{-1})}{A(z_1)A(z_2) \dots A(z_{k-1})A((z_1 z_2 \dots z_{k-1})^{-1})} \quad (6.2.11)$$

It will be seen in the next two sections that equation (6.2.11) is important in the role of the inverse cumulants.

### 6.3 The Inverse Cumulants

In this section, we give the basic definition of the inverse cumulants and describe the relations between the inverse cumulants and the original ARMA system. Its



application with deconvolution and parameter identification will be presented in the next section.

For the system (6.2.1) or (6.2.2), with  $k$ th order cumulants (6.2.9) and  $k$ th order polyspectra (6.2.10) (6.2.11), we define the inverse cumulants and inverse polyspectra by simply looking for the inverse of expression (6.2.10) or (6.2.11). Thus the  $k$ th order inverse polyspectra  $SI_k^y(z_1, z_2, \dots, z_{k-1})$  is defined as :

$$S_k^y(z_1, z_2, \dots, z_{k-1})SI_k^y(z_1, z_2, \dots, z_{k-1}) = 1 \quad (6.3.1)$$

The coefficient of  $z_1^{-m_1} z_2^{-m_2} \dots z_{k-1}^{-m_{k-1}}$  of  $SI_k^y(z_1, z_2, \dots, z_{k-1})$  will be called the  $k$ th order inverse cumulants at lag  $m_1, m_2, \dots, m_{k-1}$ , and will be denoted by  $ci_k^y(m_1, m_2, \dots, m_{k-1})$ .  $ci_k^y(m_1, m_2, \dots, m_{k-1})$  and  $SI_k^y(z_1, z_2, \dots, z_{k-1})$  are related by the  $Z$ -transform.

Noting equations (6.2.8) and (6.2.11), the following equation holds.

$$ci_k^y(m_1, m_2, \dots, m_{k-1}) = \frac{1}{(2\pi)^{k-1}} \int_{-\pi}^{\pi} \dots \int_{-\pi}^{\pi} \frac{A_k(e^{j\omega_1}, e^{j\omega_2}, \dots, e^{j\omega_{k-1}})}{\gamma_k^u B_k(e^{j\omega_1}, e^{j\omega_2}, \dots, e^{j\omega_{k-1}})} e^{-j \sum_{i=1}^{k-1} \omega_i m_i} d\omega_1 d\omega_2 \dots d\omega_{k-1} \quad (6.3.2)$$

Because we assume that the ARMA model (6.2.1) does not have zeros and poles on the unit circle, the righthand sides of (6.2.8) and (6.3.2) are integrable. The inverse cumulants based on equ. (6.3.2) are well-defined.

For the ARMA model (6.2.1), by interchanging MA modes with AR modes, we can construct another noncausal ARMA process:

$$\sum_{k=-N^-}^{N^+} b_k w(t-k) = \sum_{k=-M^-}^{M^+} a_k \varepsilon(t-k) \quad (6.3.3)$$

where the input driving signal  $\varepsilon(t)$  is an i.i.d., zero mean, non-Gaussian process. It has the flat  $k$ th order polyspectra.

$$S_k^\varepsilon(\omega_1, \omega_2, \dots, \omega_{k-1}) = \gamma_k^\varepsilon = \frac{1}{\gamma_k^u} \quad (6.3.4)$$

The  $k^{\text{th}}$  order cumulants are:

$$c_k^\varepsilon(m_1, m_2, \dots, m_{k-1}) = \frac{1}{\gamma_k^u} \delta(m_1) \delta(m_2) \dots \delta(m_{k-1}) \quad (6.3.5)$$

The output signal  $w(t)$  is a stationary, zero mean, ergodic process. It is easy to verify that the  $k$ th order cumulants of  $w(t)$  are the  $k$ th order inverse cumulants of  $y(t)$ , i.e. ,

$$c_k^w(m_1, m_2, \dots, m_{k-1}) = c_k^y(m_1, m_2, \dots, m_{k-1}) \quad (6.3.6)$$

Also,  $w(t)$  has the  $k$ th order polyspectra equal to  $\frac{A_k(e^{j\omega_1}, e^{j\omega_2}, \dots, e^{j\omega_{k-1}})}{\gamma_k^u B_k(e^{j\omega_1}, e^{j\omega_2}, \dots, e^{j\omega_{k-1}})}$ .  $A_k$  and  $B_k$  are the denominator and numerator of the r.h.s. of equ.(6.2.11) .

Model (6.3.3) shows the important dual property between the cumulants and inverse cumulants. It demonstrates that reversing the signal flow through the ARMA system will generate the  $k$ th order cumulants which are the inverse cumulants of the original system.

## 6.4 Inverse Cumulants Based Algorithms for System Deconvolution and Parameter Identification

In the previous section we introduced the inverse cumulants. Here we use the non-causal autoregressive model to approximate the original system. Also, algorithms are presented for estimating the inverse cumulants, identifying and deconvolving the system both in the frequency domain and time domain. We demonstrate more details in the following.

Given the output stationary signal  $\{y(t), t = 0, 1, 2, \dots\}$  generated from the model (6.2.1), we can always design a noncausal AR process for characterizing the original model and deconvolving the received signal  $y(t)$ :

$$u(t) = \beta_0 y(t) + \sum_{i=-\infty}^{-1} \beta_i y(t-i) + \sum_{i=1}^{+\infty} \beta_i y(t-i) \quad (6.4.1)$$

Denoting:

$$\Phi(z) = \sum_{i=-\infty}^{+\infty} \beta_i z^{-i} \quad (6.4.2)$$

Assuming  $\beta_0 = 1.0$ ,  $\Phi(z)$  is the deconvolution filter. The original model (6.2.1) will be rewritten as a noncausal AR filter:

$$\frac{1}{\Phi(z)} = \frac{B(z)}{A(z)} \quad (6.4.3)$$

Noting the equations (6.2.11, 6.3.1, 6.4.3), we have:

$$SI_k^y(z_1, z_2, \dots, z_{k-1}) = \frac{1}{\gamma_k^u} \Phi(z_1) \Phi(z_2) \dots \Phi((z_1 z_2 \dots z_{k-1})^{-1}) \quad (6.4.4)$$

Equation (6.4.4) reveals the fact that within a scale ambiguity the  $k^{th}$  order inverse

cumulants of  $y(t)$  are the same as the  $k^{\text{th}}$  order cumulants of  $w(t)$  generated by the deconvolution filter  $\Phi(z)$ .

$\Phi(z)$  has to be truncated for practical realization. So define:

$$\hat{\Phi}(z) = \sum_{-M}^N \beta_i z^{-i}$$

$$(\beta_{-M} \neq 0, \beta_0 = 1)$$
(6.4.5)

$\hat{\Phi}(z)$  will approximate the deconvolution filter. Generally speaking, the choice of  $M$  and  $N$  will depend upon the location of the zeros of the ARMA system (6.2.1). The closer the zeros to the unit circle, the larger the  $M$  and  $N$  will have to be chosen for a good approximation.

It follows immediately that the parameters  $\beta_i$  obey the following equation:

$$c_k^y(m_1, m_2, \dots, m_{k-1}) = \frac{1}{\gamma_k^y} \sum_{i=-M}^{N-m_{k-1}} \beta_i \beta_{i+m_1} \dots \beta_{i+m_{k-1}}$$

$$0 \leq m_1 \leq m_2 \leq \dots \leq m_{k-1} \leq (M + N)$$
(6.4.6)

Using the symmetric properties, we can refer to the cumulants at other lags. For the third order cumulants, the following symmetric condition holds:

$$c_3(m_1, m_2) = c_3(m_2, m_1) = c_3(-m_1, m_2 - m_1)$$

$$= c_3(m_2 - m_1, -m_1) = c_3(m_1 - m_2, -m_2) = c_3(-m_2, m_1 - m_2)$$

$$-(M + N) \leq m_1, m_2 \leq (M + N)$$
(6.4.7)

The nonredundant cumulant samples lie on the triangle described by  $0 \leq m_1 \leq m_2 \leq M + N$ .

To minimize numerical sensitivity and achieve good performance in estimating the parameters  $\beta_i$  of the inverse filter using equation (6.4.6), we construct the following objective function for matching the inverse cumulants:

$$J(\theta) = \sum_{m_{k-1}=0}^{\frac{2}{3}(M+N)} \dots \sum_{m_1=0}^{m_2} e(m_1, m_2, \dots, m_{k-1})^2 \quad (6.4.8)$$

where,

$$e(m_1, m_2, \dots, m_{k-1}) = ci_3(m_1, m_2, \dots, m_{k-1}) - \frac{1}{\gamma_k^u} \sum_{i=-M}^{N-m_{k-1}} \beta_i \beta_{i+m_1} \dots \beta_{i+m_{k-1}}$$

here,  $\beta_0 = 1$ ,  $\theta = [\beta_{-M}, \dots, \beta_{-1}, \beta_1, \dots, \beta_N, \gamma_k^u]^T$ . The character  $y$  has been omitted for easy notation. Here, we only use a center part of the inverse cumulants for our matching because a larger error will be involved for the estimates of the inverse cumulants close to the boundary due to the boundary effects.

Let  $\beta_j = 0$  for  $j < -M$  or  $j > N$ . For the case of using third order inverse cumulants, e.i.,  $k = 3$ , the derivative of  $J$  with respect to  $\beta_l$  ( $-M \leq l \leq N$ ,  $l \neq 0$ ), is:

$$\frac{\partial J}{\partial \beta_l} = -2\gamma \sum_{m_2=0}^{\frac{2(M+N)}{3}} \sum_{m_1=0}^{m_2} e(m_1, m_2) (\beta_{l+m_1} \beta_{l+m_2} + \beta_{l-m_1} \beta_{l-m_1+m_2} + \beta_{l-m_2} \beta_{l+m_1-m_2}) \quad (6.4.9)$$

where  $\gamma = 1/\gamma_3^u$ .

Taking the derivative of  $J$  with respect to  $\gamma$ , and setting the equation to zero,  $\gamma$  can easily be estimated in terms of other parameters:

$$\hat{\gamma} = \frac{\sum_{m_2=0}^{\frac{2(M+N)}{3}} \sum_{m_1=0}^{m_2} ci_3(m_1, m_2) (\sum_{i=-M}^{N-m_2} \beta_i \beta_{i+m_1} \beta_{i+m_2})}{\sum_{m_2=0}^{\frac{2(M+N)}{3}} \sum_{m_1=0}^{m_2} (\sum_{i=-M}^{N-m_2} \beta_i \beta_{i+m_1} \beta_{i+m_2})^2} \quad (6.4.10)$$

By this means, we can reduce the total number of unknowns by one dimension.

Also, the initial value guess is important for gradient based schemes to achieve

good results. Based on (6.4.6), very roughly we have the following equation:

$$ci_3(M + N, M + j) \approx \frac{1}{\gamma_3^u} \beta_{-M} \beta_N \beta_j \quad (6.4.11)$$

So, it is easy to see that:

$$\beta_j \approx \frac{ci_3(M + N, M + j)}{ci_3(M + N, 0)} \beta_{-M} = f ci_3(M + N, M + j) \quad (6.4.12)$$

$$j = -M, -M + 1, \dots, 0, \dots, N$$

$\beta_0 = 1$  can be utilized to determine the unknown constant  $f$ . Thus, we can use the following form to guess the initial values although sometimes it is not quite satisfactory:

$$\beta_j^{(0)} = \frac{ci_3(M + N, M + j)}{ci_3(M + N, M)} \quad (6.4.13)$$

$$j = -M, -M + 1, \dots, 0, \dots, N$$

We comment that the problem of stability does not arise because the deconvolution AR filter is basically noncausal. We can always identify any unstable causal poles as the stable anticausal poles. The only assumption about the underlying system is that it has no poles or zeros on the unit circle.

In the above development, it has been assumed that the inverse cumulants are already available. In practice, what we can get at hand is the received signal  $y(t)$  or sampled cumulants. We need to estimate the inverse cumulants using these quantities. In the following two subsections, we provide the algorithms to calculate the inverse cumulants both in the frequency and time domains.

## 6.4.1 Inverse Cumulants Estimation in the Frequency

### Domain

Suppose we are given the measurements of the signal  $y(t)$  for  $0 \leq t \leq L - 1$ , where  $L$  is the sample length. Practically, we use the sample cumulants  $\hat{c}_k(m_1, m_2, \dots, m_{k-1})$  being the estimates of theoretical cumulants of the random process. The estimates up to the fourth order are given by the following equations:

$$\begin{aligned}\hat{c}_2(m) &= \frac{1}{L} \sum_{i=0}^{L-m-1} y(i)y(i+m), \quad 0 \leq m \leq L-1 \\ \hat{c}_3(m_1, m_2) &= \frac{1}{L} \sum_{i=0}^{L-m_2-1} y(i)y(i+m_1)y(i+m_2) \quad 0 \leq m_1 \leq m_2 \leq L-1 \quad (6.4.14) \\ \hat{c}_4(m_1, m_2, m_3) &= \frac{1}{L} \sum_{i=0}^{L-m-1} y(i)y(i+m_1)y(i+m_2)y(i+m_3) \\ &\quad - \hat{c}_2(m_1)\hat{c}_2(m_2-m_3) - \hat{c}_2(m_2)\hat{c}_2(m_3-m_1) - \hat{c}_2(m_3)\hat{c}_2(m_1-m_2) \\ &\quad 0 \leq m_1 \leq m_2 \leq m_3 \leq L-1\end{aligned}$$

Generally speaking, we can directly use the FFT algorithm to estimate the inverse cumulants by noting the equations (6.2.6),(6.3.1) and (6.3.2). The basic steps are as follows.

First we construct the  $k^{th}$  order spectrum estimates:

$$\hat{S}_k(f_1, f_2, \dots, f_{k-1}) = \sum_{m_1, \dots, m_{k-1} = -L+1}^{L-1} \hat{c}_k(m_1, m_2, \dots, m_{k-1}) e^{-j \sum_{i=1}^{k-1} \frac{2\pi n_i m_i}{N_f}} \quad (6.4.15)$$

where  $N_f$  is a sufficient large positive integer of power 2,  $N_f \geq 2L - 1$ ,  $f_j = \frac{n_j}{N_f}$ ,  $j = 1, \dots, k-1$ ,  $n_j = 0, 1, \dots, N_f - 1$ . Let  $\hat{c}_k(m_1, m_2, \dots, m_{k-1}) = 0$  if any variable  $m_i$  is outside of the range  $(-L + 1, L - 1)$ . Obviously, we can set up a  $k - 1$  dimensional FFT algorithm to calculate  $\hat{S}_k(f_1, f_2, \dots, f_{k-1})$ . Thus, we can get the

estimates of the inverse polyspectra:

$$\hat{S}I_k(f_1, f_2, \dots, f_{k-1}) = \frac{1}{\hat{S}_k(f_1, f_2, \dots, f_{k-1})} \quad (6.4.16)$$

Because the system does not have any poles or zeros on the unit circle, equation (6.4.16) will not cause any existence problem.

The  $k^{\text{th}}$  order inverse cumulants then can be estimated by calculating:

$$\hat{c}i_k(m_1, m_2, \dots, m_{k-1}) = \frac{1}{(N_f)^{k-1}} \sum_{n_1 \dots n_{k-1}}^{N_f-1} \phi \hat{S}I_k(f_1, f_2, \dots, f_{k-1}) e^{j \sum_{i=1}^{k-1} \frac{2\pi n_i m_i}{N_f}} \quad (6.4.17)$$

where,  $\phi$  is the phase shift depending on  $n_i$ . Surely, equation (6.4.17) can be computed by using a  $k - 1$  dimensional IFFT algorithm.

A variational procedure can be employed to estimate the inverse cumulants, which uses the received signal  $y(t)$  directly. There is no necessity to estimate the sampled cumulants in advance. In this approach, we split the data into segments and estimate the polyspectra in each segment, then average the whole estimate to achieve numerical robustness. The details are as follows.

Divide the data  $y(t)$ ,  $0 \leq t \leq L - 1$ , into  $K$  segments, each containing  $L_s$  samples, so,  $L = KL_s$ . Each segment is formed as:

$$\begin{aligned} y^{(i)}(t) &= y(t + (i - 1)L_s) \\ 0 \leq t \leq L_s - 1, \quad 1 \leq i \leq K \end{aligned} \quad (6.4.18)$$

Suppose  $w^{(i)}(t)$  is a selected window function,  $L_s$  is an integer of power 2. The Fourier transform of  $y^{(i)}(t)$  is :

$$Y^{(i)}(f_i) = \sum_{t=0}^{L_s-1} y^{(i)}(t) w^{(i)}(t) e^{-j \frac{2\pi n_i t}{L_s}} \quad 1 \leq i \leq K \quad (6.4.19)$$



where,  $f_l = \frac{n_l}{L_s}$ ,  $n_l = 0, 1, \dots, L_s - 1$ . The FFT algorithm can be used to calculate the  $Y^{(i)}(f_l)$  in each segment.

Taking the average, we obtain the form of the bispectrum estimates as:

$$\hat{S}_3(f_1, f_2) = \frac{1}{KL_s} \sum_{i=1}^K Y^{(i)}(f_1)Y^{(i)}(f_2)Y^{(i)}(-f_1 - f_2) \quad (6.4.20)$$

Thus, the third order inverse cumulants can be calculated using the IFFT as:

$$\hat{c}i_3(m_1, m_2) = \frac{1}{(L_s)^2} \sum_{n_1, n_2=0}^{L_s-1} \frac{1}{\hat{S}_3(f_1, f_2)} e^{j \sum_{i=1}^2 \frac{2\pi m_i n_i}{L_s}} \quad (6.4.21)$$

For estimating the fourth order inverse cumulants, we calculate the periodogram for each segment:

$$I^{(i)}(f_l) = \frac{1}{L_s} |Y^{(i)}(f_l)|^2 \quad (6.4.22)$$

and computing:

$$X(f_l) = \sum_{i=-L_s+1}^{L_s-1} e^{-j2\pi f_l i} = \frac{\sin(2L_s - 1)\pi f_l}{\sin \pi f_l} \quad (6.4.23)$$

$$G^{(i)}(f_1, f_2, f_3) = \frac{1}{L_s} Y^{(i)}(f_1)Y^{(i)}(f_2)Y^{(i)}(f_3)Y^{(i)}(-f_1 - f_2 - f_3) \quad (6.4.24)$$

Taking the average for all segments:

$$I(f_l) = \frac{1}{K} \sum_{i=1}^K I^{(i)}(f_l) \quad (6.4.25)$$

$$G(f_1, f_2, f_3) = \frac{1}{K} \sum_{i=1}^K G^{(i)}(f_1, f_2, f_3) \quad (6.4.26)$$

Then the trispectrum takes the form:

$$\begin{aligned} \hat{S}_4(f_1, f_2, f_3) = & G(f_1, f_2, f_3) - I(f_1)I(f_2)X(f_2 + f_3) \\ & - I(f_2)I(f_3)X(f_3 + f_1) - I(f_3)I(f_1)X(f_1 + f_2) \end{aligned} \quad (6.4.27)$$

Finally, the fourth order spectrum will be estimated and the fourth order inverse cumulants can be calculated via the IFFT algorithm.

All these FFT based algorithms are simple, efficient and easy to implement. No linear equations need to be solved of any kind.

## 6.4.2 Inverse Cumulants Estimation in the Time Domain

Noting equation (6.3.1), and taking the inverse  $Z$  transform on both sides, we have:

$$\begin{aligned} \sum_{l_1, \dots, l_{k-1} = -\infty}^{+\infty} c_k(m_1 - l_1, m_2 - l_2, \dots, m_{k-1} - l_{k-1}) ci_k(l_1, l_2, \dots, l_{k-1}) \\ = \delta(m_1, m_2, \dots, m_{k-1}) \end{aligned} \quad (6.4.28)$$

In practice, we have to approximate the infinite summation by truncation. Based upon the third order inverse cumulants, let

$$S = \{(i, j) \mid -(M + N) \leq i \leq M + N, -(M + N) \leq j \leq M + N\}$$

$$S^c = \{(i, j) \mid i < -(M + N) \text{ or } i > (M + N) \text{ or } j < -(M + N) \text{ or } j > (M + N)\}$$

Define the truncation error:

$$\begin{aligned} \xi(m, n) &= \sum_{(i, j) \in S} c_3(m - i, n - j) ci_3(i, j) - \delta(m, n) \\ &= - \sum_{(i, j) \in S^c} c_3(m - i, n - j) ci_3(i, j) \end{aligned} \quad (6.4.29)$$

Because of the symmetrical property, the total unknowns of  $ci_3$  is  $\frac{(M+N+1)(M+N+2)}{2}$ . We choose the range of  $(m, n)$  as  $\tilde{S} = \{(m, n) \mid -(M + N) \leq m \leq n \leq (M + N)\}$ , so we have a total  $(M + N + 1)(2M + 2N + 1)$  equations. The estimation criterion now is defined as the sum of the least squares of the truncation error for  $(m, n) \in \tilde{S}$ :

$$E_r = \sum_{(m, n) \in \tilde{S}} \xi^2(m, n) \quad (6.4.30)$$

Define:

$$R_1(m, n, l) = c_3(m - l, n) + c_3(m, n - l) + c_3(m + l, n + l) \quad (6.4.31)$$

$$R_2(m, n, l) = c_3(m - l, n - l) + c_3(m + l, n) + c_3(m, n + l) \quad (6.4.32)$$

$$\begin{aligned} R_3(m, n, k, l) = & c_3(m - k, n - l) + c_3(m - l, n - k) + \\ & c_3(m + k, n + k - l) + c_3(m + k - l, n + k) + \\ & c_3(m + l, n - k + l) + c_3(m - k + l, n + l) \end{aligned} \quad (6.4.33)$$

By utilizing the symmetrical property of the inverse cumulants, we can write equation (6.4.29) in the form:

$$\begin{aligned} \xi(m, n) = & c_3(m, n)ci_3(0, 0) + \sum_{i=1}^{M+N} R_1(m, n, i)ci_3(i, 0) + \\ & \sum_{i=1}^{M+N} R_2(m, n, i)ci_3(i, i) + \sum_{i=2}^{M+N} \sum_{j=1}^{i-1} R_3(m, n, i, j)ci_3(i, j) - \delta(m, n) \\ & (m, n) \in \tilde{S} \end{aligned} \quad (6.4.34)$$

Divide all unknowns into two parts:

$$\begin{aligned} \zeta_a = & [ci_3(0, 0), ci_3(1, 0), ci_3(1, 1), \dots, ci_3(\frac{2(M+N)}{3}, \frac{2(M+N)}{3}), \\ & ci_3(M+N, 0), ci_3(M+N, 1), \dots, ci_3(M+N, M+N)]^T; \end{aligned} \quad (6.4.35)$$

$$\begin{aligned} \zeta_b = & [ci_3(\frac{2(M+N)}{3} + 1, 0), ci_3(\frac{2(M+N)}{3} + 1, 1), \dots, \\ & ci_3(M+N-1, 0), \dots, ci_3(M+N-1, M+N-1)]^T \end{aligned} \quad (6.4.36)$$

Now collecting all the equations for  $(m, n) \in \tilde{S}$  and constructing the standard norm regression form for a least squares solution, we obtain:

$$E_r = (\Psi\zeta - a_c)^T(\Psi\zeta - a_c) \quad (6.4.37)$$

where  $\zeta = [\zeta_b^T, \zeta_a^T]^T$  and  $\Psi$  and  $a_c$  can be formed by using the equ.(6.4.34). Denoting the integer  $P$  by  $P = M + N + 1$ , we note that  $\Psi$  is  $P(2P - 1) \times \frac{1}{2}P(P + 1)$ ,  $\zeta$  and  $a_c$  are  $\frac{1}{2}P(P + 1)$ .

Actually we are only interested in  $\zeta_a$  for the AR parameter matching and initialization. The length of  $\zeta_b$  and  $\zeta_a$  are roughly the same, i.e., only half of the total unknowns needs to be estimated. Also, only one element of the constant vector  $a_c$  is 1, all others are zero. In order to take advantage of this part, the forward regressional orthogonal algorithm proposed in [19] has been utilized because of its simplicity and effectiveness. It can be used as a pruning least squares algorithm and it also can take the numerical advantage of special structure of the constant vector  $a_c$ .

The algorithm can be realized in the following steps:

1. Step 1: Writing the  $\Psi$  as:

$$\Psi = \begin{pmatrix} \alpha_{1,1} & \alpha_{1,2} & \dots & \alpha_{1,P_2} \\ \alpha_{2,1} & \alpha_{2,2} & \dots & \alpha_{2,P_2} \\ \dots & \dots & \dots & \dots \\ \alpha_{P_1,1} & \alpha_{P_1,2} & \dots & \alpha_{P_1,P_2} \end{pmatrix}$$

where  $P_1 = (M + N + 1)(2M + 2N + 1)$ ,  $P_2 = \frac{1}{2}(M + N + 1)(M + N + 2)$ ,  $a_c = [1, 0, 0, \dots, 0]^T$ ,  $[\zeta_b^T, \zeta_a^T]^T = [\zeta_1, \zeta_2, \dots, \zeta_{P_2}]^T$ .

2. Step 2. Denoting and calculating:

$$\eta_{1,1} = 1$$

$$\lambda_{j,1} = \alpha_{j,1} \quad (j = 1, 2, \dots, P_1)$$

$$g_1 = \frac{\lambda_{1,1}}{\sum_{j=1}^{P_1} \lambda_{j,1}^2}$$

3. Step 3. Computing:

$$\eta_{i,k} = \frac{\sum_{j=1}^{P_1} \lambda_{j,i} \alpha_{j,k}}{\sum_{j=1}^{P_1} \lambda_{j,i}^2}$$

$$\lambda_{j,k} = \alpha_{j,k} - \sum_{i=1}^{k-1} \eta_{i,k} \lambda_{j,i}$$

$$g_k = \frac{\lambda_{1,k}}{\sum_{j=1}^{P_1} \lambda_{j,k}^2}$$

$$k = 2, 3, \dots, P_2, \quad i = 1, 2, \dots, k-1, \quad \eta_{k,k} = 1$$

4. Step 4. Estimating:

$$\hat{\zeta}_{P_2} = g_{P_2}$$

$$\hat{\zeta}_i = g_i - \sum_{k=i+1}^{P_2} \eta_{i,k} \hat{\zeta}_k$$

$$i = P_2 - 1, P_2 - 2, \dots, P_2 - \tau_a + 1$$

Where  $\tau_a$  is the length of  $\zeta_a$ .

We make the following comment that if the matrix  $\Psi$  has full rank then the estimates of the inverse cumulants  $ci_3(m, n)$  will satisfy the normal equation of (6.4.37) and are the least squares solution. Also the procedure can be modified as an adaptive algorithm easily.

## 6.5 Numerical Simulation Results

In this section, some typical numerical results will be shown to demonstrate the performance of our approach. For simulating our algorithms, the independent identical one-sided exponential distributed input driving process with zero mean and random antipodal input sequences are generated for using the third order and fourth order inverse cumulants. In each example, 8300 random input samples are produced which

convolve with the true LTI model to generate the output signals. The first 54 and last 54 output samples are discarded to remove the transient effects of the response. Zero mean white i.i.d. Gaussian noise, or colored noise  $\nu(t)$  are added to the output signal  $y(t)$  to generate the various signal-to-noise ratios. The signal-to-noise ratio(SNR) is defined as  $10 \log_{10}(\frac{E\{y^2(t)\}}{E\{\nu^2(t)\}})$ . The colored noise was produced by passing the i.i.d. white Gaussian noise through an MA filter  $T(z) = 1 + 0.5z^{-1} - 1.5z^{-2}$ .

**Example 1. (Noncausal ARMA(2,2) model)**

The model we simulated in our first example is the second order noncausal ARMA(2,2):

$$H(z) = \frac{0.3752(1 + 0.8z^{-1})(1 + 0.1z)}{(1 - 0.2725z^{-1})(1 + 0.6359z)}$$

The system has one stable causal pole at 0.2725, one stable anticausal pole at  $-1.5725$ , one minimum phase zero at  $-0.8$  and one nonminimum phase zero at  $-10$ . The true coefficient values  $(\beta_{-2}, \beta_{-1}, \beta_0, \beta_1, \beta_2, \beta_3, \beta_4)$  of the deconvolution AR filter are  $(-0.1595, 1.5948, 1.000, -1.5263, 1.2210, -0.9768, 0.7815)$ . One-sided exponential i.i.d. input sequences are generated with  $\sigma^2 = 0.630$ ,  $\gamma_3 = 1.000$  for estimating the inverse cumulants. Fig.6.1(a) shows the true third order inverse cumulants  $ci_3(i, j)$  for  $-12 \leq i, j \leq 12$  of the model.

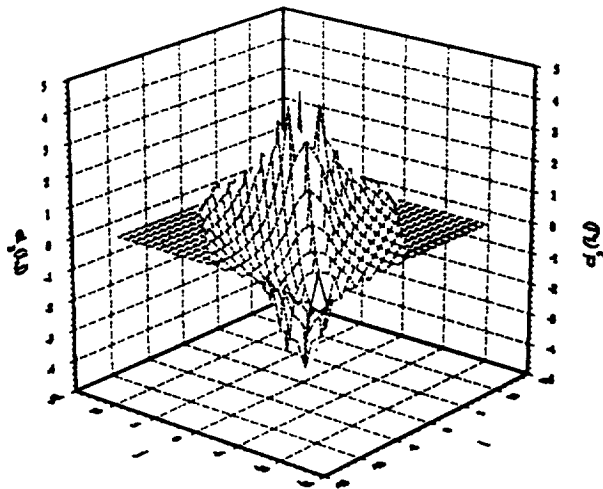


Fig.6.1(a) The true third order inverse cumulants  $ci_3(i, j)$  for  $-12 \leq i, j \leq 12$ .

For using the frequency domain formulation, we divide the output samples into 16 segments, each containing 512 points. White i.i.d. Gaussian noise, or colored Gaussian noise are added to the output signal to produce the various signal-to-noise ratios for testing the performance of the algorithm. Equations (6.4.19), (6.4.20) and (6.4.21) are used to calculate the inverse cumulants via 512 points 1-D FFT and  $512 \times 512$  points 2-D FFT algorithms. Weight signals  $w(t)$  are selected as rectangular windows for simplicity. For the output signals contaminated by the i.i.d. white Gaussian noise with SNR=30dB, Fig.6.1(b) demonstrates the estimated third order inverse cumulants  $ci_{3,F}(i, j)$  for  $-12 \leq i, j, \leq 12$  in the frequency domain (averaged over 20 Monte Carlo runs). Fig.6.1(c) presents the estimated error  $Di_{3,F}(i, j) = ci_3(i, j) - ci_{3,F}(i, j)$ .

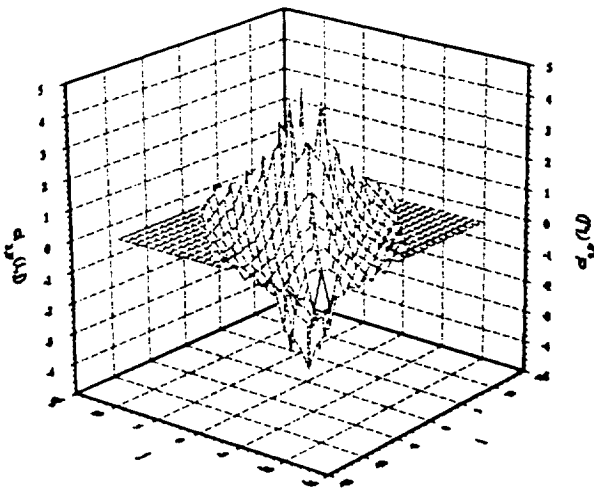


Fig.6.1(b) The estimated third order inverse cumulants  $ci_{3,F}(i, j)$  in the frequency domain via the FFT algorithms.

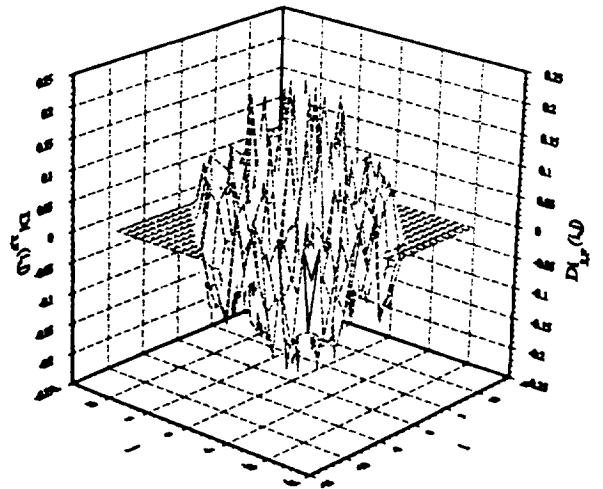


Fig.6.1(c) The error for the estimated third order inverse cumulants using the frequency domain formulation.

For estimating the inverse cumulants using the time domain least squares formu-





lation, we need to estimate the third order cumulants. We average the estimates over all 16 segments for reducing the numerical sensitivity, i.e.,

$$\begin{aligned}\hat{c}_3(m, n) &= \frac{1}{16} \sum_{k=1}^{16} \hat{c}_3^{(k)}(m, n) \\ &= \frac{1}{16} \sum_{k=1}^{16} \frac{1}{512} \sum_{i=0}^{511-m} y^{(k)}(i)y^{(k)}(i+m)y^{(k)}(i+n)\end{aligned}$$

We choose  $M = 5, N = 20$ . The i.i.d.white Gaussian noise is added to produce the SNR=30dB. Fig.6.1(d) gives the plot of estimated inverse cumulants  $ci_{3,T}(i, j)$  for  $-12 \leq i, j \leq 12$  (averaged over 20 Monte Carlo runs ). Fig.6.1(e) shows the estimation error  $Di_{3,T}(i, j) = ci_3(i, j) - ci_{3,T}(i, j)$ .

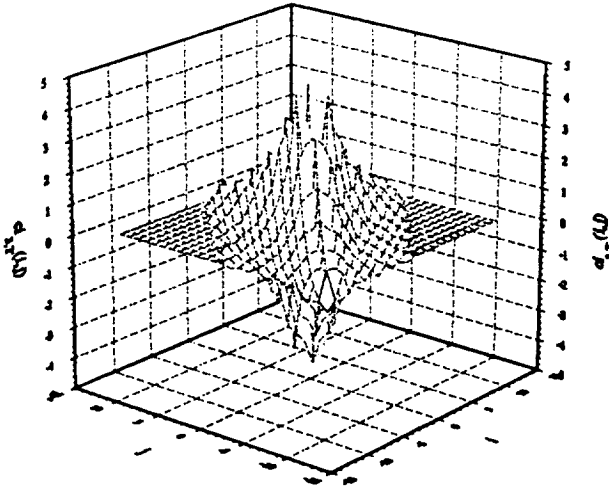


Fig.6.1(d) The estimated third order inverse cumulants  $ci_{3,T}(i, j)$  in the time domain via the least square algorithm.

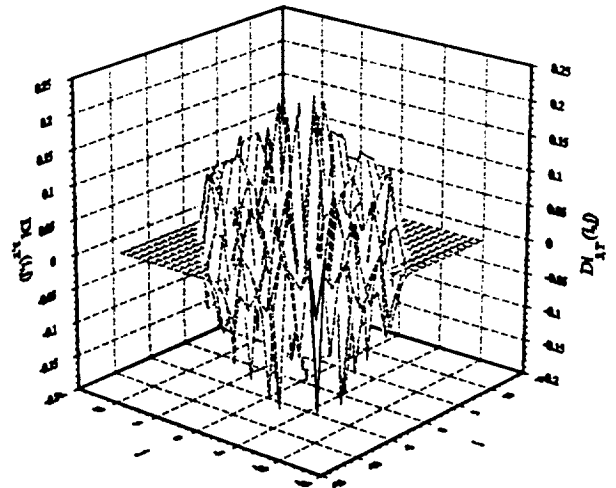


Fig.6.1(e) The error for the estimated third order inverse cumulants in the time domain via the LS algorithm.

Based upon the simulation, we have found that for a large signal-to-noise ratio case, there is not much difference from the estimates of the inverse cumulants calculated via

the FFT algorithms using the frequency domain formulation or via the least squares algorithm using the time domain formulation. But for the small SNR situations, LS algorithm does a better job than the FFT algorithm.

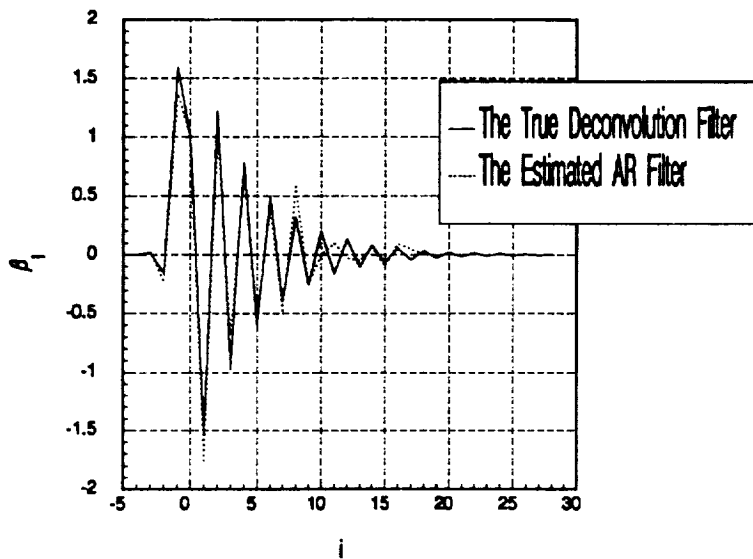


Fig.6.2(a) The true parameters of the deconvolution filter and the estimated parameters using the inverse cumulants calculated via the FFT algorithms.

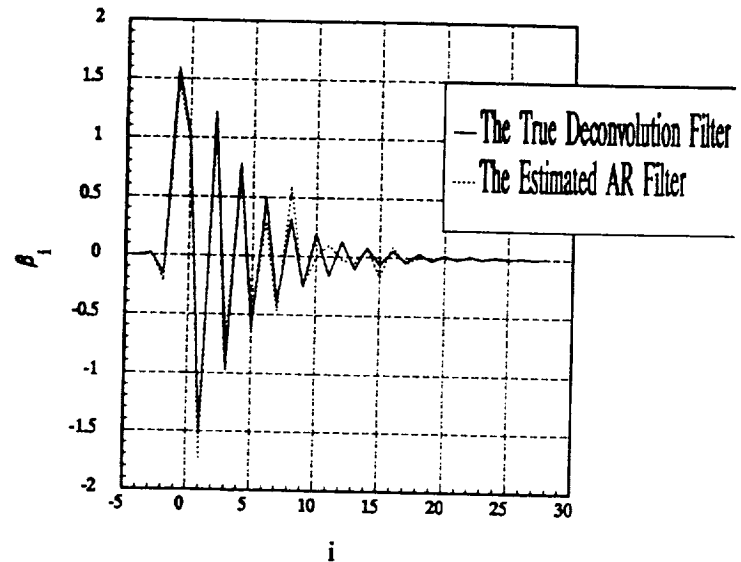


Fig.6.2(b) The true parameters of the AR deconvolution filter and the estimated parameters via the third order inverse cumulants calculated in the time domain.

After obtaining the estimates of the inverse cumulants, we use the Fletcher and Powell optimization algorithm to minimize the matching error function (6.4.8) and get the estimates of the AR parameters. In the situation of  $SNR=20dB$  for the additive colored noise, the mean and the standard deviation of the parameter estimates we got ( from the total 20 Monte-Carlo runs ) via the third order inverse cumulants calculated in the frequency domain are  $(\hat{\beta}_{-2}, \hat{\beta}_{-1}, \hat{\beta}_1, \hat{\beta}_2, \hat{\beta}_3, \hat{\beta}_4) = (-0.2342 \pm 0.0925, 1.3679 \pm 0.3482, -1.7762 \pm 0.4419, 1.0189 \pm 0.3827, -0.6820 \pm 0.2523, 0.6794 \pm 0.1836)$ . The estimates we obtained via the third order inverse cumulants calculated in the time

domain are  $(\hat{\beta}_{-2}, \hat{\beta}_{-1}, \hat{\beta}_1, \hat{\beta}_2, \hat{\beta}_3, \hat{\beta}_4) = (-0.2178 \pm 0.0784, 1.4623 \pm 0.3215, -1.7298 \pm 0.3764, 1.0787 \pm 0.3521, -0.7219 \pm 0.3621, 0.6932 \pm 0.1832)$ . Fig.6.2(a) and 2(b) give the plots of the true deconvolution parameters and the estimated parameters. So the time domain least squares inverse cumulant estimation slightly outperforms the frequency domain FFT estimation.

### Example 2.(Noncausal ARMA(2,3) model)

The second example we are going to simulate is the noncausal nonminimum phase ARMA(2,3) system:

$$H(z) = \frac{1.2013(1 + 0.55z)(1 + 0.6z^{-1})}{(1 + 0.37z)(1 - 0.62z^{-1})(1 + 0.35z^{-1})}$$

The system has two stable causal poles at  $(0.62, -0.35)$ , one stable anticausal pole at  $-2.70$ , one minimum phase zero  $-0.6$  and one nonminimum phase zero  $1.82$ . The true coefficient values of the approximate noncausal deconvolution filter are  $(\beta_{-2}, \beta_{-1}, \beta_0, \beta_1, \beta_2, \beta_3, \beta_4) = (0.1331, -0.2420, 1.0000, -0.7920, 0.2946, -0.1767, 0.1060)$ .

In this example, the input driving process  $u(t)$  is a binary random i.i.d. signal taking the values  $\{-1, 1\}$  with the equal probability 0.5.  $\gamma_3^u = 0.0$  and  $\gamma_4^u = 1.0$ . The skewness of  $u(t)$  is zero so we utilize the fourth order cumulants and fourth order inverse cumulants. Fig.6.3(a) and Fig.6.3(b) present the true fourth order inverse cumulant lags  $ci_4(i, j, 0)$  and  $ci_4(i, j, 1)$  for  $-8 \leq i, j \leq 8$ .

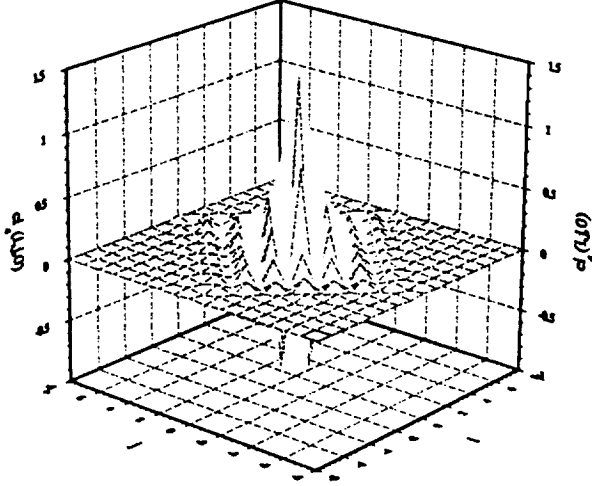


Fig.6.3(a) The true fourth order inverse cumulants  $ci_4(i, j, 0)$  for  $-8 \leq i, j \leq 8$ .

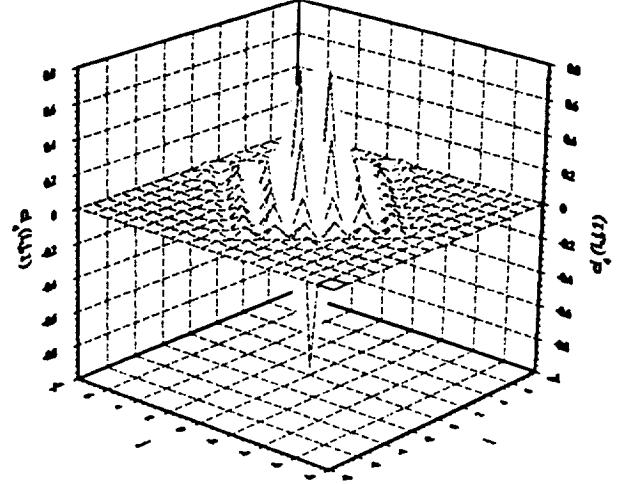


Fig.6.3(b) The true fourth order inverse cumulants  $ci_4(i, j, 1)$  for  $-8 \leq i, j \leq 8$ .

The  $M$  and  $N$  have been selected as 12. For the output signals contaminated by the i.i.d. white Gaussian noise with SNR= 30dB, Fig.6.4(a,b) show the fourth order inverse cumulants  $ci_{4,F}(i, j, 0)$  and  $ci_{4,F}(i, j, 1)$  for  $-8 \leq i, j \leq 8$  estimated in the frequency domain via the FFT algorithms (averaged over 20 Monte-Carlo runs).

Fig.6.4(c) and Fig.6.4(d) demonstrate the estimation error  $Di_{4,F}(i, j, 0) = ci_4(i, j, 0) - ci_{4,F}(i, j, 0)$  and  $Di_{4,F}(i, j, 1) = ci_4(i, j, 1) - ci_{4,F}(i, j, 1)$ .

Fig.6.5(a,b) plot the fourth order inverse cumulants  $ci_{4,T}(i, j, 0)$  and  $ci_{4,T}(i, j, 1)$  calculated in the time domain using the least squares algorithm. Fig.6.5(c)(d) give the difference  $Di_{4,T}(i, j, 0) = ci_4(i, j, 0) - ci_{4,T}(i, j, 0)$  and  $Di_{4,T}(i, j, 1) = ci_4(i, j, 1) - ci_{4,T}(i, j, 1)$ .

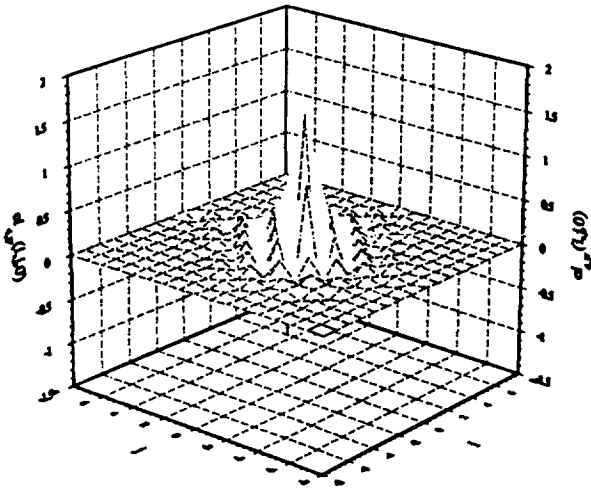


Fig.6.4(a) The estimated fourth order inverse cumulants  $ci_{4,F}(i, j, 0)$  for  $-8 \leq i, j \leq 8$  in the frequency domain via the FFT algorithms.

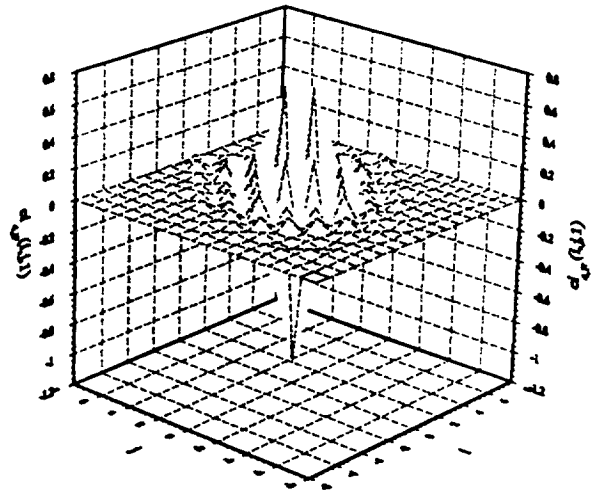


Fig.6.4(b) The estimated fourth order inverse cumulants  $ci_{4,F}(i, j, 1)$  for  $-8 \leq i, j \leq 8$  using the FFT algorithms.

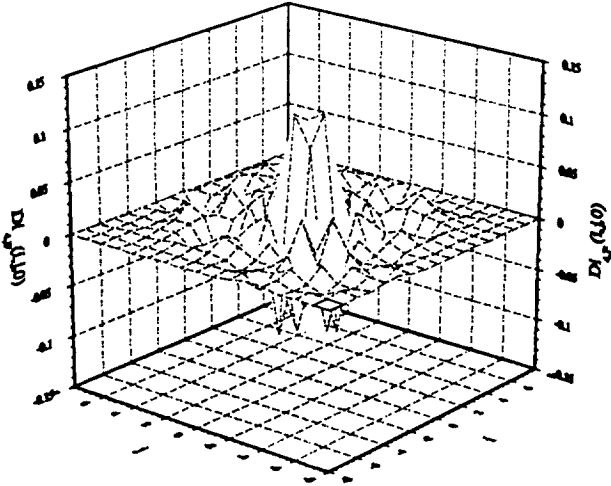


Fig.6.4(c) The error for the estimated fourth order inverse cumulants  $ci_4(i, j, 0)$  for  $-8 \leq i, j \leq 8$  in the frequency domain via the FFT algorithms.

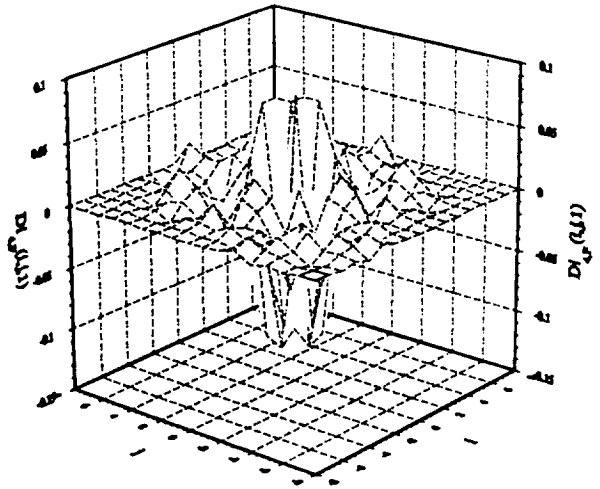


Fig.6.4(d) The error for the estimated fourth order inverse cumulants  $ci_4(i, j, 1)$  for  $-8 \leq i, j \leq 8$  using the FFT algorithms.

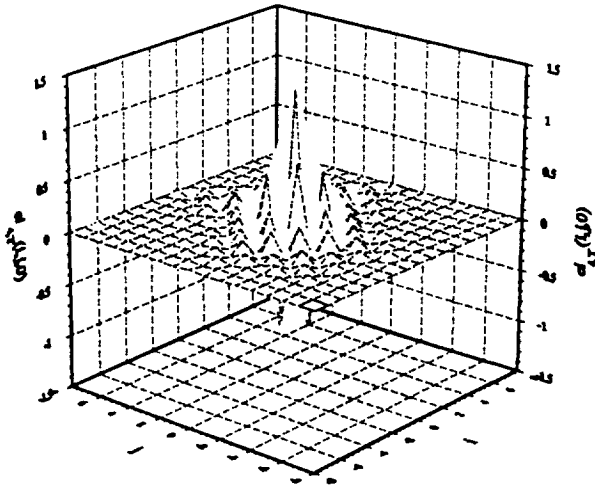


Fig.6.5(a) The estimated fourth order inverse cumulants  $ci_{4,T}(i, j, 0)$  for  $-8 \leq i, j \leq 8$  in the time domain via the least square algorithm.

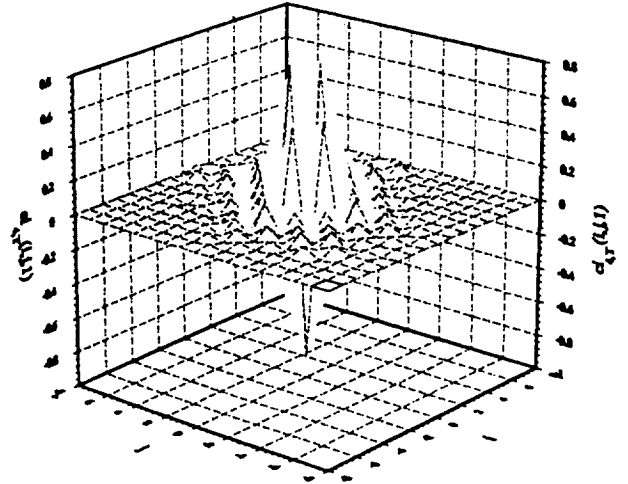


Fig.6.5(b) The estimated fourth order inverse cumulants  $ci_{4,T}(i, j, 1)$  for  $-8 \leq i, j \leq 8$  using the least square algorithms.

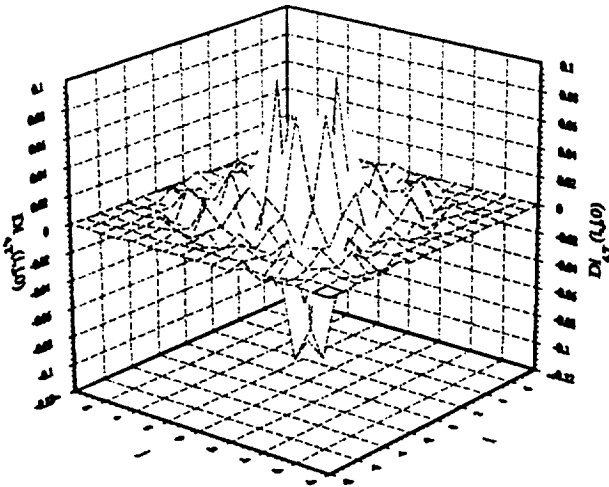


Fig.6.5(c) The error for the estimated fourth order inverse cumulants  $ci_4(i, j, 0)$  for  $-8 \leq i, j \leq 8$  in the time domain via the LS algorithms.

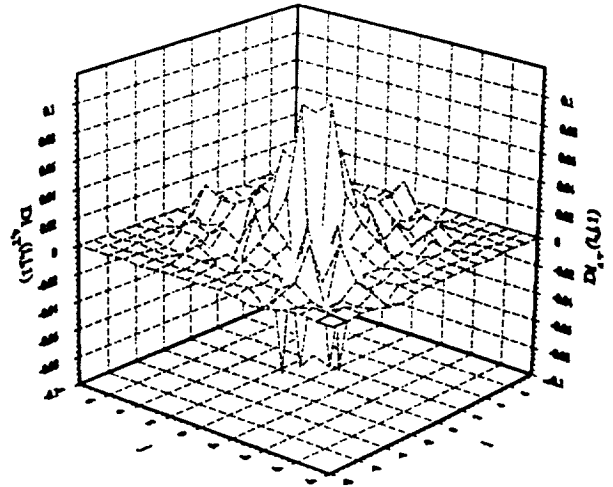


Fig.6.5(d) The error for the estimated fourth order inverse cumulants  $ci_4(i, j, 1)$  for  $-8 \leq i, j \leq 8$  using the LS algorithms.

In the case of SNR=15dB for additive white noise, the mean and standard deviation of parameter estimates of the AR filter obtained from a total of 20 Monte-Carlo runs via the fourth order inverse cumulants calculated in the frequency domain are  $(\hat{\beta}_{-2}, \hat{\beta}_{-1}, \hat{\beta}_1, \hat{\beta}_2, \hat{\beta}_3, \hat{\beta}_4) = (0.0547 \pm 0.0253, -0.3243 \pm 0.0863, -0.6250 \pm 0.2328, 0.3669 \pm 0.1429, -0.2450 \pm 0.0953, 0.049 \pm 0.022)$ . The parameter estimates we got using the inverse cumulants computed via the LS algorithm are  $(\hat{\beta}_{-2}, \hat{\beta}_{-1}, \hat{\beta}_1, \hat{\beta}_2, \hat{\beta}_3, \hat{\beta}_4) = (0.2178 \pm 0.0965, -0.1353 \pm 0.0826, -0.9483 \pm 0.3544, 0.2101 \pm 0.0673, -0.0924 \pm 0.0556, 0.0628 \pm 0.0338)$ . Fig.6.6(a) and Fig.6.6(b) plot the actual AR parameters and the estimated parameters.

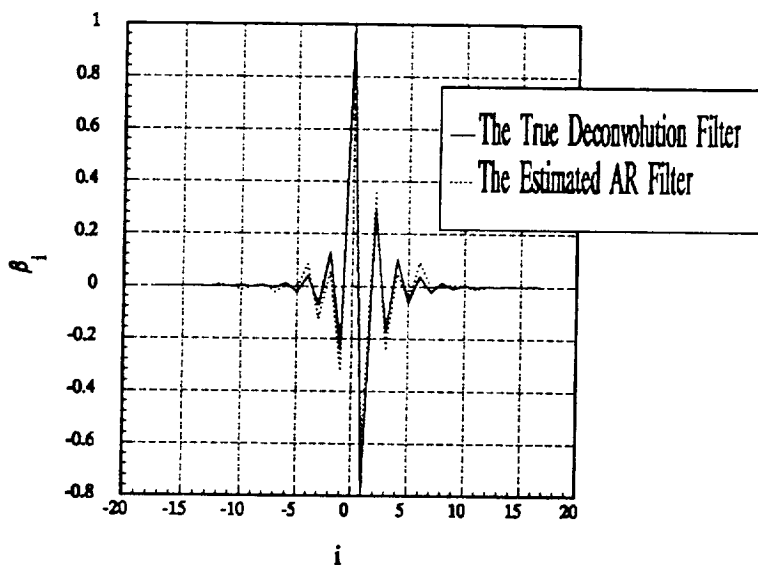


Fig.6.6(a) The true parameters of the deconvolution AR filter and the estimated parameters using the fourth order inverse cumulants calculated via the FFT algorithms.

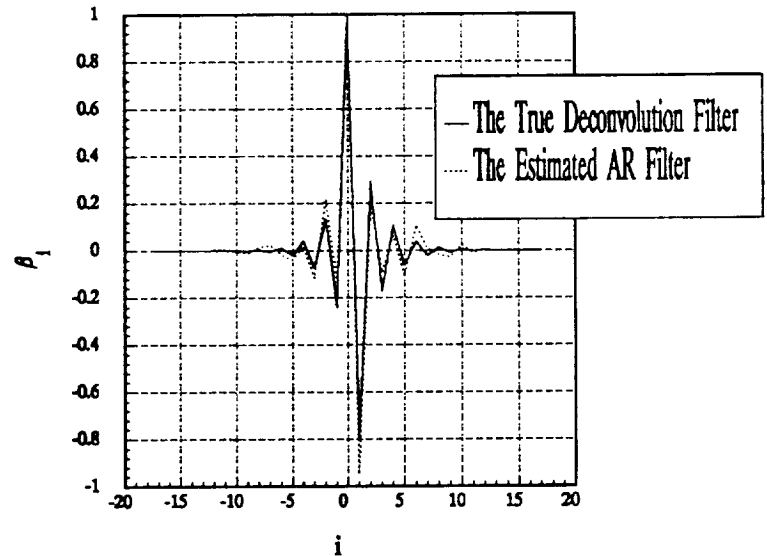


Fig.6.6(b) The true parameters of the deconvolution AR model and the estimated parameters using the fourth order inverse cumulants computed via the LS algorithm.

Also in this example, we deconvolve the output signals with the estimated AR filters to reconstruct the input driven process. For the i.i.d. random binary input

sequence  $\{-1, 1\}$ , we choose zero as the threshold value for detecting the input signals. If the data coming out from the deconvolution filter is larger than zero, we classify it as 1, otherwise we classify it as  $-1$ . The probability error  $P(e)$  of the classification is defined as the total number of the errors in the detection of the input signals divided by the length of the driven input data. For 8000 input data and various SNR cases of a total of 40 Monte-Carlo runs, Fig.6.7 demonstrates the effectiveness of our deconvolution scheme. For small SNR situations, there are some differences between the frequency domain estimation and time domain estimation. The performance of the latter is slightly better than the former. Also, for additive i.i.d. white gaussian noise and colored gaussian noise the results will change slightly. For large SNR cases, all these differences vanish and both estimation procedures give the same performance.

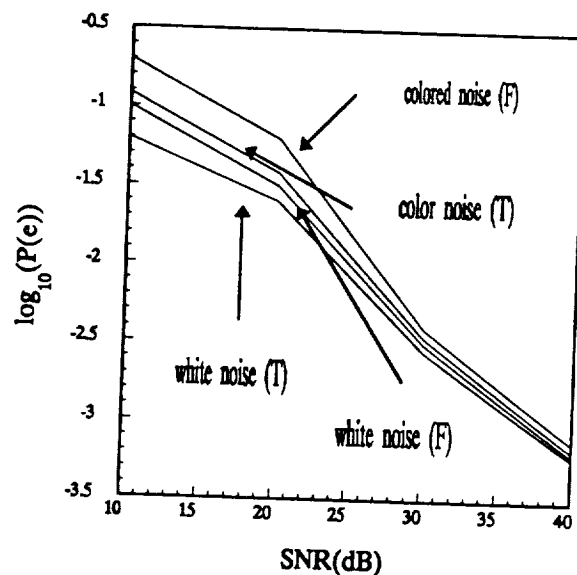


Fig.6.7 The probability error of reconstructing the input random binary antipodal signals for noncausal ARMA(2,3) system of example 2 versus SNR of white and colored Gaussian noise.

The simulation results have shown that it is possible to identify the deconvolution



model accurately in the presence of moderate additive noise based upon the method proposed in this paper. Similar to other nonminimum phase system identification schemes, a long length of sample data is required in order to get good estimates of the cumulants and the inverse cumulants. Short data records and low SNR will give a large estimate variance.

## 6.6 Concluding Remarks

In this chapter we have introduced the inverse cumulants and inverse polyspectra for parameter identification and system deconvolution. The inverse polyspectra and inverse cumulants are generalizations of the inverse power spectra and inverse auto-correlation proposed in [Chat79, Clev72]. It has been shown that there is duality between cumulants and inverse cumulants which relates to the AR modes and MA modes of the system. The basic scheme is that we use the noncausal AR filter to approximate the original system and identify this deconvolution filter directly using the inverse cumulants. Unlike the approach specified in [Chia90, Niki87], which can only be used for finite MA systems, our method can apply to the more general noncausal nonminimum phase ARMA systems. There is no necessity to know the order of the system. The only assumption about the model is that it does not have any poles or zeros on the unit circle.

Also, we have presented a procedure for estimating the inverse cumulants both in the frequency domain using an FFT algorithm and in the time domain using a least squares algorithm. It is hard to make the claim relating to the issue of consistency of the parameter estimation because of the inverse cumulants involved. The Monte-Carlo numerical simulation results demonstrate the performance of our approach. We

point out here that it is easy to modify our algorithm to an adaptive scheme so that we can track the magnitude and phase response of the system and reconstruct the input signals in time.

## Bibliography

- [Astr75] Åstrom, K.J., *Lectures on System Identification, Chapt. 3: Frequency Response Analysis*. Report 7504 , Dept. of Automatic Control, Lund Inst. of Tech., Sweden, Feb.1975.
- [Astr81] Astrom, K.J. (1981), *Maximum Likelihood and Prediction Error Methods*, Trends and Progress in System Identification, ed. by P.Eykhoff, Pergamon Press, Oxford, pp145-168.
- [Aud177] D.J.Audley, “ A Method of Constructing Minimal Approximate Realization of Linear Input-Output Behavior ”, *Automatica*, vol-13, pp409~415 , (1977).
- [Bell65] R.E.Bellman, and R.E.Kalaba, *Quasilinearization and Nonlinear Boundary Value Problems*, New York, American Elsevier, 1965.
- [Benv80] A.Benveniste, M.Goursat, and G.Ruget, “ Robust Identification of a Non-minimum Phase System: Blind Adjustment of Linear Equalizer in Data Communications ” , IEEE Trans. Automat. Contr., vol.AC-25, pp385 ~ 398, June 1980.
- [Bill89] S.A.Billings, S.Chen, and M.J.Korenberg, ” Identification of MIMO nonlinear systems using a forward-regression orthogonal estimator ”, *Int. J. Control*, vol.49, No.6, pp2157-2189, 1989.
- [BoxG70] G.E.P.Box and G.M.Jenkins, *Time Series Analysis, Forecasting and Control* , San Francisco, CA : Holden Day, 1970.

- [Bril67] D.R.Brillinger and M.Rosenblatt, " Computation and interpretation of kth-order spectra ", in *Spectral Analysis of Time Series*, B.Harris, Ed. New York : Wiley, 1967 , pp 189 ~ 232.
- [Bril70] D.R.Brillinger, " The identification of polynomial systems by means of higher order spectra " , J. Sound Vib., vol-12, pp301 ~ 313, 1970.
- [Chan82] Y. T. Chan and R. P. Langford, " Spectral Estimation via the High-Order Yule-Walker Equations " , IEEE Trans. on Acoust., Speech, Signal Processing, vol-30, No.5, pp 689-698, Oct. 1982.
- [Chat79] C.Chatfields, "Inverse Autocorrelations " , J. R. Statist. Soc. A, vol-142, pp 363-377, 1979.
- [Chia90] Hsing-Hsing Chiang, and Chrysostomos L. Nikias, "Adaptive Deconvolution and Identification of Nonminimum Phase FIR Systems Based on Cumulants " , IEEE Trans. on Automat. Contr., vol-35, No.1, January 1990.
- [Clev72] William S. Cleveland, " The inverse autocorrelations of a time series and their applications " , *Technometrics*, vol-14, No.2, May 1972.
- [CoTB90] T.B.Co and B.E.Ydstie, " System Identification Using Modulating Functions and Fast Fourier Transforms " , *Computers Chem. Engng* , vol.14, No.10, pp 1051-1066, 1990.
- [Dasg89] Soura Dasgupta, Yash Shrivastava and George Krenzer, " Persistent Excitation in Bilinear Systems " , Proc. 28th of the Conference on Decision and Control, Tampa, Florida, Dec. 1989.
- [Denn83] J.E.Dennis, Jr. and R.B.Schnable, *Numerical Methods for Unconstrained Optimization and nonlinear Equations*. Englewood Cliff, NJ: Prentice-Hall, 1983.

- [Fraz88] C. Frazho, and P. Sherman, " A Geometric Approach to the Maximum Likelihood Spectral Estimator for Sinusoids in Noise ", IEEE Trans. on Inform. Theory, vol-IT-34, No.5, pp 1066-1070, 1988.
- [Frie89] Benjamin Friedlander and Boaz Porat, "Adaptive IIR Algorithms Based on High-order Statistics " , IEEE Trans. on Acoust., Speech, Signal Processing, vol-37, no.4, April 1989.
- [Gang86] D.Gangsaas, K.R.Bruce, J.D.Blight, and U.-L.Ly, "Application of modern synthesis to aircraft control: Three case studies", IEEE Trans. Automat. Control, vol.AC-31, pp 995 ~ 1104, Nov.1986.
- [Gian89] Georgios B. Giannakis and Jerry M. Mendel, " Identification of Nonminimum Phase System Using Higher Order Statistics " , IEEE Trans. on Acoust., Speech, Signal Processing, vol-37, pp 360 ~ 377, Mar., 1989.
- [Gian90] Georgios B. Giannakis, " On the Identifiability of Non-Gaussian ARMA Models Using Cumulants " , IEEE Trans. on Automat. Contr., vol.35, No.1 , January 1990.
- [Gian90] Georgios B. Giannakis, and Ananthram Swami, "On Estimating Noncausal Nonminimum Phase ARMA Models of Non-Gaussian Processes " , IEEE Trans. on Acoust., Speech, and Signal Processing, vol.38, No.3, March 1990.
- [Good84] G.C. Goodwin and K.S. Sin, " Adaptive Filtering, Prediction and Control " , Prentice Hall, 1984.
- [HuXi87] X.Hu, "FF-Pade Method of Model Reduction in Frequency Domain " , IEEE Trans. on Automat. Control, vol.AC-32, No.3, Mar. 1987.

- [Inou83] Y.Inouye, "Approximation of Multivariable Linear Systems with Impulse Response and Autocorrelation Sequences", *Automatica*, vol-19, pp 265 ~ 277, (1983).
- [John82] D. H. Johnson and S. T. DeGraaf, "Improving the Resolution of Bearing in Passive Sonar Arrays by Eigenvalue Analysis", *IEEE Trans. on Acoust., Speech, Signal Processing*, vol-30, pp 638-647, Aug. 1982.
- [Jord90] J.R.Jordan, S.A.Jalali-Naini and R.D.L.Mackie, "System Identification with Hermite Modulating Functions", *IEE Proceedings*, vol.137, No.2, pt.D, March 1990.
- [Kala82] R.Kalaba and K.Spingarn, *Control, Identification and Input Optimization*, New York, Plenum, 1982.
- [Kave86] M. Kaveh and A. J. Barabell, "The Statistical Performance of the MUSIC and the Minimum-Norm Algorithms in Resolving Plane Waves in Noise", *IEEE Trans. on Acoust., Speech, Signal Processing*, vol-34, pp 331-341, Apr. 1986.
- [Kay84] Kay, S. M., "Accurate Frequency Estimation at Low Signal-to-Noise Ratios", *IEEE Trans. on Acoust., Speech, Signal Processing*, vol-32, pp 540-547, June 1984.
- [Kuma85] Kumaresan, R., and A. K. Shaw, "High Resolution Bearing Estimation Without Eigendecomposition", pp 576-579, *Proc. IEEE Intl. Conf. on ASSP*, Tampa, Florida, 1985.
- [Lari83] W.E.Larimore, "System Identification, Reduced Order Filtering and Modeling Via Canonical Variate Analysis", in *Proc. 1983 Amer. Contr. Conf.*, San Francisco, CA, June 1983, pp 445~451.

- [LeeF84] Lee F.C., "Time Limited Identification of Continuous Systems Using the Modulating Function Method", Ph.D dissertation, Division of Engineering, Brown University, Providence, RI (1984).
- [LeeH91] H. B. Lee and M. S. Wengrouitz, "Statistical Characterization of the MUSIC Null Spectrum", IEEE Trans. on Acoust., Speech, Signal Processing, vol-39, No.6, pp 1333-1347, June 1991.
- [Levi47] N. Levinson, "The Wiener RMS error criterion in filter design and prediction", J. Math Phys., vol.25, pp 261-278, Jan. 1947.
- [LiiK82] K.S.Lii and M.Rosenblatt, "Deconvolution and estimation of transfer function phase and coefficient for non-Gaussian linear processes", *Ann. Stat.*, pp 1195 ~ 1208, 1982.
- [Ljun87] Lennart Ljung, *System Identification: Theory for the User*, Prentice Hall Englewood Cliffs, 1987.
- [Mark71] J.D.Markel, "FFT Pruning", IEEE Trans. Audio Electroacoust., vol,AU-19, pp 305 ~ 311, Dec. 1971.
- [Moor81] B.C. Moore, "Principle Component Analysis in Linear Systems: Controllability and Model Reduction", IEEE Trans. Automat. Control, vol.AC-26, pp 17 ~ 32, 1981.
- [Mose88] R. Moses, J. Li and P. Stoica, "Accuracy Properties of High Order Yule-Walker Equation Estimators of Sinusoidal Frequencies", in *Proc. 8th IFAC Symp. Identification Syst. Parameter Estimation*, Aug. 27-31, 1988.
- [Mull76] C.T.Mullis and R.A.Roberts, "The Use of Second-Order Information in the Approximation of Discrete-Time Linear System", IEEE Trans. Acoust., Speech, Signal Processing, vol.ASSP-24, pp 226 ~ 238, (1976).

- [Niki87] C.L.Nikias and H.H.Chiang, "Higher-order spectrum estimation via non-causal autoregressive modeling and deconvolution ", IEEE Trans. on Acoust., Speech, Signal Processing, vol-36, Dec. 1988; Also in CDSP center Northeastern University, Boston, pub.CDSP-86/87-CLN-113, March 1987.
- [OhSG91] S. G. Oh and R. L. Kashyap, " A Robust Approach for High Resolution Frequency Estimation ", IEEE Trans. on Acoust., Speech, Signal Processing, vol-30, No.3, March 1991.
- [OngB79] B. G. Ong and L. L. Campbell, " Estimation of Frequencies of Sinusoids in the Presence of Noise ", *The Canadian Journal of Statistics* , vol.7, No.1, pp 11-19, 1979.
- [Park81] Sydney R. Parker, and Francis A. Perry, " A discrete ARMA model for nonlinear system identification ", IEEE Trans. on Circuits and Systems, vol.CAS-28, No.3, pp 224-233, March 1981.
- [Pear79] Pearson A.E., " Nonlinear System identification with limited time data ", *Automatica* , 5 , pp 73-84 (1979).
- [Pear85a] A.E.Pearson and F.C.Lee, " On the Identification of Polynomial Input-Output Differential System", IEEE Trans. on Automat. Control, vol.AC-30, No.8, Aug. 1985.
- [Pear85b] Pearson,A.E. and F.C.Lee, "Parameter Identification of Linear Differential Systems Via the Fourier Based Modulating Functions ", *Control-Theory and Adv. Tech.*, vol.1, No.4, pp 239 ~ 266, 1985.
- [Pear88a] A.E.Pearson, " On the equation error identification of nonlinear differential systems ", Proc. of the 1988 Conference on Information Science and System, Princeton University, Princeton, N.J., March 1988.



- [Pear88b] A. E. Pearson, “ Least Squares Parameter Identification of Nonlinear Differential I/O Models ”, Proc. of 27th IEEE Conf. on Dec. and Contr., Austin, TX, pp 1831–1835, 1988.
- [Pear89] A.E. Pearson, “ Identifiability and well-posedness in nonlinear system I/O modeling ”, Proc. of the 28th conference on decision and control, Tampa, Florida, Dec. 1989.
- [PearAE] Pearson, A. E., “ Explicit Least Squares System Parameter Identification for Exact Differential Input/Output Models ”, in *Proc. of 8th ICMCM*, X. J. R. Avula, ed., Pergamon Press, Oxford, UK (to appear).
- [Pear91] A.E.Pearson and J.Q.Pan, “ Frequency Analysis Via the method of Moment Functionals ”, *Proceedings of the 30th IEEE CDC* , Brighton, England, Dec. 1991.
- [Pres90] William H.Press, and etc. , *Numerical Recipes in C - The Art of Scientific Computing* , Cambridge University press 1990.
- [Rose85] M.Rosenblatt, *Stationary Sequences and Random Fields*, Boston : Birkhauser, 1985.
- [Saha82] Saha, D.C. and G.P. Rao, “ General algorithm for parameter identification in lumped continuous system – The Poisson moment functional approach ”, IEEE Trans. Automatic Control, vol.AC-27, pp 223-225, 1982.
- [Saha83] Saha C.S. and G.P.Rao, *Identification of Continuous Dynamical Systems: The Poisson Moment Functional (PMF)* , Springer-Verlag, New York (1983).
- [Sana63] Sanathanan, C. K., and J. Koerner, “ Transfer Function Synthesis as a Ratio of Two Complex Polynomials ”, IEEE Trans. on Autom. Control, vol-8, pp 56-58, 1963.

- [Scha91] Louis L. Scharf, *Statistical Signal Processing: Detection, Estimation, and Time Series Analysis*, Addison-Wesley Publishing Company, 1991 .
- [Schm86] R. O. Schmidt, “ Multiple Emitter Location and Signal Parameter Estimation ”, IEEE Trans. on Antennas Propagt., vol-34, pp 276-280, 1986.
- [Sham75] Y. Shamash, “Multivariable System Reduction via Model Methods and Padè Approximation”, IEEE Trans. Auto. Control, AC-20, pp 815 ~ 817 (1975).
- [Sher91] P. J. Sherman and K. N. Lou, “ On the Family of ML Spectral Estimates for Mixed Spectrum Identification ”, IEEE Trans. Acoust., Speech, Signal Processing, vol-39, No.3, March 1991.
- [Shin57] Shinbrot, M., “On the Analysis of Linear and Nonlinear Systems ”, Trans. ASME, vol.79, pp 547 ~ 552, 1957.
- [Söde89] Söderström, T. and P. Stoica, *System Identification*, New York: Prentice Hall, 1989.
- [Stah84] Stahl, H., “ Transfer Function Synthesis Using Frequency Response Data ”, Int. J. of Control, vol-39, pp 541-550, 1984.
- [Stoi86] P. Stoica, B. Friedlander, and T. Söderström, “ On Instrumental Variable Estimation of Sinusoid Frequencies and the Parsimony Principle ”, IEEE Trans. on Automat. Contr., vol-31, No.8, pp 793-795, Aug. 1986.
- [Stoi91] P. Stoica, R. L. Moses, T. Söderström, and J. Li, “Optimal High-Order Yule-Walker Estimation of Sinusoidal Frequencies”, IEEE Trans. on Acoust., Speech, Signal Processing, Vol-39, No.6, pp 1360-1368, June 1991.
- [Tuft82] D. W. Tufts and R. Kumaresan, “ Estimation of Frequencies of Multiple Sinusoids: Making Linear Prediction Perform Like Maximum Likelihood ”, Proc. IEEE, vol-70, No.9, pp 975-989, Sept. 1982.

- [Tugn86] J.T.Tugnait, "Order Reduction of SISO Nonminimum-Phase Stochastic Systems ", IEEE Trans. Automat. Control, vol.AC-31, No.7, pp 623 ~ 632, July, 1986.
- [Unbe87] H. Unbehauen and G. P. Rao, *Identification of Continuous Systems* , vol-10, North-Holland Systems and Control Series, Elsevier Science Publishers, B.V., 1987.
- [Wagi86] D.A.Wagie and R.E.Skelton, " A Projection Approach to Covariance Equivalent Realizations of Discrete System ", IEEE Trans. Automat. Control, vol.AC-31, pp 1114 ~ 1120, (1986).
- [Wahl90] B.Wahlberg, " ARMA Spectral Estimation of Narrow-Band Processes Via Model Reduction ", IEEE Trans. Acoust. Speech and Signal Processing, vol-38, No.7, July 1990.
- [Walk71] A. M. Walker, " On the Estimation of a Harmonic Component in a Time Series With Stationary Independent Residuals ", *Biometrika*, vol.58, pp 21-36, 1971.
- [YooD88] Do Hyun Yoo, " Order determination in linear differential system identification " , M.S. thesis, Division Eng., Brown University, Providence RI, May 1988.
- [Youn81] Young, P.C., " Parameter estimation for continuous time models – A survey ", *Automatica*, vol.17, pp 23-29, 1981.



